SEDIMENTOLOGICAL, CYCLOSTRATIGRAPHICAL
AND SEQUENCE STRATIGRAPHICAL ANALYSIS OF
CRETACEOUS ÜZÜMLÜ FORMATION (NW TURKEY)

A THESIS SUBMITTED TO
THE GRADUATE SCHOOL OF NATURAL AND APPLIED SCIENCES
OF
MIDDLE EAST TECHNICAL UNIVERSITY

BY

SALİH YİĞİT KESKİNLER

IN PARTIAL FULFILLMENT OF THE REQUIREMENTS
FOR
THE DEGREE OF MASTER OF SCIENCE
IN
GEOLOGICAL ENGINEERING

APRIL 2007

Approval of the Graduate School of Natural and Applied Sciences

_____
Prof. Dr. Canan Özgen
Director

I certify that this thesis satisfies all the requirements as a thesis for the degree of Master of Science.

_____
Prof. Dr. Vedat Doyuran
Head of Department

This is to certify that we have read this thesis and that in our opinion it is fully adequate, in scope and quality, as a thesis for the degree of Master of Science.

_____
Assistant Prof. Dr. İ. Ömer Yılmaz
Supervisor

Examining Committee Members

Prof. Dr. Demir Altıner   (METU, GEOE)   _____

Assistant Prof. Dr. İ. Ömer Yılmaz   (METU, GEOE)   _____

Prof. Dr. Asuman Türkmenoğlu   (METU, GEOE)   _____

Prof. Dr. Atilla Çiner   (Hacettepe Univ, GEOE) _____

Assoc. Prof. Dr. Uğur Kaan Tekin   (Hacettepe Univ, GEOE) _____

I hereby declare that all information in this document has been obtained and presented in accordance with academic rules and ethical conduct. I also declare that, as required by these rules and conduct, I have fully cited and referenced all material and results that are not original to this work.

Name, Last name: Salih Yiğit Keskinler

Signature   :

ABSTRACT

SEDIMENTOLOGICAL, CYCLOSTRATIGRAPHICAL
AND SEQUENCE STRATIGRAPHICAL ANALYSIS OF
CRETACEOUS ÜZÜMLÜ FORMATION (NW TURKEY)

Salih Yiğit Keskinler

M.Sc., Department of Geological Engineering

Supervisor: Assistant Prof. Dr. İ. Ömer Yılmaz

April 2007, 113 pages

High resolution sampling was performed along the Üzümlü Formation exposed near the Yeniceşıhlar village of Mudurnu (Bolu). Field and thin-section analyses showed that the Üzümlü Formation is composed of cm to m scale cycles of 4th and 5th order. The 4th order cycles are equivalencies of parasequences and have 0.4 Ma average duration. 5th order cycles are interpreted as episodic. Upper Albian (OAE1c or OAE1d) and Cenomanian/Turonian (OAE2) anoxic events are observed as black shale levels in the studied section. Position of black shale levels is interpreted using cyclostratigraphy and sequence stratigraphy. Four types of cycle are determined. A and B-type cycles are placed in transgressive and Highstand System Tract. C and D-type cycles are placed in Lowstand System Tract. Two type 3 and one type 1 sequence boundaries are recorded. The boundary between the Soğukçam Limestone and the Üzümlü Formation is interpreted as the first type 3 sequence boundary. The second

one separates the Üzümlü Formation and the Yenipazar Formation and is observed at the top of the section. Type 1 boundary is represented by a conglomeratic level in the middle of the succession. Provenance analysis of sandstones indicates that during the Cenomanian the source area changed from magmatic arc setting to continental setting

Keywords: Mudurnu, OAE, cyclostratigraphy, sedimentology, sequence stratigraphy.

ÖZ

KRETASE YAŞLI ÜZÜMLÜ FORMASYONUNUN (KB ANADOLU)
SEDİMENTOLOJİK, DEVİRSEL STRATİGRAFİK
VE SEKANS STRATİGRAFİK ANALİZİ

Salih Yiğit Keskinler

Yüksek Lisans, Jeoloji Mühendisliği Bölümü

Tez Yöneticisi: Yard. Doç. Dr. İ. Ömer Yılmaz

Nisan 2007, 113 sayfa

Mudurnu ilçesinin Yeniceşıhlar köyünde yüzeyleyen Üzümlü Formasyonu'nda bir stratigrafik kesit ölçülmüş ve örnekleme yapılmıştır. Arazi ve ince kesit analizleri Üzümlü Formayonu'nun cm ve m ölçekli devirlerden oluştuğunu göstermiştir. Çalışılan istifte 4. ve 5. derecede devirler tespit edilmiştir. 4. derece devirler parasekansların eşleniği olarak yorumlanmış ve her bir devirin ortalama 0.4 milyon yılı temsil ettiği anlaşılmıştır. 5. derece devirler sürekli olmayan episodik devirler olarak tespit edilmiştir. Üzümlü Formasyonu'nda Geç Albiyen ve Senomaniyen/Turoniyen anoksik olayları siyah şeyil seviyesi olarak gözlemlenmiştir. Siyah şeyl seviyeleri devirsel stratigrafi ve sekans stratigrafi kullanılarak yorumlanmıştır. 4 tip devirsel ardalanma tesbit edilmiştir. A- ve B-tipi devirsel ardalanmaları transgresif ve deniz seviyesinin yüksek olduğu kesimlerdedir. C- ve D-tipi devirsel ardalanmaları ise deniz seviyesinin düşük olduğu kesimlerdedir. İki tip 3

sekans sınırı ve bir tip 1 sekans sınırı belirlenmiştir. Soğukçam Kireçtaşı ve Üzümlü Formasyonu arasındaki sınır, birinci tip 3 sekans sınırı olarak yorumlanmıştır. İkinci tip 3 sekans sınırı ise Üzümlü Formasyonu ve Yenipazar Formasyonu'nun sınırındadır. Tip 1 sınırı çalışılan kesitin ortasındaki konglomera seviyesidir. Ölçülen istifteki kumtaşlarının provenans analizleri kaynağın Geç Senomaniyende mağmatik yay ortamından kıtasal ortama geçtiğini göstermektedir.

Anahtar Kelimeler: Mudurnu, OAE, sedimentoloji, devirsel stratigrafi, sekans stratigrafi.

To my mother and my brother

ACKNOWLEDGEMENTS

TABLE OF CONTENTS

LIST OF TABLES

TABLES

LIST OF FIGURES

FIGURES

xiv

CHAPTER 1

INTRODUCTION

1.1 Purpose and Scope

This study consists of a series of sedimentological, cyclostratigraphical and sequence stratigraphical investigations along a stratigraphic section measured near Yeniceşıhlar village of Mudurnu town (Bolu). The studied section is 40.55 m in thickness and composed of alternations of siliciclastic and carbonate rocks of the Üzümlü Formation. The facies are studied both in the field and laboratory by using thin sections in petrographic analysis and sedimentary structures. Changes in lithofacies types are used to detect the cyclicity in different scales. Occurrences of black shale/mudstones in the stratigraphic section are evaluated in the scope of sequence stratigraphy and global oceanic anoxic events (OAE).

The boundary between the Soğukçam Limestone and the Üzümlü Formation is also analyzed within the scope of tectonic setting of the area. Classification of sandstones, provenance and tectonic setting of sandstones and paleogeographic conditions of upper Albian will be interpreted and oceanic anoxic events (OAEs) at that time will be investigated.

1.2 Geographic Setting

The study area is located near the Yeniceşıhlar village of the Mudurnu (Bolu, NW Turkey) (Figure 1). The Mudurnu town is located 52 km south-west of Bolu City Centrum. The study area is located at the entrance of the Yeniceşıhlar village and can be reached from Mudurnu along a main transportation road.

GPS coordinates of the measured stratigraphic section are 0341082 easting, 4485124 northing at the top and 0341080 easting, 4485070 northing at the bottom.

1.3 Methods of Study

The lithofacies along the measured stratigraphic section are first investigated in the field by hand lens and their physical and descriptive characteristics have been noted in cm-scale. A total number of 125 samples are collected along the section; samples have been examined in thin section under the microscope. Afterwards, in the light of the field description and microscopic analyses, facies changes along the formation are determined. Whole samples are analyzed quantitatively using point-counting measurement by a James Swift brand mechanical stage mounted on the microscope. Detailed facies analysis under the microscope and point-counting allowed determination of the ratio between matrix and components within the individual lithofacies and the percentage variations of matrix, quartz, total terrigeneous material and glauconite along the measured section. The variations of these components versus thickness graphs are drawn and correlated with the vertical lithofacies change. Depositional environments are interpreted by investigating the vertical facies associations. On the basis of lithofacies changes, interpretations of different-order depositional cycles in the section are plotted. The determination of vertical variations

allows the recognition of relative sea-level changes. Fossil identifications were carried out by Prof. Dr. Demir Altıner and Assoc. Prof. Dr. İ. Ömer Yılmaz.
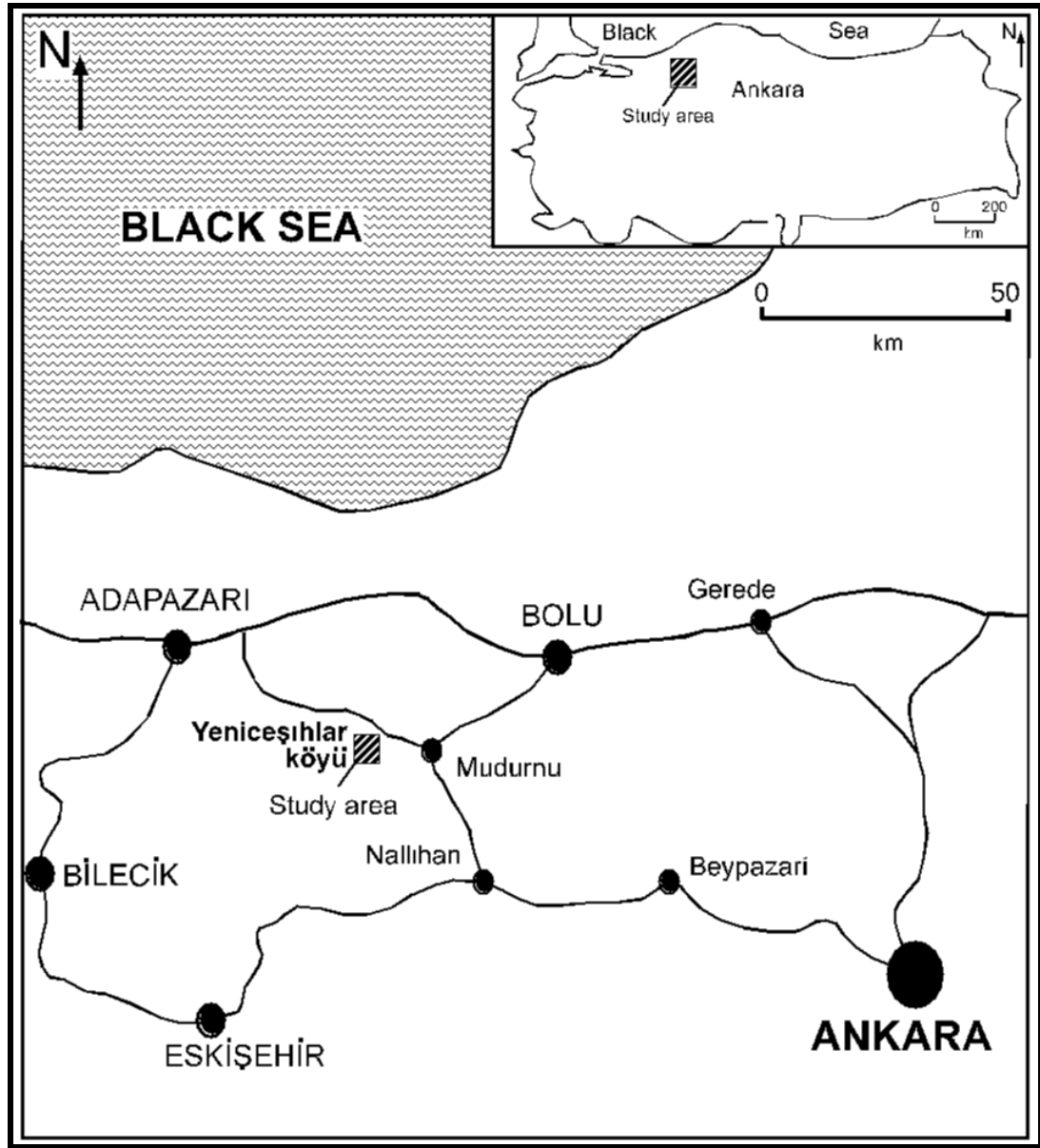
Figure 1: Location map of the study area (modified from Özkan Altıner, 1999)

1.4 Previous Studies

Geologic studies in Mudurnu goes back to 1950's in time, Abdüselamoğlu (1959), Türkünal (1960), Fourquin (1975), Altınlı (1975), Toker (1975), Saner (1980a, b), Varol and Kazancı (1981), Yılmaz et al. (1981), Görür et al. (1983), Önal et al. (1988), Altıner et al. (1991), Altıner (1991), Altıner and Özkan (1991), Koçyiğit et al. (1991), Okay and Tüysüz (1999), Koçyiğit and Altıner (2002), Yılmaz (2002), Yılmaz et al. (2005), Yılmaz and Altıner (2005a, 2005b and 2006a).

Abdüsselamoğlu (1959) studied the geology of Almacıkdağı, Mudurnu and Göynük areas. In his comprehensive study, he investigated the stratigraphic units from the pre-Devonian to Quaternary, igneous activities, tectonic activities, paleogeography and geomorphology of the area. He prepared a 1/100 000 scaled geologic map of the region. Abdüsselamoğlu described the calcareous and flysch facies in the Mudurnu region and he assigned an age of Late Cretaceous to these units. He also recognized the Lower Cretaceous calcareous units in the southern part of the Mudurnu town.

Türkünal (1960) surveyed an area between Nallıhan, Mudurnu and Seben. He described the area as an orogen zone developed along ENE-WSW direction and he claimed that this zone was composed of a Sillon and Cordilleres. The Sillon is comprised of several basins including Mudurnu basin, Vakıfaktaş basin, Şıhlar village basin, Köstebekçayı basin. These basins are represented by clayey, *Globotruncana* bearing multicolored limestone, spillite-basalt and trachite and syenite of Cretaceous ageforming flysch formations. The Cordilleres has been embodied by Tavgat Mountain, Nalıhan Mountains, Sarıçal Mountain, Çal Mountain which are composed of marly limestone of Lower Cretaceous. He has investigated and correlated the sedimentary successions of these zones and adjacent zones to interpret the paleogeography and the tectonics of the region.

Altınlı (1975) compiled the data obtained from 41 graduate theses about the geology of the area between the Bursa, Nallıhan, Mekece and Söğüt countries. In addition to the Basement Complex and the Quaternary he has differentiated, named and mapped, 5 formations- 9 members in the Mesozoic deposits including the Soğukçam Limestone and the Üzümlü Formation.

Toker (1975) studied the region and outlined the general stratigraphy and tectono-stratigraphy of the region.

Saner (1980a) published his site investigations in the western Pontides and interpretation of geophysical data. He discussed the Upper Cretaceous evolution of the region, these findings have been correlated with the areas between Russian, Carpathian and Caucasus plates, and also he interpreted the geological structure and geotectonic constitution of the area.

Saner (1980b) studied units outcropping in the Mudurnu-Göynük basin and interpreted their paleogeographic evolution after the Jurassic. He investigated the stratigraphic units in the basin in four different locations; Bilecik-Gölpazarı, Mudurnu, Nallıhan and the north of the Göynük River. He correlated the stratigraphic units in the aforesaid locations then he has defined their properties and paleogeographic evolutions. He recognized fourteen different formations in the basin, consisting of the Bayırköy Formation, Bilecik Formation, Soğukçam Limestone, Mudurnu Formation, Vezirhan Formation, Üzümlü Formation, Yenipazar Formation, Seben Formation, Selvipınar Formation, Kızılçay Formation, Çataltepe Formation, Halidiye Formation, Ciciler Formation and granitic basement.

Yılmaz (1981) studied the tectonic evolution of the southern margin of the Sakarya Continent; he claimed that southern part of the Sakarya Continent is composed of different rock groups which evolved in diverse times, environments and conditions. These are the northern autochthonous units underlain by basement granite and metabasic rocks. Rock units of Upper Cretaceous are represented by southern ophiolite

association in the area. The northern granitic land was covered by a Liassic to Late Cretaceous aged shallow carbonate platform, at the same time flysch-like sediments were deposited against the leading edge of the continent. He has defined three tectonic units: a) granitic rocks, metabase and overlying rocks, b) ophiolite complex and its metamorphic equivalent (metaophiolite) and c) dynamic metamorphosed rocks (also introduced as pulverized zone). Yılmaz (1981) claims that the rocks observed to the north of the Sakarya River are formed in different times, environments and conditions than those observed in the south of the Sakarya River.

Varol and Kazancı (1981) studied the Upper Jurassic/Lower Cretaceous limestones in the Seben - Nallıhan - Atça region including Soğukçam Limestone. According to Varol and Kazancı (1981) Upper Jurassic flysch like pelagic and resedimented limestones have been deposited in the slope and basin facies, in the region. They have defined the Jurassic/Cretaceous boundary by Calpionella biozones with the index foraminifera in the pelagic limestones, and Dasycladaeean algae in the massive biocalcarenites.

Görür et al. (1983) carried out sedimentological study of various Liassic sequences in the Pontides to identify outlines of the geomorphological, depositional, and tectonic characteristics of their environment of deposition. According to Görür et al (1983) Mudurnu region was a basin at the end of the Liassic.

Önal et al. (1988) investigated the area between Yeşilyurt, Kızılöz, Emincik, Çeğiköy, Dudaş and Sama villages which are located north of Çayırhan. Late Jurassic to Early-Paleocene aged sedimentary rocks were studied to reveal their stratigraphy, facies zones and depositional environments. The studied stratigraphic section includes the Soğukçam Limestone, Nardin Formation and the Kızılçay Group. The Soğukçam Limestone was divided into three different lithofacies from bottom to top which are, cherty micritic limestone, sandstone-shale repetation interbedded with tuffite and the

massive limestone. The age of the Soğukçam Limestone was determined as Berriasian to Albian. Three different units have been distinguished in the Nardin Formation which are olistostromal Yeşilyurt Sandstone, reefal Çeğiköy unit and sandstone-mudstone repetition. The formation was aged as Late Campanian to Maastrichian. The Kızılçay group was aged as Danian, which is claimed to be deposited in shallow water and continental environments.

Altiner et al. (1991) carried out a detailed stratigraphic study of Ammonitico Rosso bearing Jurassic-Lower Cretaceous successions of the southern part of the north-western Anatolia. Altıner et al. (1991) studied the Mudurnu area and interpreted the paleogeographic evolution of the area from Hettangian to Aptian. They have redefined the Soğukçam Limestone which is interpreted as Late-Jurassic-Early Cretaceous pelagic sedimentary sequence by Saner 1980 and Yılmaz et al., 1981, and divided it into three distinctive units as Soğukçam Limestone, Kurcalıkdere and the Yosunlukbayırı Formations.

Altıner (1991) studied the microfossil associations which comprises essential basis for the chronostratigraphic subdivision of carbonate units of Callovian to Aptian age in southern part of North-Western Anatolia. He established biostratigraphic framework of the Jurassic-Lower Cretaceous units of North-Western Anatolia including the Mudurnu Trough.

Altıner and Özkan (1991) studied the calpionellid zonation in North-Western Anatolia, including the Mudurnu-Kabalar region. They have established biostratigraphic framework at the Jurassic Cretaceous boundary and calibrated the stratigraphic ranges of several benthic foraminiferal associations occurring in the Tithonian-Hauterivian interval in association with the calpionellids and Lower Cretaceous planktonic foraminifers.

Koçyiğit et al. (1991) documented the Sedimentological evidence for the opening history of the northern branch of Neo-Tethys and its Late Jurassic-Aptian evolution in north-western Anatolia. They claim that initial volcanic activity in the Mudurnu area before the Callovian after the Pliensbachian.

Okay and Tüysüz (1999) studied Tethyan sutures of Turkey, the İzmir-Ankara-Erzincan and the Intra-Pontide sutures. They summarized the Jurassic-Eocene stratigraphy of the Sakarya Zone in two sections from the western and central part (Mudurnu-Göynük) of the Sakarya Zone. Lower to Middle Jurassic continental to shallow marine clastic rocks with ammonitico rosso horizons, Upper Jurassic-Lower Cretaceous carbonates, Upper Cretaceous-Paleocene volcanic and sedimentary rocks.

Yılmaz (2002) studied the sequence stratigraphy, cyclostratigraphy, chemostratigraphy of the Barremian-Albian inner platform deposits of the Zonguldak and Seydişehir areas and pelagic deposits of the Mudurnu and Nallıhan areas. In this study he distinguished fifth and fourth order cycles in the Soğukçam Limestone. The stable isotope (carbon and oxygen) and microfacies analyses and the point-counting method were used to determine the cyclicity of the studied sections. He correlated results of cyclostratigraphy and sequence stratigraphy studies of Lower Cretaceous platform carbonates deposited on two opposite continental margins of Neotethyan Ocean within these of their pelagic counterparts.

Koçyiğit and Altıner (2002) studied the Jurassic - Lower Cretaceous stratigraphical, sedimentological and structural evolutionary history of the northern branch of Neo-Tethys within the 6-km-thick basin fill exposed throughout the northern Turkey. They have interpreted this basin fill as the North Anatolian Paleorift (NAPR) which comprises the south-facing passive continental margin of north Neo-Tethys. They have defined the structural units of NAPR as interior grabens, subplatforms, platforms, palaeohighs, rift-related unconformities (proto-, syn- and post-rift unconformities) and

8

rift-related faults. Within these structural units Mudurnu area is described as an interior graben.

Yılmaz et al. (2005) have studied Seydişehir village in Central Taurides, Nallıhan and Mudurnu villages in Sakarya, Zonguldak city, Kozlu and Çengellidere in Western Pontides. They carried out stable isotope studies on Barremian-Aptian pelagic carbonates of Soğukçam Formation in the Sakarya Continent. They detected the global anoxia in Mid-Aptian within the pelagic successions on Sakarya Continent.

Yılmaz and Altıner (2005a) studied the Soğukçam, Nallıhan and Mudurnu areas. Studied sections comprise slope/basin pelagic carbonates of Barremian-Aptian age and the overlying turbiditic siliclastics of "Albian" age. They recorded OAE1b and OAE1c.

Yılmaz and Altıner (2005b) carried out cyclostratigraphic, sequence stratigraphic and sedimentological studies and platform to platform, platform to basin correlations on Tauride and Pontide platforms and Mudurnu-Nallıhan basins. In Mudurnu and Nallıhan areas they carried out high resolution cyclostratigraphic studies on slope/basin pelagic carbonates of Barremian-Aptian age. They recognized the global sea level changes in the Barremian-Aptian age within the successions of the Tauride and the Pontide platforms and in their pelagic counterparts within the Mudurnu - Nallihan basins.

Yılmaz and Altıner (2006a) studied two stratigraphic sections of pelagic carbonates of Barremian-Aptian age and the overlying turbiditic siliclastics of Albian-Cenomanian age in Mudurnu. They recorded OAE1c and OAE2 and carried out cyclic and sequence stratigraphic analysis of the measured sections. Yılmaz and Altıner (2006) recorded the Milancovitch cycles and cyclic alternation of pelagic limestones and silty black

shales/mud stones at the bottom of the sections and alternation of bioturbated sandstones and silty/sandy shales-mudstones.

1.5 Geological Setting

The studied Üzümlü Formation belongs to Sakarya Continent of Şengör & Yılmaz (1981), Sakarya Zone of Okay (1984), Okay and Tüysüz (1999) (Figure 2), Mudurnu Göynük trough (Figure 3) of Altıner et al. (1991), Koçyiğit et al. (1991).

In the Toarcian-Bathonian interval the Mudurnu area subsided, deepened and was filled with rift volcanics (Koçyiğit et al. 1991). During the Early Callovian-Tithonian interval the volcanic activity accompanied to the carbonate deposition in the Mudurnu depression (Koçyiğit et al. 1991). Starting from the Late Oxfordian-Early Kimmeridgian up to Late Valanginian; Aktaş (Gerede)-Sekinindoruk (Çerkeş) line uplifted and formed a submarine sill dividing the Mudurnu depression into two troughs the Mudurnu and Doğdu troughs (Koçyiğit et al. 1991). Accordingly, the subsidence and deepening of these two troughs continued and they were filled by as much as 2 km thick pelagic carbonates and carbonate turbidites (Koçyiğit et al. 1991). In the Late Valanginian-Early Hauterivian interval, due to extentional events that resulted from the downward pulling effect of progressively enlarging, cooling and being heavier ocean floor on the adjacent continental margin the submarine sill separating the Mudurnu and Doğdu troughs emerged at the end of Valanginian and became a site of erosion up to the Santonian in which it subsided suddenly, submerged, was covered by the Santonian red pelagic carbonates, and formed one of the palaeohighs (Koçyiğit et al. 1991). As to the Aptian, the rate of both sedimentation and block-faulting processes relatively decreased, and except from the Aktaş-Sekinindoruk high, the whole area was covered by the pelagic carbonates (Koçyiğit et al. 1991). Thus a fully developed divergent margin, the Sakarya divergent margin, dominated by a wide carbonate platform, the Biga-Bursa-Bilecik carbonate platform, and two major deep troughs, the

Mudurnu and Doğdu troughs separated by an intervening high appeared (Koçyiğit et al. 1991).

The Pre-Jurassic basement of the Sakarya zone is represented by the Karakaya Complex which is unconformably overlain by sedimentary rocks of Liassic Bayırköy Formation, and Liassic-Dogger volcanogenetic rocks of Mudurnu Formation, (Saner, 1980). These units are capped by Upper Jurassic- Lower Cretaceous Bilecik Limestone (Altınlı, 1975). It is known that, Bilecik Limestone is locally truncated and encountered periods of non-deposition at its basement (Altıner et al. 1991). The Soğukçam Limestone which is composed of micritic limestones, calciturbidites and olistostroms overlies the Bilecik Formation (Altınlı 1975). The overlying Upper Cretaceous units continue with different facies (Okay et al. 2006).

The oldest unit in the study area (for the geological map, see figure 4) is the Mudurnu Formation which is composed of volcanoclastics and defined by Saner (1980) as the Middle-Jurassic deep-sea deposit. In contrast, the same unit is dated as Liassic and defined as shallow marine deposit with rift volcanics representing Northern Branch of Neo-Tethys (Şengör &Yılmaz, 1981). On the other hand, the Mudurnu Formation is considered as marine deposits and dated as Dogger (Altıner et al. 1991). The Mudurnu Formation is overlain by Kurcalıkdere Formation described by Altıner et al. (1991), as a transitional zone between the Mudurnu and Yosunlukbayırı Formations and the age of the Formation ranges from the Callovian to Kimmeridgian. The Kurcalıkdere Formation includes olistostromes with pebbles derived from reefal and high energy depositional environments, tuffaceous, siliceous and basaltic levels and pelagic mudstones. The Kurcalıkdere Formation is conformably overlain by the Yosunlukbayırı Formation. The age of the formation ranges from Tithonian to Late Berriasian (Altıner et al., 1991). The Yosunlukbayırı Formation is composed of argillaceous limestones and packstones interbedded mudstones. The Kurcalıkdere Formation is overlain by the Soğukçam Limestone consisting of pelagic limestones with micritic facies.
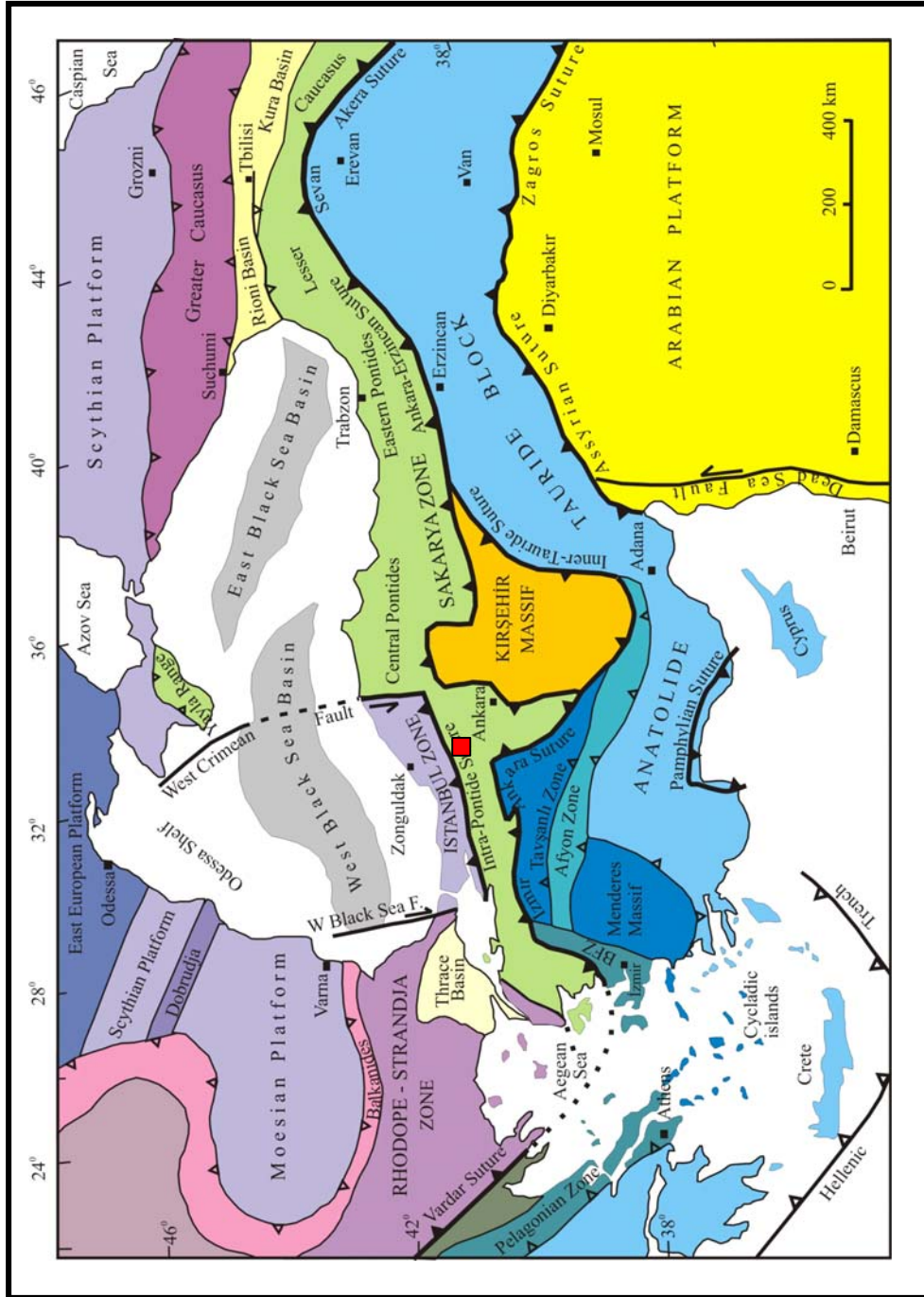
Figure 2: Tectonic units and major suture zones of Turkey and surrounding areas (Okay & Tüysüz, 1999). Red-colored area represents the study area.

12
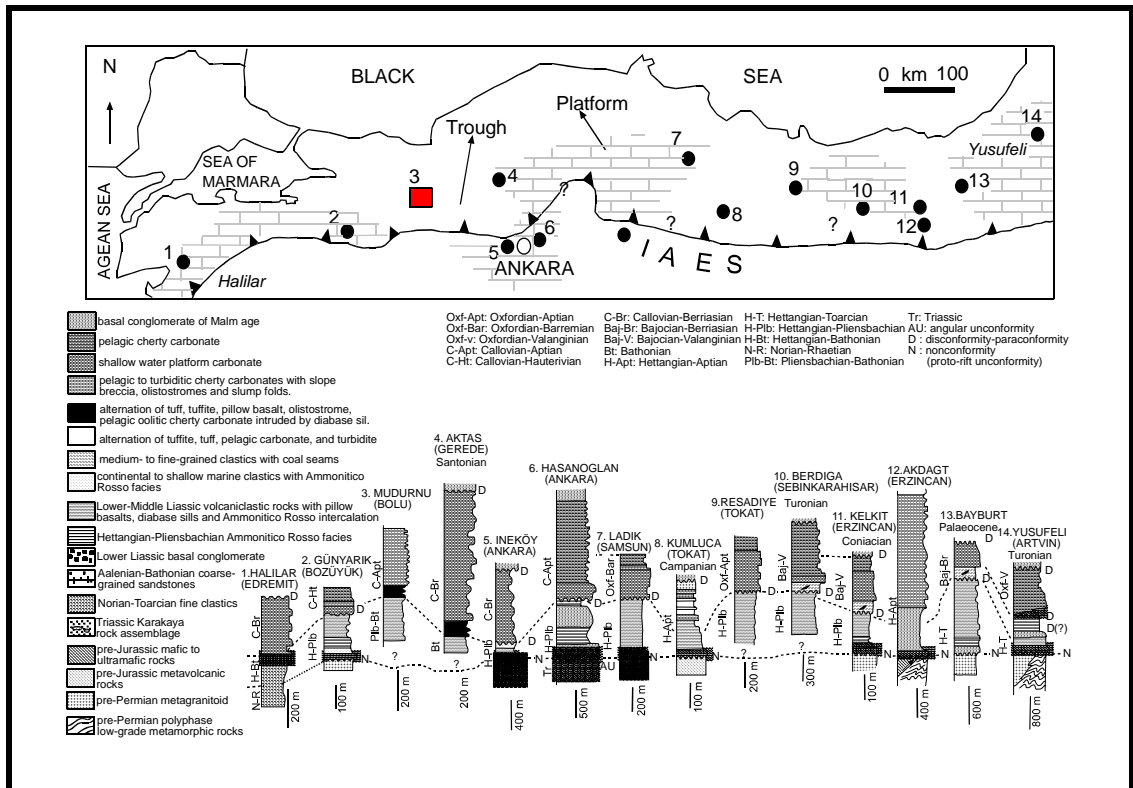
Figure 3: Simplified map showing type localities (Numbers 1 through 14) of the North Anatolian Palaeorift infill. ÜAES- İzmir-Ankara-Erzincan Suture; (B) Stratigraphical sections showing both the lateral and vertical facies distribution of the North Anatolian Palaeorift infill. Koçyiğit and Altıner (2002). Red-colored area represents the study area.

They are interpreted to represent the most stable and calm period of the carbonate regime that prevailed since the Callovian (Altıner et al., 1991). This formation is capped by Üzümlü and Yenipazar Formations which are dated as Albian to Early Maastrichtian. These formations include volcanic litharenites, purple to red glauconitic limestones and a flyschoid sequence at the top (Altıner et al., 1991).

The studied Üzümlü Formation was described by Altınlı (1975) as 250-950m thick and composed of alternation of siltstone, mudstone, sandstone and shale with micrite,

calcarenite and conglomerate lenses. He also stated that the repetition of fine and coarse rocks might be cyclic or rhythmic (Altınlı, 1975).
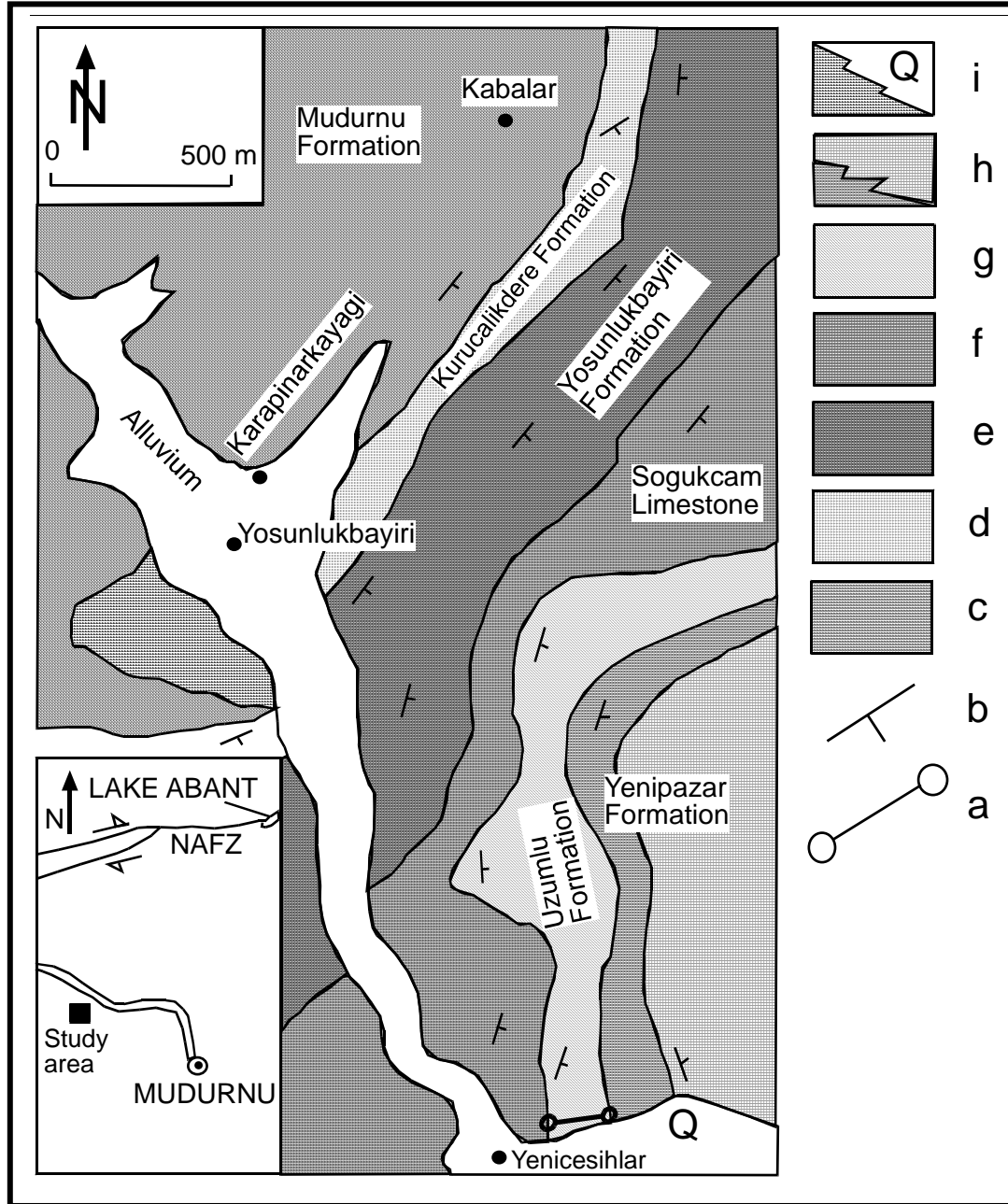
Figure 4: Geological map of the study area (a: Stratigraphic section, b: Strike and dip, c:Mudurnu Formation, d: Kurcalıkdere Formation, e: Yosunlukbayırı Formation, f: Soğukçam Limestone, g: Üzümlü Formation, h: Yenipazar Formation, i: Alluvial, NAFZ: North Anatolian Fault Zone (Altıner et al. 1991).

On the other hand, Yılmaz (2002) defined the Üzümlü Formation as succession starting with litharenitic sandstones of volcanic origin and limestones with glauconite at the bottom and flyschoidal sandstone succession at the top. The age interval assigned to Üzümlü and Yenipazar formations is Albian-Maastrichtian (Altıner et al., 1991).

CHAPTER 2

LITHOSTRATIGRAPHY

The stratigraphic succession in the Mudurnu region (for geological map, see figure 4) starts with the Middle Jurassic at the bottom. The formations observed in the study area can be listed as Mudurnu, Kurcalıkdere, Yosunlukbayırı formations, Soğukçam limestone, Üzümlü and Yenipazar formations, overlain by alluvium and alluvial cones of Quaternary (for generalized columnar section, see figure 5). In this chapter, Cretaceous Üzümlü Formation will be described in detail, yet other units will be discussed briefly.

Mudurnu, Kurucalıkdere, Yosunlukbayırı formations and the Soğukçam Limestone were defined within the Kabalar Group (Altiner et al., 1991) which extends from Beypazarı to Gerede. Both the Mudurnu and Kurucalıkdere formations are volcanogenic in character (Altiner et al., 1991). The Mudumu Formation constitutes volcanic tuffs, tuffite, and spilitic basalts, whereas the Kurucalıkdere Formation shows a succession with radiolarites, volcanic tuffs, litharenitic sandstones, pelagic limestones, and spilitic basalts (Altiner et al., 1991). The Kurucalıkdere Formation starts on the upper most basaltic layer of the Mudurnu Formation and overlain by the pelagic limestones of Yosunlukbayırı Formation. Yosunlukbayırı Formation is composed of calciturbiditic limestones and limestones of lime mudstone facies rich in calpionellids (Altiner et al., 1991). The age interval assigned to this formation is Tithonian to

Valanginian (Altıner et al., 1991). Soğukçam Limestone overlies the Yosunlukbayırı Formation (Altiner et al., 1991). It starts with cherty limestones transitionally overlying the Yosunlukbayırı Formation at the base and continues upward with lime mudstones/wackestones with planktonic foraminifera, radiolaria, sponge spicules, and *Globachaete* (Yılmaz 2002). Toward the top of the unit, the presence of marl/shale and limestone alternations is one of the characteristic features of the formation (Yılmaz 2002). The formation is overlain at the top by Üzümlü and Yenipazar Formations. Depositional age interval of the formation is attributed to Valanginian - Aptian (Altıner et al., 1991).

Üzümlü Formation overlies the Soğukçam Formation with a sudden facies change observed in the Mudurnu area (Altıner et al., 1991). Although this boundary seems to be conformable, there is a time gap between these formations. Üzümlü Formation starts with purple - red colored litharenitic sandstones of volcanic origin and limestones with glauconite at the bottom and continues upward with flyschoidal sandstone successions (Yılmaz 2002). The age interval assigned to Üzümlü and Yenipazar formations is Albian-Maastrichtian (Altıner et al., 1991).

The measured section starts with foraminifera bearing wackestones of the Soğukçam Limestone the section passes upward to the grey to brown colored greywackes of the Üzümlü Formation. These greywackes are intercalated by limestones and grey – black shales. This alternation capped by mudstone – marl and limestone alternation. Towards the middle of the section remarkable increase in grain size is recorded as alternation of conglomerate and sandstone facies. This alternation is overlain by carbonaceous mudstone/marl-limestone repetitions. The repetition continues to the top of the measured section. The simplified log of the measured section is shown in figures 6 and 7. The biozones were identified by Prof. Dr. Demir Altıner and Assoc. Prof. Dr. İsmail Ömer Yılmaz. The age intervals and key fossils are shown in figures 6 and 7.
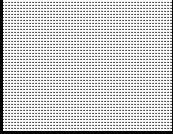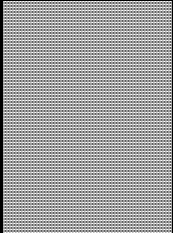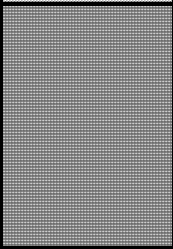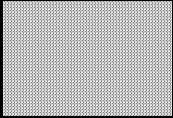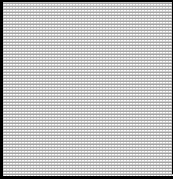
Age	Formation	Lithology	Descriptions
Quaternary	Alluvium and alluvial cones		Alluvial cones and talus breccia
Albian-Maastrichtian	Yenipazar		─── Unconformity ───
Albian-Maastrichtian	Üzümlü (studied section)		Volcano sedimentary sequence (sandstones and conglomerates) including pelagic micritic limestones
Valanginian-Aptian	Soğukçam		Alternation of micritic limestones with planktonic foraminifera and marls/blackshales
Tithonian-Valanginian	Yosunlukbayırı		Volcano sedimentary sequence with olistrostromes, diabase dikes and detritic pelagic limestones
Collavian-Kimmeridgian	Kurucalıkdere		Limestones with radiolaria, tuffs, and olistrostromes
Dogger	Mudurnu		Tuffs, volcanogenic sandstones, and spillitic basalts

Figure 5: Generalized columnar section of the study area (Altiner et al., 1991).

18
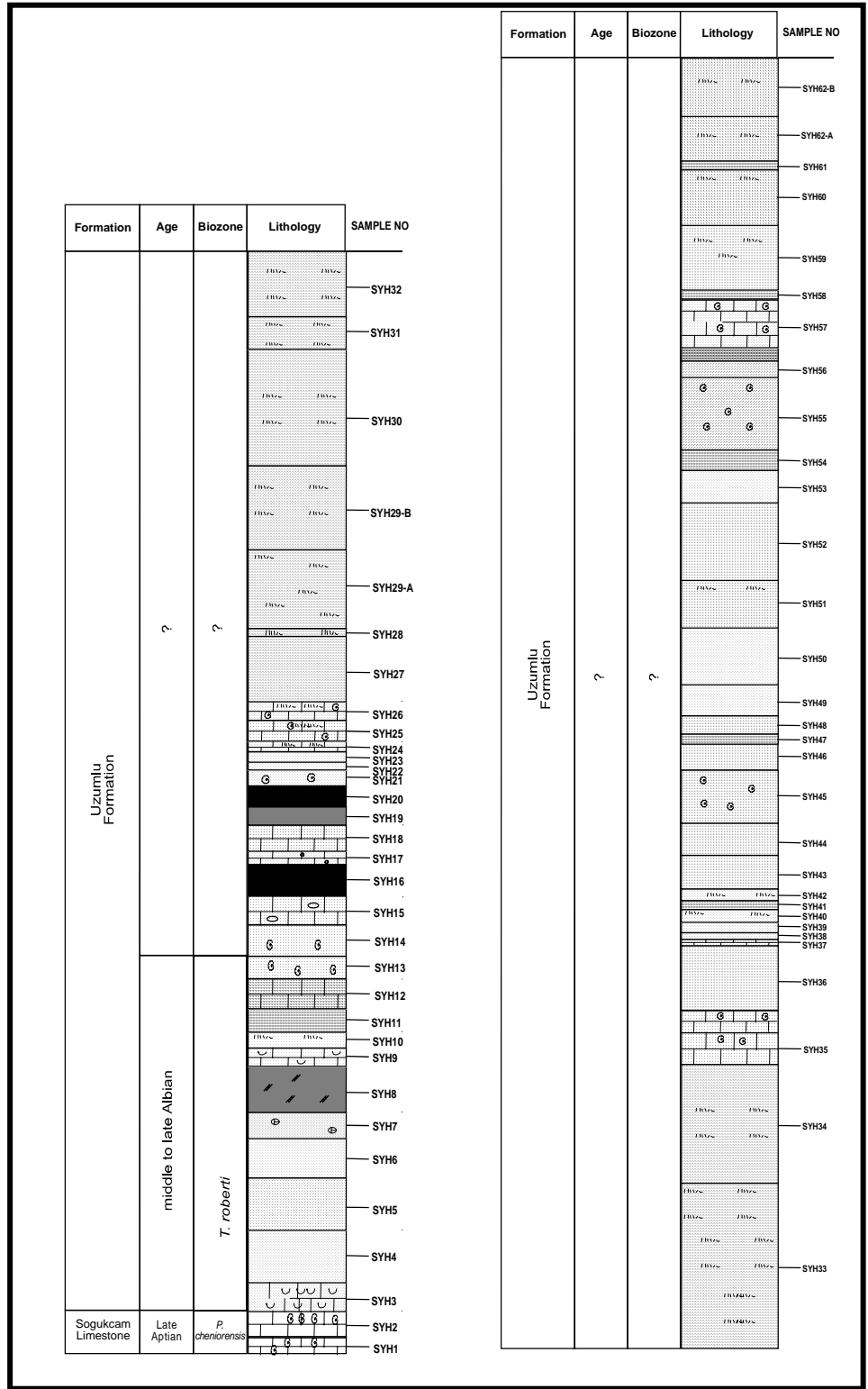
Figure 6: Simplified log of the studied section. For legend see figure 33.
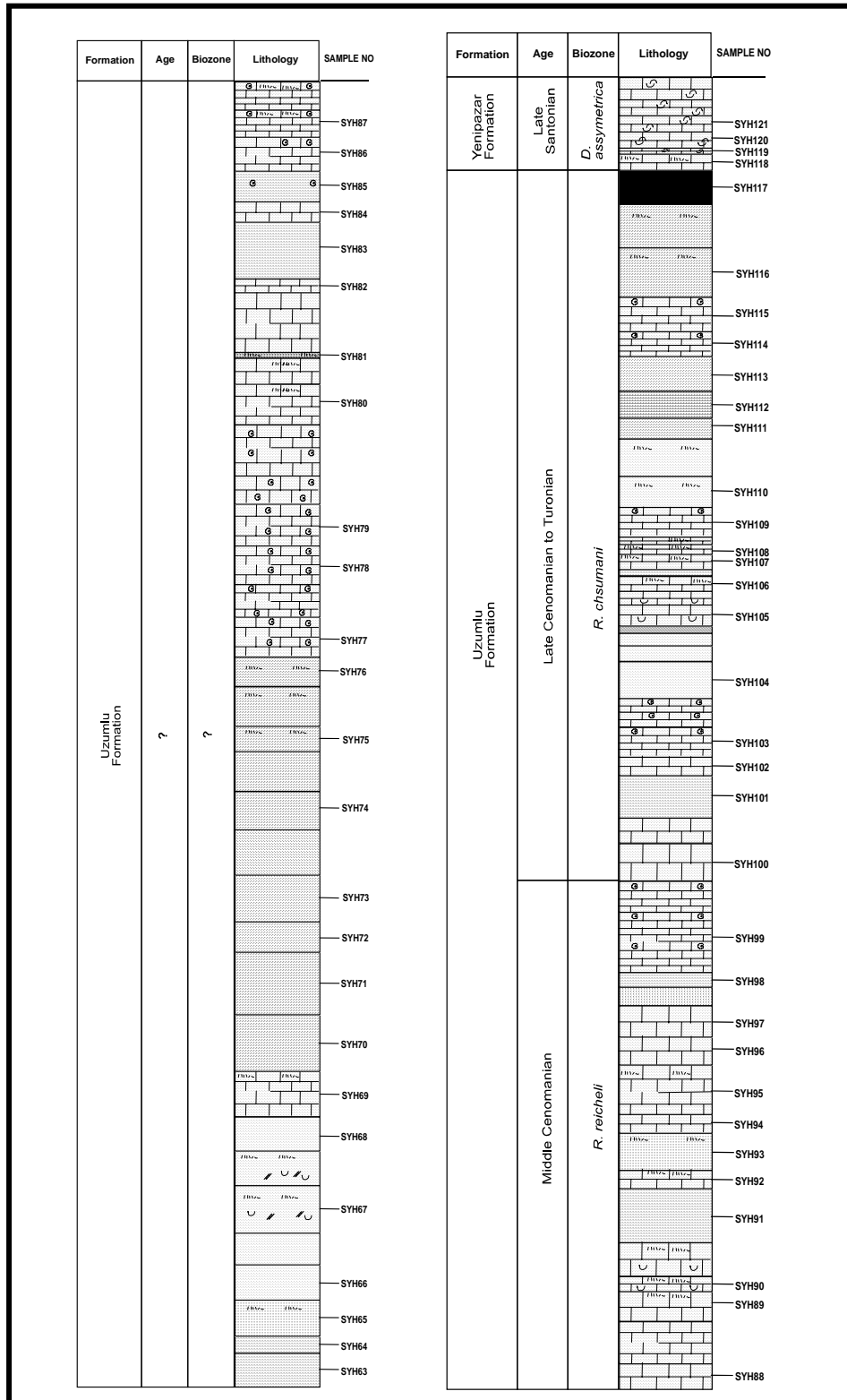
Figure 7: Simplified log of the studied section. For legend see figure 33.

CHAPTER 3

SEDIMENTOLOGY

3.1 Lithofacies

Seven different lithofacies are recognized in the studied section. These are sandstone facies, conglomerate facies, marl facies, mudstone facies, siltstone facies, shale facies and limestone facies. These facies were differentiated by the field observations, thin section investigations and point-counting method. A total of 1000-1500 points were counted for each sample.

3.1.1 Sandstone Facies

Sandstone facies (Figures 8, 9) are observed throughout the studied section of the Üzümlü Formation. They are generally dark grey, light grey and green colored. The thickness of sandstone beds vary between 5 cm to 60 cm. Point counting results indicate that the sandstones are matrix-dominated and classified as greywacke but feldspar, quartz and rock fragment ratios display variations. Quartz contents of studied thin sections are generally low and calcareous matrix is dominant yet still some of the sandstones have clay matrix. Although, a quantitative grain size analysis was not carried out, observations in the field indicate that sandstones are generally fine grained with silt, mud and lime content.

Sandstone samples are classified according to Pettijhon (1975) (Figure 10), also known as QFR classification. Percentage values of quartz, feldspar and rock fragments are obtained by point-counting method. The ternary diagrams are drawn by using PAST software and edited by freehand 10. A total of 28 sandstones were analyzed (Fig 11). Three different types of sandstone facies are recognized as arkosic wacke, feldspathic greywacke and lithic greywacke (Figure 11). Parallel lamination, normal grading and bioturbation are the most common sedimentary structures recorded in the greywackes. Thin section photograph of a feldspathic greywacke is shown in figure 12.

Figure 8: Typical View of Sandstone Facies.

Figure 9: Field photograph of sandstone (syh.23).

It is possible to recognize a number of varieties of greywacke. Those rich in rock fragments have been called lithic greywackes; those rich in feldspar are the feldspathic greywackes and those rich in quartz are named as quartzwackes (Pettijhon, 1972).

From a modal analysis of sandstone, the percentages of various combinations of grains are plotted on triangular diagrams. These diagrams are used to differentiate the different provenance terrains.
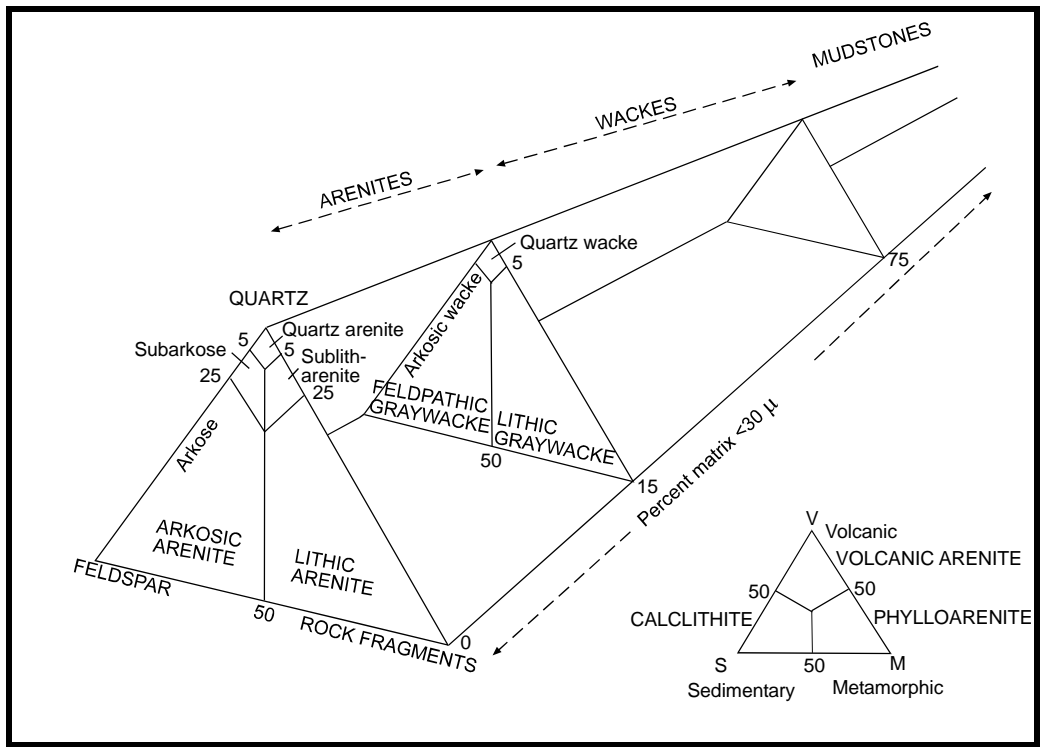
Figure 10: Sandstone classification after Pettijohn (1975).
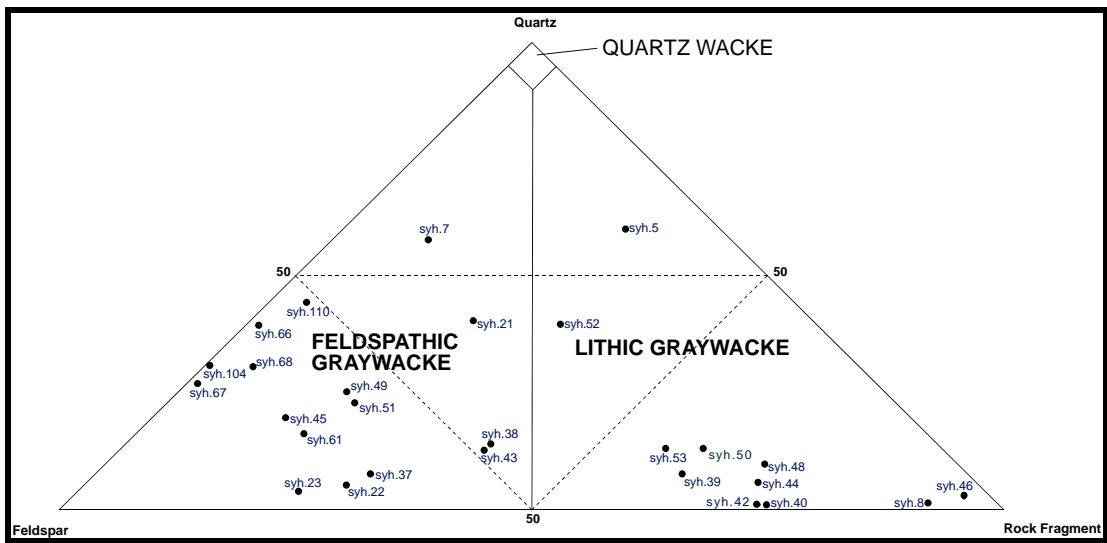
Figure 11: Ternary plots of the sandstone facies.

24
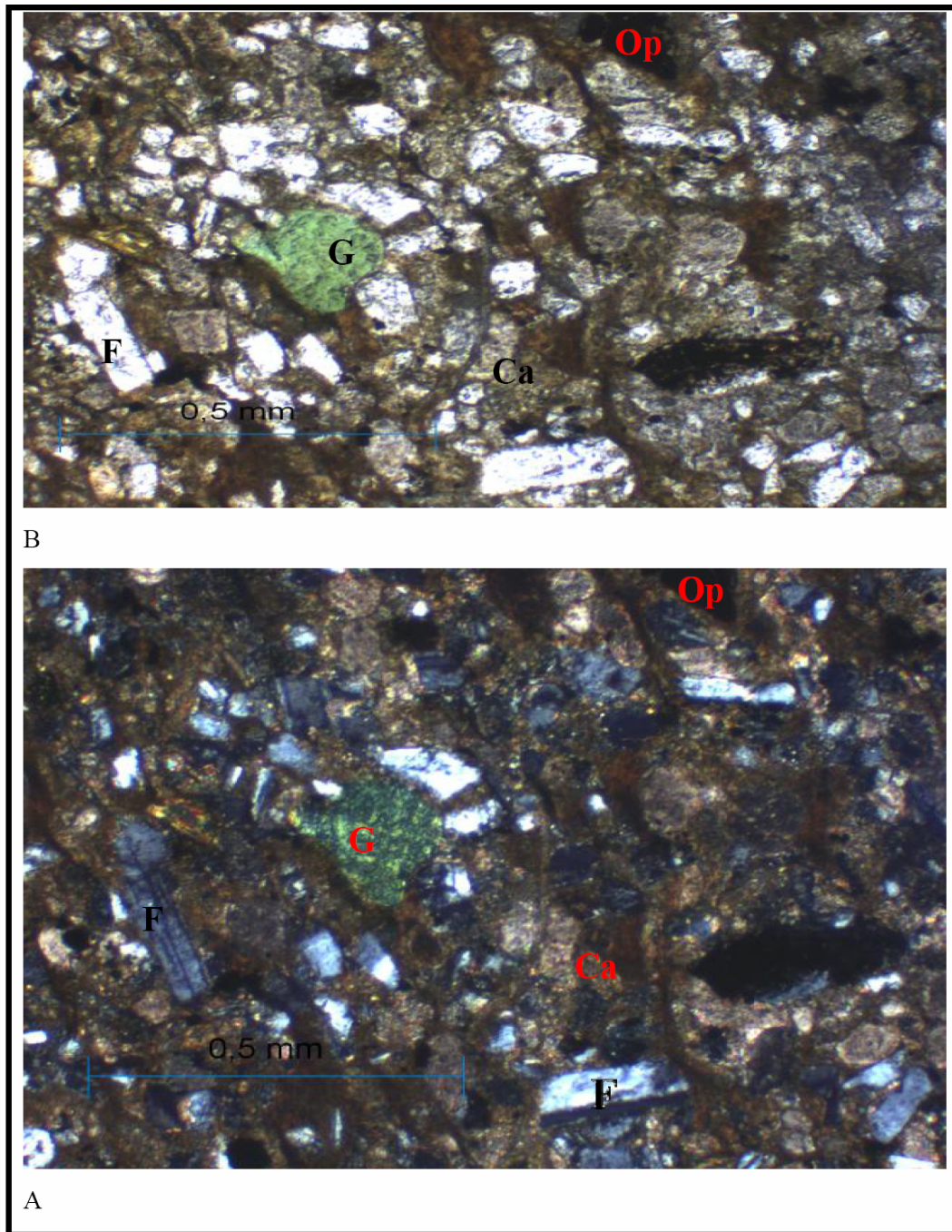
Figure 12: Thin section photograph of feldspathic greywacke (syh 21) G: glauconite, F: feldspar, Ca: calcite grain, Op: opaque. A. crossed polars, B. plane polarized light. Scale 0,5mm.

The mineralogical composition and the tectonic provenance of sandstone are related. Dickinson (1985) distinguished four major provenance terrains (Figure 13) in his work on ancient sands. (1) Stable craton, (2) basement uplift, (3) magmatic arc and (4) recycled orogen.
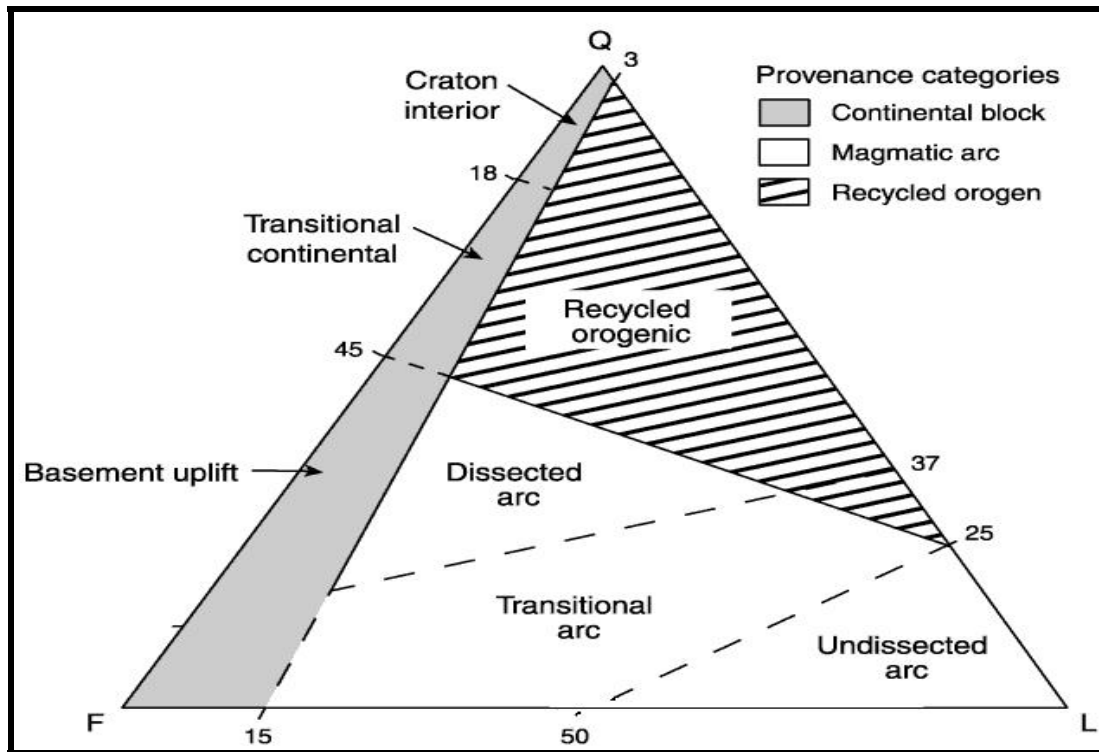
Figure 13: Provenance of sandstones after Dickinson (1985).
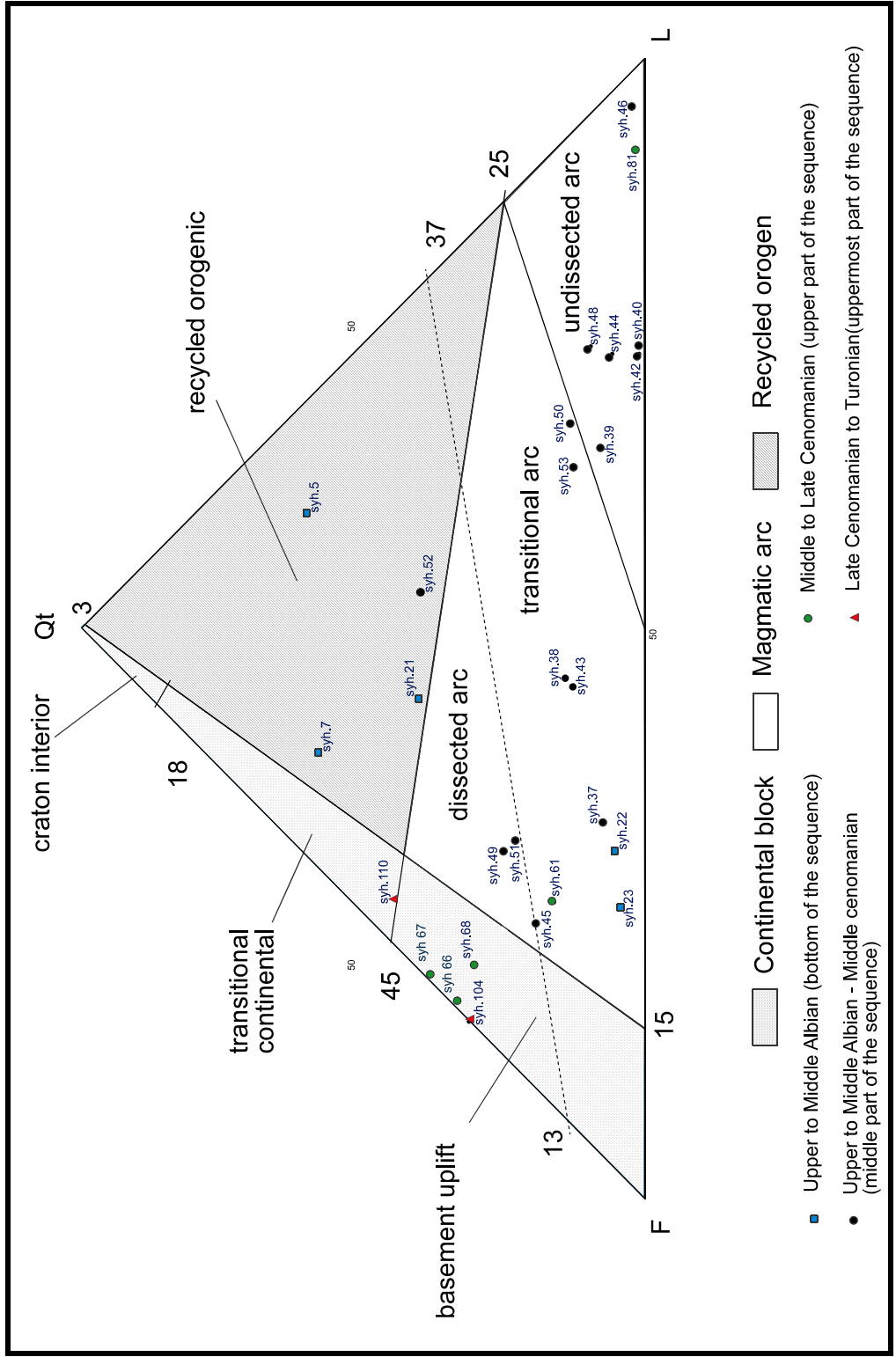
Figure 14: Provenance of the sandstones in the studied section.

The provenance of sandstones was determined by plotting a ternary diagram and correlated with Dickinson's provenances (figure 13). Although, 300 samples or more needed for an accurate analysis of the provenance of sandstones, this analysis gives a rough approximation to the provenance of sandstones throughout the section as follows. At the bottom of the studied section Upper to Middle Albian three distinct provenances of greywackes are distinguished. (1) Transitional arc (2) recycled orogen and (3) basement uplift the transitional arc and recycled orogen are the most abundant. On the other hand the greywackes observed in the middle of the section (upper to middle Albian-middle Cenomanian) have four different provenances which are transitional arc, undissected arc, dissected arc and recycled orogenic. Within these provenances, the magmatic arc region (transitional arc, undissected arc, and dissected arc) is the dominant one. The upper level of the sequence (Middle to Late Cenomanian) is characterized by randomly distributed greywacke depositions within limestone, marl, and mudstone beds. These greywackes have four different provenances: transitional arc, undissected arc, basement uplift and transitional continental. The mineral constitution of the top most greywackes (Upper Cenomanian to Turonian) of the section indicates basement uplift and transitional continental provenances.

After the Soğukçam Limestone, which is mainly composed of micritic pelagic composed of limestone and shales; Üzümlü Formation starts with sandy limestone, or calcareous sandstone with abundant feldspars, quartz, and some volcanic rock fragments, over Soğukçam Limestone. In the scope of provenance analysis, this content change and provenance study indicate that area was tectonically active. Until the Middle to Late Cenomanian a possible magmatic arc setting was present, thus magmatic arc was a site of erosion, and the Mudurnu trough was continuously subsided and was the site of deposition of pelagic/hemi pelagic siliciclastic/carbonate and volcaniclastic sedimentation (Koçyiğit et al. 1991). After the middle to late

Cenomanian, the provenance study indicates that there is a change in the source from arc related setting to basement uplift.

If provenance study is interpreted in the scope of sea level change, large scale relative sea level variations which can also be affected by tectonic movements can be stated. Towards a sequence boundary at the top of the section, "change in a relative fall in the sea level in large scale. This interpretation may also be supported by a time gap over the sequence boundary in the basin.

3.1.2 Conglomerate facies

Conglomerate facies are mostly appeared in the centre of the studied section as interbeded with sandstone facies (Figure 15). They are green to grey colored and bed thicknesses of conglomerates vary between 7 cm to 18 cm.

Conglomerates found within sandstones are also differing in composition than those found with fine grained rocks. As discussed in the previous section, the sandstones at the center of the section indicate magmatic arc setting. The conglomerates alternating with these sandstones are also indicates volcanic source. In the center of the section conglomerates contains more volcanic rock fragments and feldspars than the others, yet volcanic rock fragments are dominant components of all conglomerates observed throughout the section. Pyroxene and amphibole grains are other evidences proving volcanic source. Moreover, calcite is the dominant cement type for all conglomerates, although clay matrix is also observed.

Silt-sand sized quartz grains are emplaced within the cement, the amount of these quartz grains reached up to 9% in the mineral composition. Other quartz grains are found in the volcanic rock fragments and were not separately counted.

Figure 15: Typical view of conglomerate facies

Conglomerates alternating with sandstones in the middle of the studied section and at the top of the section have similar textures. They are composed of subrounded to rounded grains, grain supported and moderately sorted. On the other hand, conglomerate observed at the bottom of the succession is matrix supported and poorly sorted. Also this unit is laterally pinchout in two meters.

The conglomerate facies of the studied section composed of mostly from the volcanic rock fragments. the percentage of the volcanic grains generally constitutes more than 50% in composition except the uppermost conglomerate of the section. Also, the matrix is generates more than 15% of all conglomerates (Figure 16).
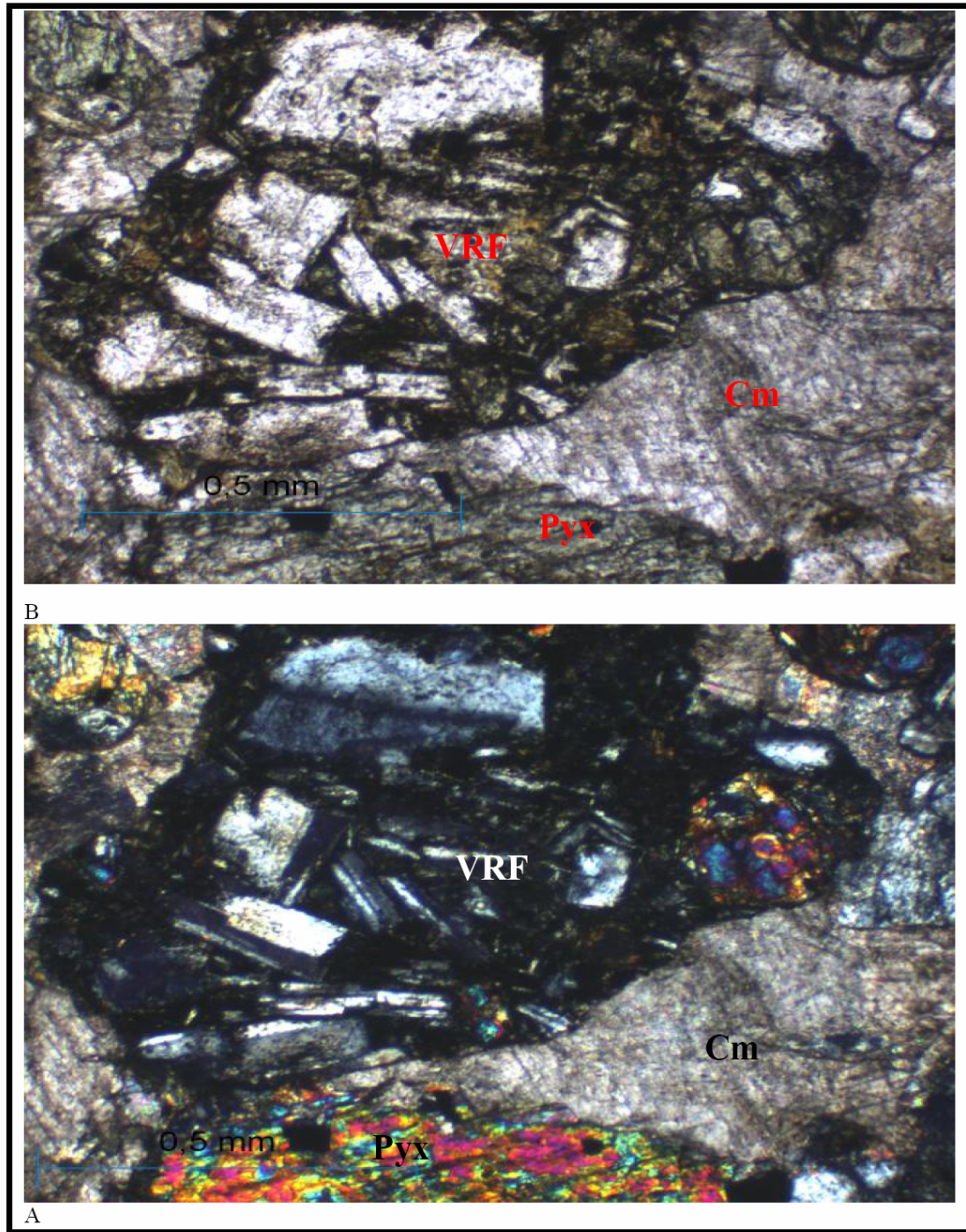
Figure 16: Thin section photograph of conglomerate. VRF: Volcanic rock fragment, Cm: calcite cement, Pyx: pyroxene. A. crossed nicols, B. plane polarized light. Scale 0.5 mm.

The conglomeratic facies in the studied section is classified under the extraformational paraconglomerates (Pettijohn, 1972) (Figure 17). The disorganized and non-laminated characteristics of these conglomerates and the vertical facies associations indicate deposition by mass movement hence the conglomerates of the studied section are named as tilloids (Pettijohn, 1972).
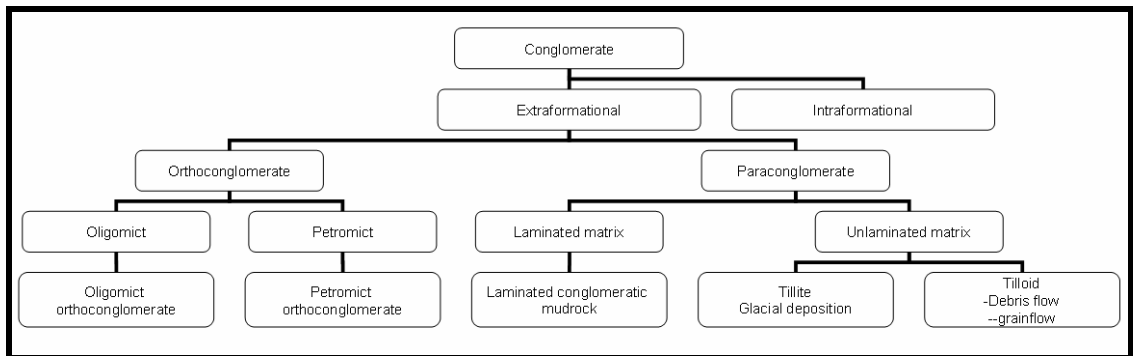
Figure 17: Flow chart of classification of conglomerates (Pettijohn, 1972).

3.1.3 Calcareous Mudstone/Marl Facies

Marls (Figure 18), (Figure 19) and calcareous mudstones (Figure 20) are alternating with limestones along the studied section. They comprise the background sedimentation with the limestones. They are deposited in quiet deep water conditions with low terrigeneous sediment influx. Mudstones observed at the bottom of the section are red colored indicating well oxygenated conditions. In contrast, mudstones observed in the middle and at the top of succession are greyish to purplish colored indicating relatively high amount of organic carbon and more oxygenated conditions.
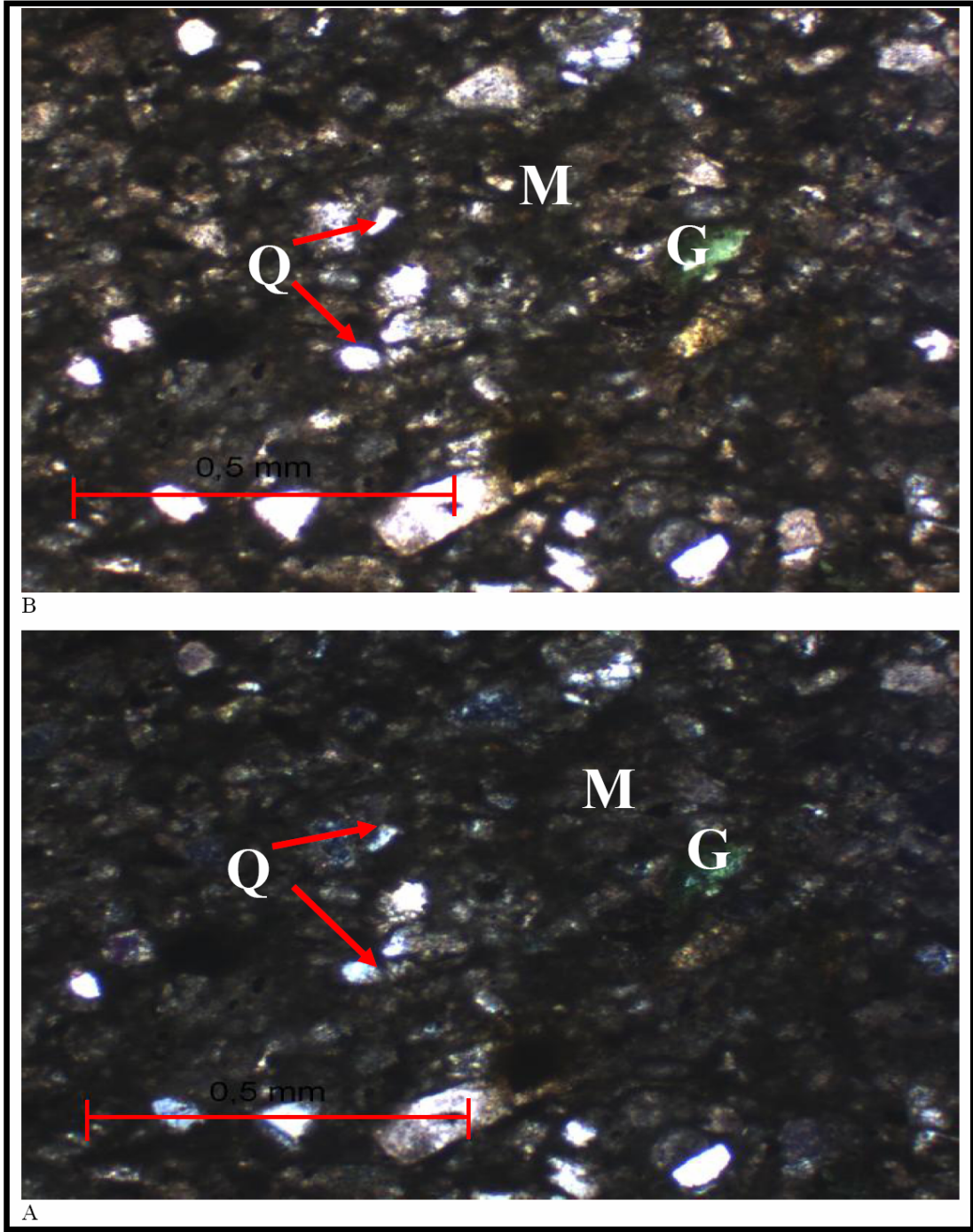
Figure 18: Thin section photograph of marl. M: carbonaceous matrix, Q: quartz, G: glauconite (green colored mineral). A. crossed polars, B. plane polarized light. Scale 0.5 mm.

Figure 19: Field photograph of purplish colored marl.

Carbonaceous mudstones and marls generally show faint lamination and bioturbation. They contain silt sized material. Feldspar constitution of the mudstones may reach up to 15% (Appendix). Pyroxene, amphibole and glauconite are found as accessory minerals (Appendix). Also they contain small amount of rock volcanic rock fragments (Appendix). These sedimentary structures and constituents indicate that carbonaceous mudstone and marl facies were deposited in quiet conditions and silt sized sediments were derived from a volcanic source.
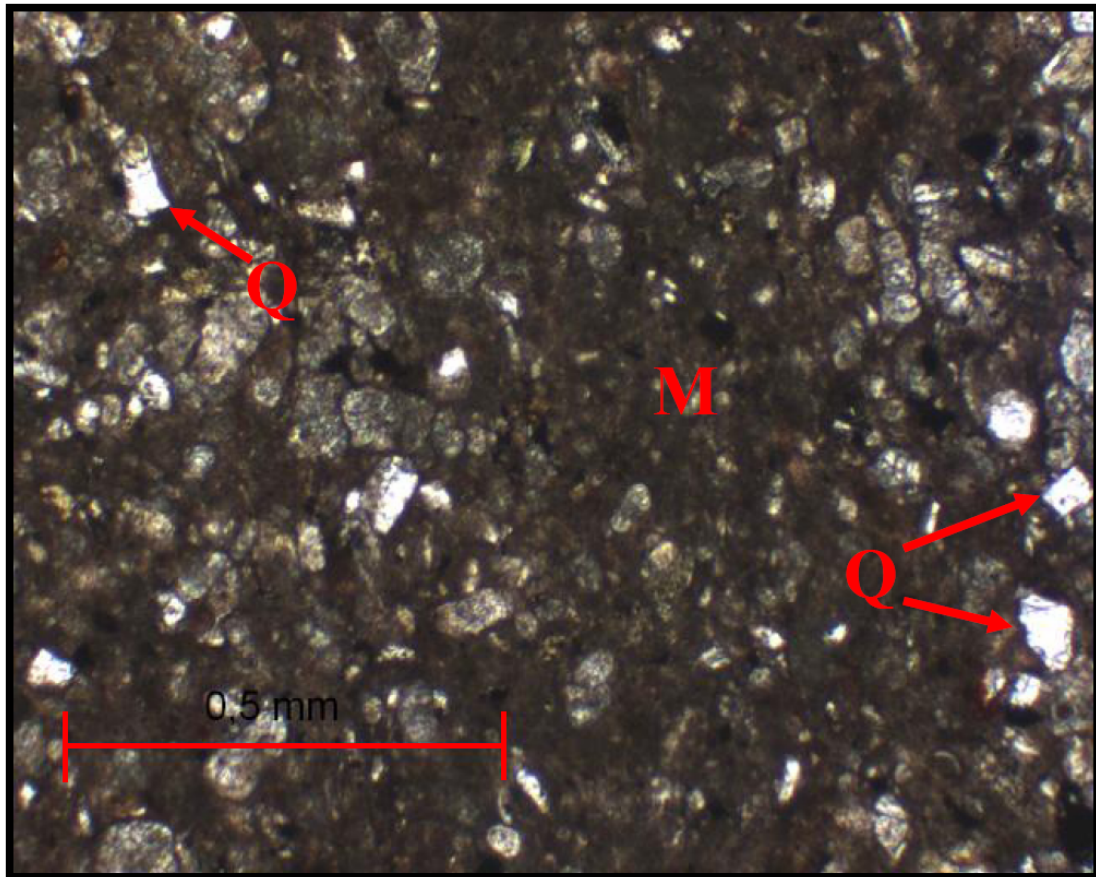
Figure 20: Thin section photograph of mudstone Q: Quartz, M: Matrix. Plane polarized light. Scale 0.5 mm.

Marls are calcium carbonate or lime-rich mud or mudstones which contain variable amounts of clays and calcite or aragonite. The lower stratigraphic units of the chalk cliffs of Dover consist of a sequence of glauconitic marl followed by rhythmically-banded limestone and marl layers (Schurrenberger, 2003). Similar Upper Cretaceous cyclic sequences in Germany have been correlated with Milankovitch orbital forcing.

3.1.4 Siltstone Facies

Hardened sedimentary rock that is composed primarily of angular silt-sized particles and that is not laminated or easily split into thin layers. Siltstones, which are hard and

durable, occur in thin layers rarely thick enough to be classified as formations. They are intermediate between sandstones and shales but are not as common as either. Siltstone facies constitutes only a small part of the succession. Indeed they appear only at the bottom of the succession just after the middle Albian. This facies is characterized by light grey to greenish colors, presence of planktonic foraminifera and sand sized grains (Figure 21).
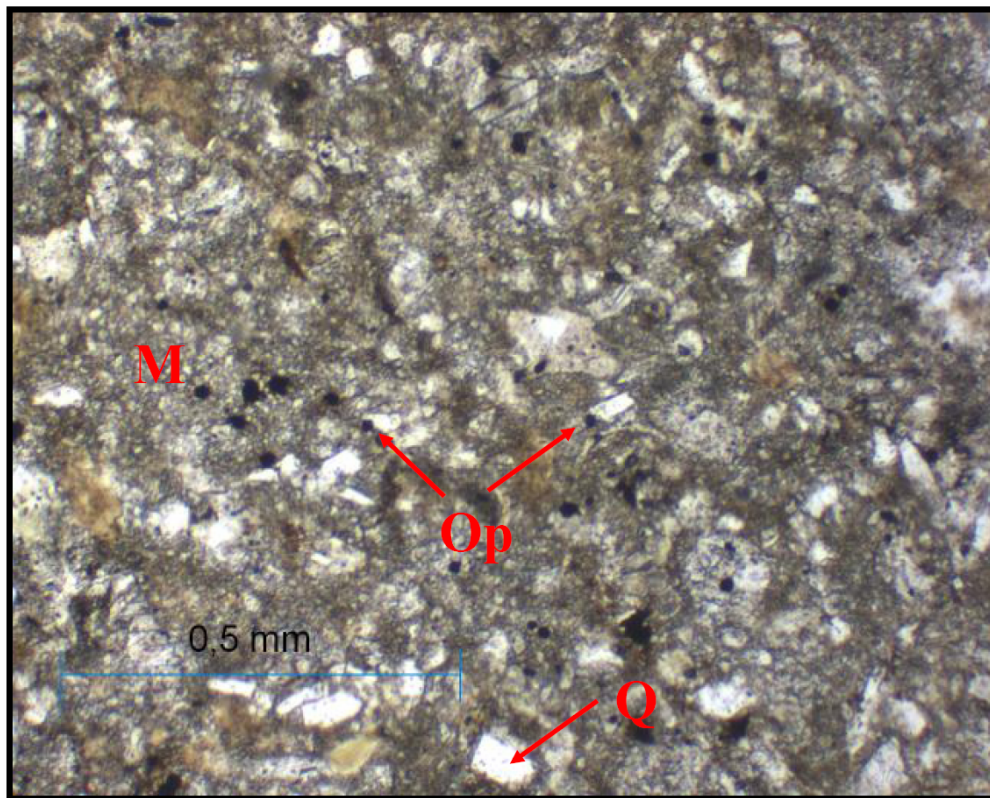
Figure 21: Thin section photograph of siltstone (syh.14) M: Matrix, Op: opaque, Q: quartz. Plane polarized light. Scale 0.5 mm.

Also, thin section analysis and point-counting (Appendix A) results show that presence of amphibole, and volcanic rock fragments, and glauconite, although their percentages in the rock are very low, they indicate that sediments are derived from a volcanic source.

3.1.5 Shale Facies

Shales are observed at the bottom and at the top of the section with sandstones and limestones. They contain calcite grains, small amount of silt sized terrigeneous material (figure 22) and fossil fragments (plant fossils). They are finely laminated and separated into 0.5-1 cm thick flakes (figure 23). Shales are defined as fissile mudrocks and differentiated from mudrocks in the field on the basis of fissility and color. Shales are classified on the basis of color. In the studied section, shales are dark grey and black colored. Black shales are of particular interest, because they are both precise environmental and depositional indicators. The depositional environments, conditions and other black shale occurrences during the Cretaceous will be discussed in section 2.3 (Black shales and OAEs).
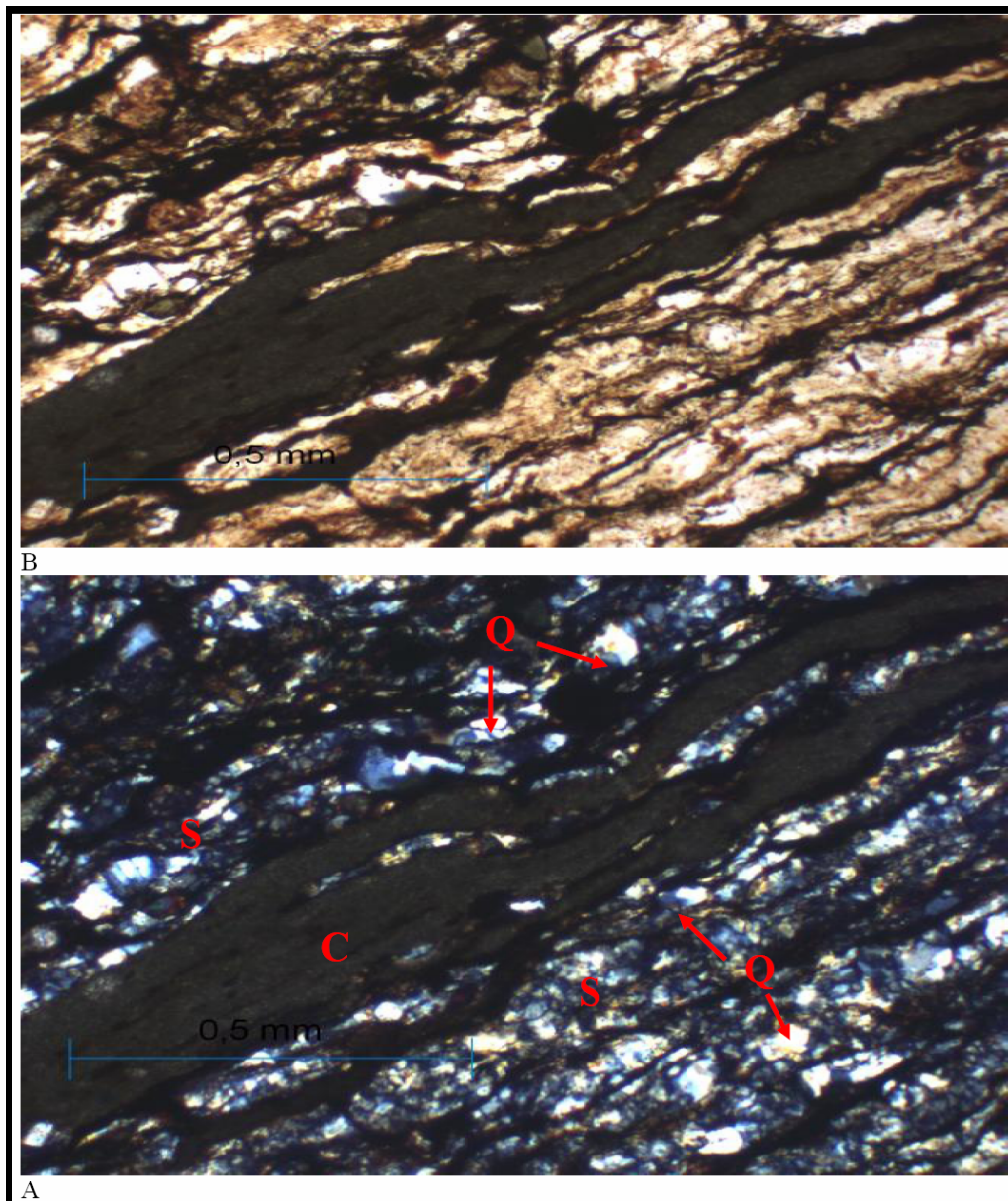
Figure 22: Thin section view of the silicified black shale. Q: quartz, C: carbon rich layer, S: silicified layer. A crossed nicols, B plane polarized light. Scale 0,5 mm.

Figure 23: Black shale separating into 0.5 -1 cm thick flakes. Sample number syh 20.

3.1.6 Limestone Facies

Two main types of limestone facies are recognized in the studied section; pure limestones and carbonate rocks with siliciclastics. Pure limestones are classified in accordance with Dunham's classification chart (1962) (Figure 24). Limestones deposited between the upper to middle Albian and upper Cenomanian to Turonian are dark grey, light grey, beige and brown colored. In contrast, at the top of the section Santonian limestones are red colored. Red color is generally indicative of iron oxidization whereas grey colors indicate high organic carbon preservation.

Allochthonous limestone original components not organically bound during deposition						Autochthonous limestone original components organically bound during deposition		
Less than 10% >2 mm components				Greater than 10% >2 mm components		Boundstone		
Contains lime mud (<0.02 mm)			No lime mud	Matrix supported	>2 mm component supported	By organisms which act as barriers	By organisms which encrust and bind	By organisms which build a rigid framework
Mud supported		Grain supported						
Less than 10% grains (>0.02 mm to <2 mm)	Greater than 10% grains							
Mudstone	Wackestone	Packstone	Grainstone	Floatstone	Rudstone	Bafflestone	Bindstone	Framestone

Figure 24: Classification of limestones after Dunham (1962) modified by Embry and Klovan (1971).

Pure limestones found at the bottom and top of the section intercalated with sandstones and mudstones. Although, they are called pure limestones, they still contain siliciclastic material, however the amount of these siliciclastic material are very low and are neglected. Micrite is appeared as a common matrix for pure limestones. Nearly all of the limestones are matrix dominated with only one or two exceptions. Wackestone, biogenic packstone are observed as types of pure limestones.

Wackestones appeared at the top, middle and bottom of the succession and contain sphericalcites, planktonic foraminifera and fewer amounts of siliciclastics. Highest amount of siliciclastics are observed in the middle of the succession, the wackestones at the top and bottom of the section contains relatively less siliciclastics (Figure 25).

40

Only one biogenic packstone (Figure 26) is recognized in the studied section, it contains closely packed shell fragments within the sandy matrix (Figure 27). Biogenic packstone of the Üzümlü Formation overlies the wackestones of the Soğukçam Limestone.
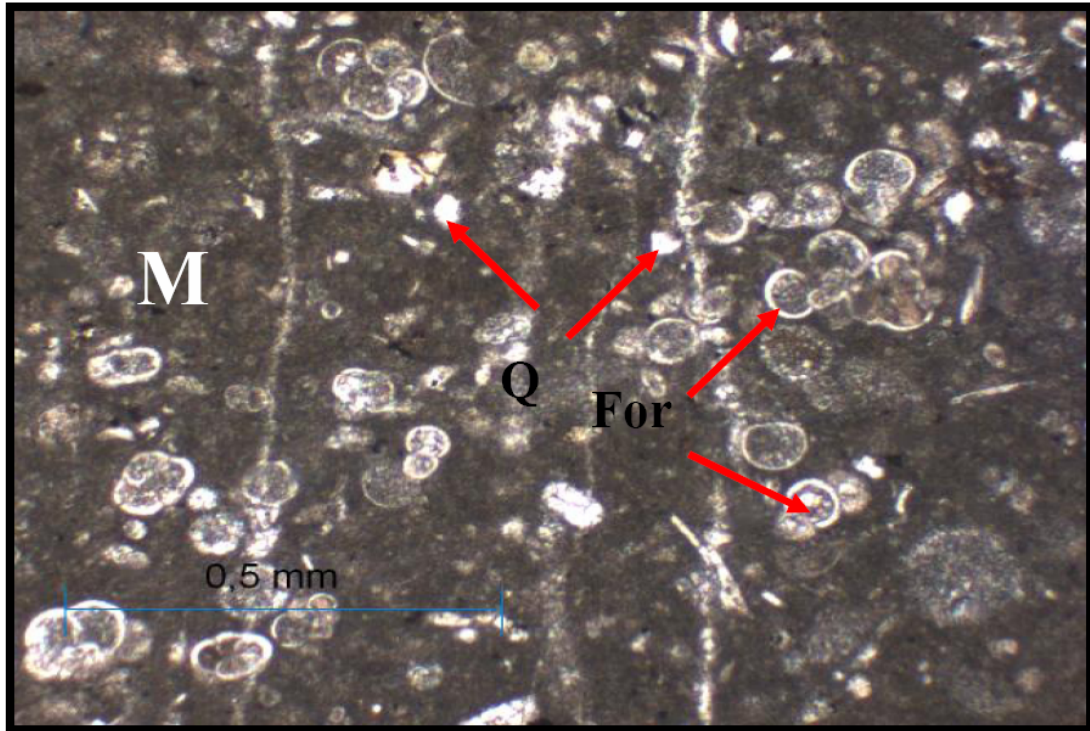
Figure 25: Thin section view of wackestone with little amount of quartz grains. Q: quartz, M matrix, For: foraminifera. Scale 0.5 mm.

Figure 26: Field photograph of biogenic packstone.
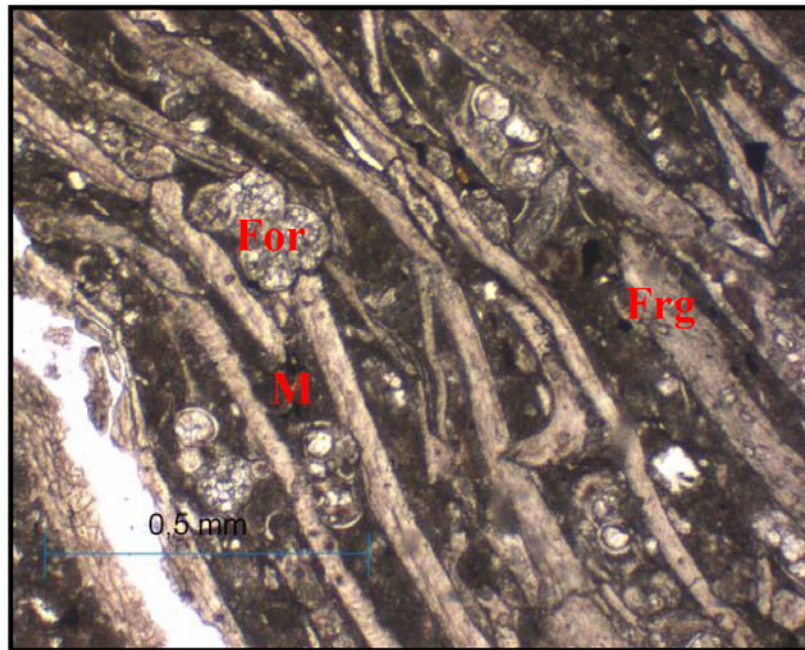
Figure 27: Thin section photograph of biogenic packstone composed of shell fragments M: sandy matrix, For: foraminifera, Frg: shell fragments. Plane polarized light. Scale 0.5 mm.

Impure limestones (Figure 28, 29) which are influenced by considerable amounts of terrigeneous material dominate the section intercalated with marls and with carbonaceous mudstones and alternating with the black shales at the bottom of the section (Figure 30). Volcanic rock fragments observed as well as limestone fragments, amphibole, pyroxene and glauconite found as accessory minerals which proves volcanic activity near the depositional environment.

Figure 28: Field photograph of impure limestone (a: grey shale, b: limestone, c: limestone, d: black shale, e: limestone, f: siltstone, g: grey shale, h: limestone, i: conglomerate).
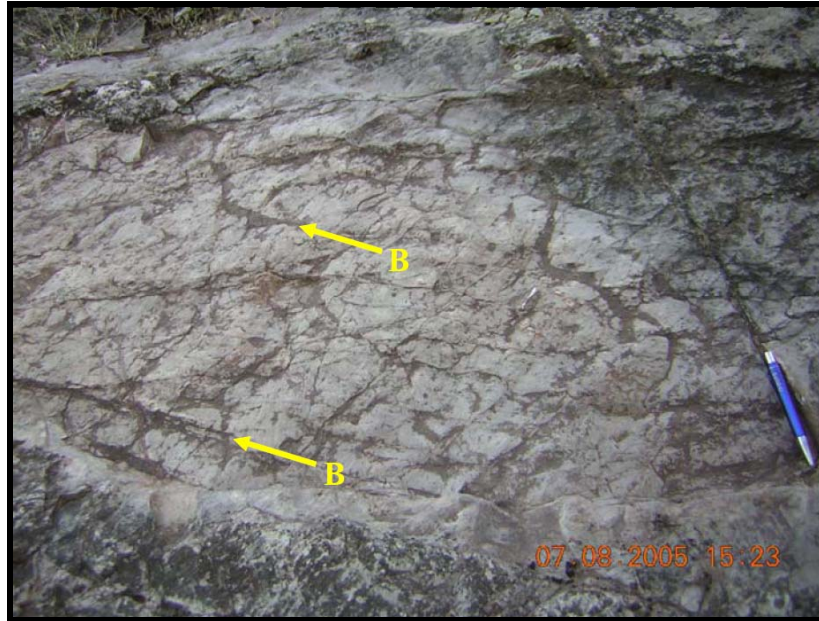
Figure 29: Bioturbated (B) Limestone.
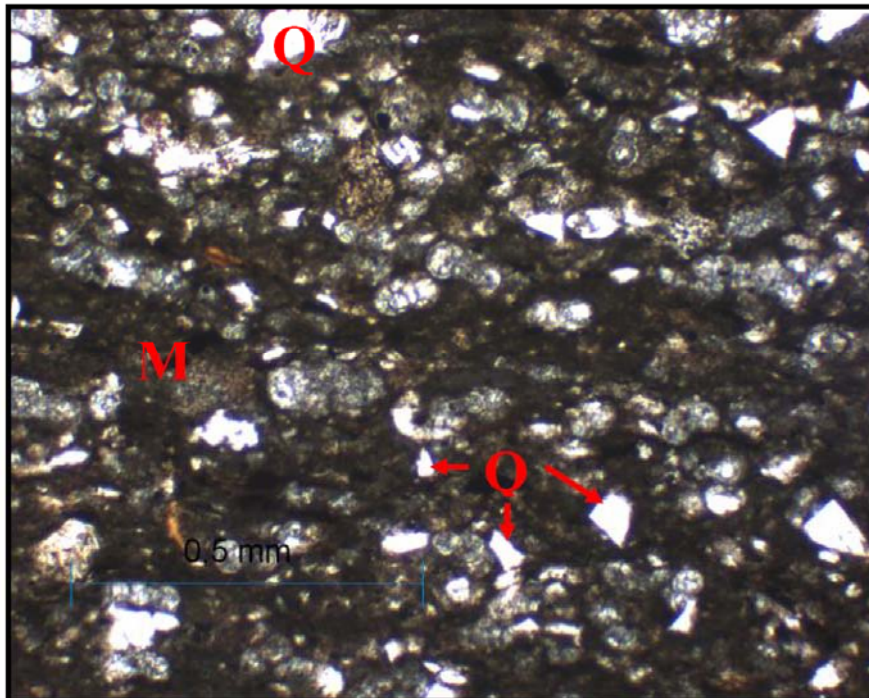
Figure 30: Thin section photograph of silty limestone. Q: quartz, M: Matrix. Plane polarized light. Scale 0.5 mm.

3.2 Depositional Environment

A depositional environment is a portion of the earth's surface characterized by a unique combination of physical, chemical, and biological processes. These processes (table 1) control how sediment is transported and deposited, what chemical modification it undergoes, and what kind of organisms live in and affect the sediment (Fichter 2000). The processes result in the characteristic and distinctive sedimentary deposits typical of each environment (table 2) by which we recognize and identify them.

Table 1: Classification of environments by depositional processes (Fichter 2000).

Classification of Environments by Depositional Processes		
Terrestrial	**Transitional**	**Marine**
Alluvial Fan	Delta Complex	Shelf (storm and tidal dominated)
Braided River	Beach	Submarine fan
Meandering River	Lagoon	Basin
(including alluvial plain)	Tidal Flat	
Lake	Dunes	
	Carbonate	
	Tidal Flat	Carbonate Barrier (reef)
	Lagoon	Shelf
		Basin

Table 2: Classification of marine environment and their related rock types, textures and sedimentary structures (Fichter 2000).

	REEF	CONTINENTAL SHELF	CONTINENTAL SLOPE AND RISE	ABYSSAL PLAIN
Rock Type	Fossiliferous limestone	Sandstone, shale, siltstone, fossiliferous limestone, oolitic limestone	Litharenite, siltstone, and shale (or limestone)	Shale, chert, micrite, chalk, diatomite
Composition	Carbonate	Terrigenous or carbonate	Terrigenous or carbonate	Terrigenous or carbonate
Color	Grey to white	Grey to brown	Grey, green, brown	Black, white red
Grain Size	Variable, frameworks, few to no grains	Clay to sand	Clay to sand	Clay
Grain Shape	---	---	---	---
Sorting	---	Poor to good	Poor	Good
Inorganic Sedimentary Structures	---	Lamination, cross-bedding	Graded bedding, cross-bedding, lamination, flute marks, tool marks (turbidites)	Lamination
Organic or Biogenic Sedimentary Structures	---	Trails, burrows	Trails, burrows	Trails, burrows
Fossils	Corals, marine shells	Marine shells	Marine shells, rare plant fragments	Marine shells (mostly microscopic)

The studied section starts with late Aptian wackestone facies of Soğukçam Limestone. These beds are overlain by dark-light grey calcareous graded, poorly sorted thinly laminated turbiditic sandstone beds. These beds are overlain by a cyclic succession of silty, clayey/pebbly limestones and black-grey colored silty black shales of pelagic origin which is also called a redox cycle (figure 31). These black-grey colored silty black shales include plant particles which were derived from the flooded vegetated lands during relatively high sea levels (Einsele and Ricken, 1991). Redox cycles composed of light colored carbonate beds and dark colored, organic-rich interbeds (Einsele 2000). The redox cycles may be restricted to the deepest sub-basins, or they can pinch out laterally in a basin of little changing water depth (Einsele 2000). The redox cycles commonly indicate repeated transitions from aerobic to anaerobic conditions because of water mass mixing and turnover (Einsele 2000). This cycle is episodically disturbed by siltstones, planar laminated sandstones, graded sandstones and conglomerate which are interpreted as sand turbidities. Turbidities are characterized simple grading without complications of floating granules and floating clasts (Shanmugam 2002). Investigation of the organic carbon in the various Cretaceous bituminous levels cored from the oceans suggests significant differences in the nature of the two major OAE's. Black shales cored from the Atlantic, for example, reveal a significant terrestrial component in the organic material from Aptian-Albian levels whereas that of Cenomanian-Turonian age is more richly planktonic (Arthur 1979; Arthur & Natland 1979). Schlanger & Jenkyns (1976) proposed that these two OAE's correlated with times of equable climate and with transgressive pulses.
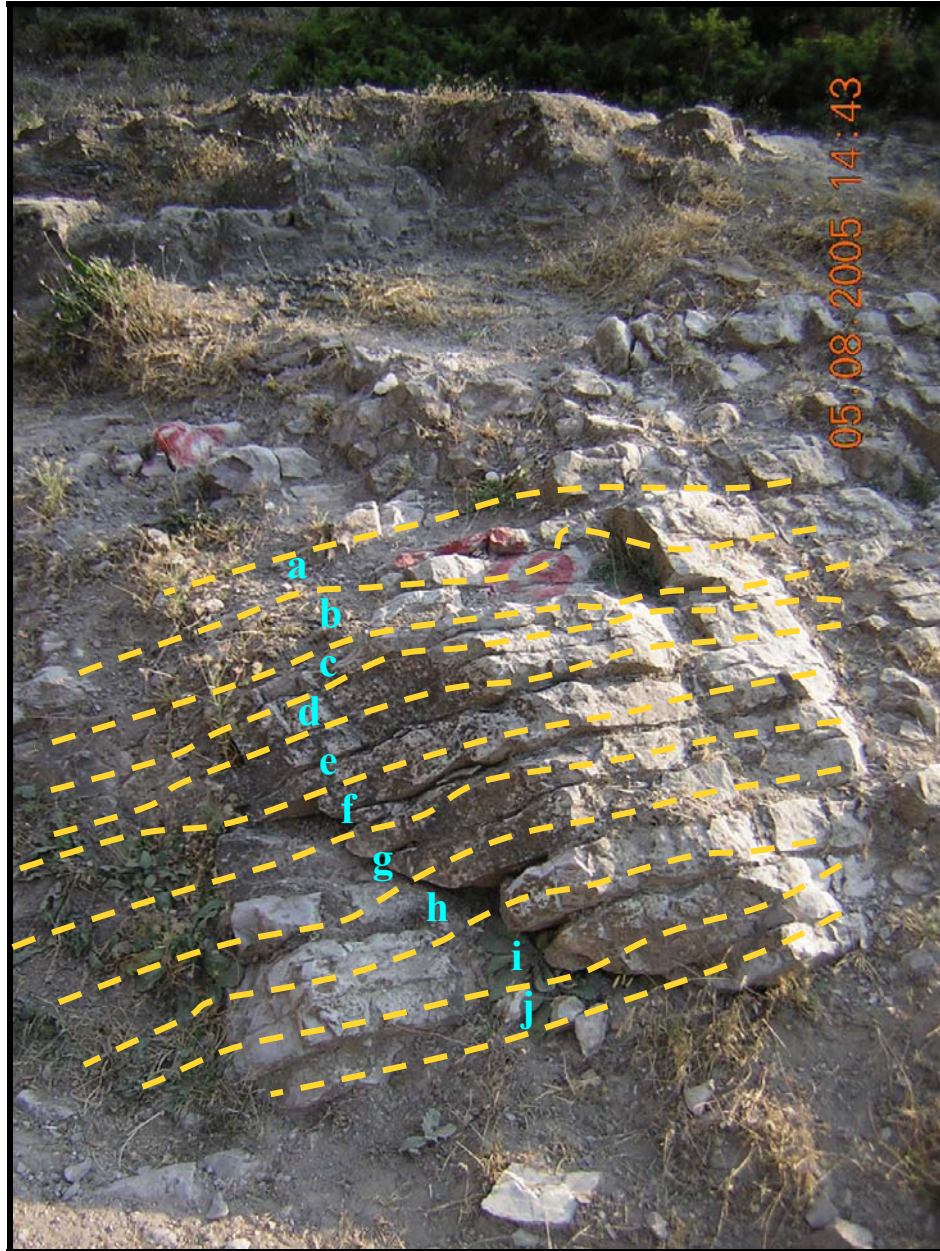
Figure 31: Redox cycle (a: grey shale, b: limestone, c: limestone, d: black shale e: limestone, f: siltstone, g: grey shale, h: limestone, i: conglomerate, j: sandstone)

After the middle Albian the turbiditic disturbance is relatively decreased and limestone/black shale cycle changes into thick marl (calcareous mudstone) and thin

limestone cycle which indicates relatively more oxygenated basin. The reddish color of marls is another evidence for the oxygenated conditions. This part of the section is also deposited in the deep sea. The generation of limestone-marl couplets requires a carbonate production rate three or four times higher than the terrigeneous silt and clay input (Einsele and Ricken 1991). This alternation is interrupted by an alternation of dark grey to brown colored sandstone beds and green to grey colored conglomerates which is another turbiditic event but the unusual thickness of this cycle is questionable. It may be either a turbiditic deposit or it is a sequence boundary which is formed due to an abrupt fall in sea level.

This alternation ends up with silty-sandy limestone. This limestone is capped by thick dark-grey to brown colored sandstone and thin green to grey colored conglomerate alternation. Increase in the grain size of the sediments indicates shallowing of the sea level.

The sandstone-conglomerate alternation is overlain by limestone/marl and limestone/carbonaceous mud alternations which are also interrupted by sandy turbidities. During the late Cenomanian the limestone/marl alternation changes into limestone/carbonaceous mudstone alternation and the studied section ends up with red sandy limestone lithofacies dated as late Santonian.

The studied section can be summarized to a limestone/marl (carbonaceous mudstone) alternation (Figures 6 and 7) deposited in the marginal sea and this deposition is episodically disturbed by turbidity currents. In other words, depositional environment of the studied section is deep sea at the toe of the continental slope. The medium-coarse grain size of the turbiditic deposits indicates a proximate slope location.

3.3 Black Shales and OAEs

In the measured section, black shale levels are observed close to the top and at the bottom of the sequence. Although, a detailed study of these black shale levels was not carried out associated dark grey and grey colored facies indicate anoxic conditions. Therefore, possible equivalencies of these black shale levels and correlation to Cretaceous anoxic events are investigated. Organic carbon–rich black shales are found extensively in different Cretaceous marine settings. Although globally distributed, the black shales are restricted to specific intervals during the Aptian–Santonian ages (Arthur et al., 1990). The mid-Cretaceous is characterized by a coincidence of intensified volcanism, increased oceanic crust production, elevated sea level, and high paleo-temperatures that peaked in the early Turonian (Larson, 1991a, b).

Black shales accumulated in oxygen-poor to anoxic environments (Pettijohn, 1949; Berry and Wilde, 1978). The concept of global oceanic anoxic events (OAEs) (Schlanger and Jenkyns, 1976) was proposed to explain times of enhanced organic carbon burial associated with the genesis of widespread marine black shales.

There are two widely accepted theories which lead to the OAEs and hence the deposition of black shales.

1-   The preservation model: Density stratification of the water masses causes decreased ventilation on the ocean floor independent of organic productivity and following enhanced carbon preservation due to limited oxygen supply (Galeotti et al., 2003).

2-   The productivity model: It is based on increase in primary organic matter productivity, related to transgressions, overwhelming oxic remineralization of organic matter as a cause for the development of

dysaerobic/anoxic environments on the sea floor (Schlanger and Jenkyns, 1976; Jenkyns, 1980).

Anoxic conditions may be caused by combination of both processes (Arthur and Schlanger, 1979). Major Cretaceous anoxic events are shown in table 3.

Table 3: Major oceanic anoxic events and related time spans in Cretaceous (Erbacher and Thurow, 1997).

OAE1	OAE1a	Early Aptian (120 million years ago)	
	OAE1b	Aptian/Albian boundary (113 to 109 million years ago)	Selli Level
	OAE1c	middle-late Albian (103 million years ago)	Amedeus level
	OAE1d	latest Albian (99 million years ago)	Breistroffer Level
OAE2	Cenomanian/Turonian (93-91 million years ago)		Bonarelli Level
OAE3	Coniacian-Santonian (89 to 84 million years ago)		

In the studied section organic-rich black shales appeared immediately after the middle to late Albian interval and in the late Cenomanian to Turonian interval. There are three different occurrences of black shales in the studied section. Two of them are observed at the bottom of the studied section just after the middle to late Albian interval (samples syh 16 and syh 20). The bed thickness of syh 16 is 24 cm and thickness of syh 20 is 16 cm. Sample syh 16 is composed of alternations of silicified and

carbonaceous laminae (figure 22); due to siliceous laminae quartz content of the sample is high (%50 in composition, appendix A). Sample syh 20 has shiny black surface and fissile. Because of the high fissility of the sample syh 20, thin section can not be prepared. Therefore point-counting of the sample did not carry out. One of them is observed in the late Cenomanian to Turonian interval (sample syh 117). It overlies the purplish colored mudstones and overlain by red colored silty limestones (figure 32). It contains considerable amounts of quartz and feldspar, and glauconite found as accessory mineral (Appendix A).

Figure 32: Field photograph of the syh 117. A: limestone, B: black shale, C: mudstone

Although, necessary analyses for determining OAEs (e.g. geochemical, isotope, ecological) was not performed, biozones and age intervals of the black shales in the studied section show similarities with the occurrences of OAE1d and OAE2 examples from the world. Therefore, the black shales of the studied section are interpreted as equivalencies of OAE1d (Breistroffer Level) and OAE2 (Bonarelli Level). The examples of these two levels from the world are given below.

Latest Albian OAE1d, is named the "Breistroffer interval" in south-eastern France and was recently recognized as another interval of Corg burial for the Cretaceous in Tethyan Atlantic regions and suggested as marked by a collapse of water-column stratification due to intensifies water mixing and reduced summer stratification. Erbacher et al. (1996); Gale et al. (1996) suggest the globally significant organic-carbon burial. Biological records indicate that this OAE event damaged planktonic foraminiferal and radiolarian populations, as well as the carbonate platforms (Erbacher et al., 1996). Albian oceanic anoxic events are also recorded in the southern Italy (Luciani et al., 2006) and Hokkaido (Japan) (Takashima et al., 2004).

Pueblo, Colorado; Oceanic Anoxic Event 2 (OAE 2), that marks the lower part of the Bridge Creek Limestone Member. The lithology consists of rhythmically bedded 10- to 20-cm-thick bioturbated micritic limestones alternating with 10- to 60-cm-thick organic rich dark shales (Kellera G. et al., 2004). Tarfaya (Morocco) and Senegal Basins, North-West Africa: three facies characterise the lateral variations of the C–T sediments. The first consists of homogenous black shales deposited in the fully marine environment. This facies dominates the western part of the Thies-Diam Niadio area and reaches maximum thickness in Casamance. The second facies is characterised by a succession of calcareous and shaly calcareous sediments typical of a transitional neritic environment. The third facies, typical of a sub-littoral to nearshore marine environment, is composed of shales with shaly siltstone intercalations (Nzoussi-Mbassania P. et al., 2005). Hokkaido, Japan OAE2 horizon has been well documented, and is placed in the middle part of the Saku Formation. Lithology consists of finely

laminated, pyrite-rich, dark grey greyish black mudstones, (Takashima R. et al., 2004). Guerrero-Morelos Platform, Huitziltepec area, Guerrero State, southern Mexico; facies successions in three stratigraphic sections (Barranca del Tigre, Axaxacoalco, and Zotoltitlan, Guerrero State, southern Mexico) that comprise middle Cenomanian to lower Turonian rocks of the central part of the Guerrero-Morelos Platform, indicate the drowning of some parts of the platform near the Cenomanian – Turonian boundary. Dark-grey and black laminated pelagic limestones and marls, (Hernandez-Romano U. et al., 1997). Calabianca–Guidaloca composite section, northwestern Sicily, Italy black shale samples from the Calabianca–Guidaloca composite section contain very high TOC (up to 26%) and moderate to high amounts of CaCO3 (on average 20%) (Scopellitia G. Et al., 2004). Proto-North Atlantic; the Cenomanian/Turonian (C/T) intervals at DSDP Sites 105 and 603B from the northern part of the proto-North Atlantic show high amplitude. The more pronounced changes in TOC are also reflected by changes in lithology from green claystones (TOCb1%) to black claystones (TOCN1%). OM-rich (TOC 1–25%) black claystones (Kuypers M. M. M. et al., 2004). Outer Carpathian Basin, Subsilesian nappe, Poland. A global oceanic event (OAE2) has been identified on the basis of lithology and radiolarian stratigraphic data. This event is marked by a series of organic-rich (TOC up to 5%) non-calcareous shales, practically devoid of benthic microfossils, indicative of bottom water anoxia, (Bak K., 2005). Crimea, Ukraine; the sediments and organic-rich claystones with total organic carbon values up to 2.6 wt. %, representing Oceanic Anoxic Event 2 (Fisher J. K. et al., 2005). Oued Mellegue, north-western Tunisia; an expanded Cenomanian-Turonian section along Oued Mellegue in north-western Tunisia provides a high-resolution record of the latest Cenomanian Oceanic Anoxic Event in an upper bathyal, pelagic to hemipelagic environment. Base of the organic-rich Bahloul Formation, which represents the Cenomanian- Turonian Boundary Event (CTBE) in Tunisia. Bahloul Formation consists of 20 to 40 m of carbonaceous limestones and marls (Nederbragt A. J. and Fiorentino A., 1999). Roter Sattel, Romandes Prealps, Switzerland; black shales interval is interpreted as consisting of deposits related to

54

maximum flooding and condensation. TOC value reaches up to 6% (Strasser A. et al., 2001).

3.4 Petrographic Analysis

In this chapter, the counted minerals or rock fragments will be considered and the petrographic features and variations through the studied section will be discussed. Also, their changes in percentages in the rock composition along the measured section (in different lithofacies and similar lithofacies) will be investigated. In addition, mineralogical implications of the depositional environments and processes are evaluated. Percentages of counted minerals are shown in appendix A, percentage versus thickness graphs are shown in the appendix B.

Recognized minerals and rock forming clasts are: quartz, feldspar (orthoclase and plagioclase), rock fragments, matrix (calcite or clay), calcite grains, skeletal grains, pyroxene, amphibole, glauconite, biotite, muscovite and opaque minerals. Opaque minerals will not be mentioned because the required study for identification of them was not carried out.

Quartz is the one of the most important rock forming minerals for siliciclastic sedimentary rocks. Folk (1975) states that quartz forms 35-50% of terrigeneous fractures of sedimentary rocks. They are found in significant percentages in fine grained rocks as well as sandstones along the measured section. The quartz percentage of the rocks along the studied section is generally low yet it is found within all sediments. Percentage of quartz grains are rapidly increased during the turbiditic processes relative to the above and underlying background sediments. Except the conglomerate facies because as stated before these conglomerates are composed

mostly volcanic rock fragments and the quartz grains within these sediments were not counted separately.

Feldspars are also important terrigeneous components of siliciclastic sedimentary rocks. They make up 10-15% of terrigeneous fraction of sedimentary rocks (Folk, 1980). In the studied section, feldspar percentages reach up to 38%. They are generally in high percentages in turbiditic sandstone facies but the percentages of feldspars are also high in the background sediments especially in calcareous mudstones and marls. The presence of feldspar grains in both fine and coarse grained rocks indicates a volcanic source.

Rock fragments are generally found in coarse grained rocks of the measured section, on the contrary fine grained rocks contain few or no rock fragments. Not surprisingly they attain the highest percentages in conglomerate and sandstone facies. They are especially abundant in the middle of the studied section. In conglomerates they constitutes more than 50% of overall rock composition. Almost all lithic components in studied section are volcanic rock fragments with a few expectations in limestones where limestone clasts dominate. Metamorphic rock fragments are absent in all recognized lithofacies. Volcanic rock fragments are indicators of sediments which are derived from volcanic sources.

Matrix, from the textural point of view, described as the fine-grained background material that surrounds larger crystals, pebbles, or fossils in rock (Boggs, 1995). The studied section is composed of matrix supported sedimentary rocks. Matrix constitutes the major part of all siliciclastic and carbonaceous rocks in the measured section. Even the conglomerates are show matrix supported textures. Percentage values of matrix reach up to 85%. The matrix of the lithofacies in the studied section is calcareous, although some parts are clay. The dominance of the calcareous matrix is an evidence of deposition above the calcium compensation depth, the high amount of it proves that

depositional environment is above the lysocline too. High percentage values of matrix in the sandstones and conglomerates indicate that these rocks are products of turbiditic currents.

Glauconite is generally observed in the fine grained carbonaceous rocks of the measured section. Although, it is an accessory mineral its environmental implications are very important. It indicates deposition in quiet environments with low sediment influx. Glauconite is supposed to form under marine, mildly reducing to mildly oxidizing conditions and is abundant in modern offshore muds (Folk, 1980).

Pyroxene and amphibole are other important accessory minerals which are observed in the studied section. Amphibole is seen more frequently than the pyroxene. Both amphibole and pyroxene is mostly observed in sandstone and conglomerate turbiditic facies, and less frequently seen in fine grained background facies. Pyroxenes and amphiboles are less stable minerals and are less likely to survive during transportation. They are commonly first-cycle sediments that reflect the composition of proximate sources (Boggs, 1995).

Biotite and muscovite are very rarely observed in small amounts. They are usually seen in carbonaceous mudstones, marls and limestones. In conglomerates biotite is very rarely seen, in fact only one of the conglomerates contains biotites. Micas are derived from metamorphic source rocks as well as from some plutonic igneous rocks (Boggs, 1995).

Skeletal grains are only seen in limestones which are placed at the top and at the bottom of the studied section. They are mostly planktonic foraminifera and radiolarian shell fragments, the bivalve shell fragments are only seen in a skeletal packstone at the bottom of the section.

The petrographic features and variations through the studied section will be evaluated as the intervals of 0-5.54 m, 5.54-11.82 m, 11.82-17.64 m, 17.64-23.33 m, 23.33-29.94 m, 29.94-36.52 m, 36.52-40.55 m.

Between 0 and 5.54 m interval of the studied section (Figure 33), following statements can be interpreted: Quartz content throughout this interval is directly proportional to the grain content only with minor differences. However, a few exceptions are still observed such as syh-11 and syh-28. At these samples, although quartz content decreases rapidly, total grain content continues to decrease. Such increases are resulted by changes in rock fragment content. When glauconite content (Figure 34) is evaluated, a strong inverse proportion between quartz and glauconite contents is observed so that when siliciclastic content is high, no glauconite is observed. Hence, it can be stated that glauconite is a primary mineral.

Between 5.54 and 11.82 m interval, when we compare the quartz, matrix and total grain contents (Figure 35), the strong relationship between the variations of quartz grains and those of total grains continue and variations of total grains depend on quartz grains. However, as a major difference at this interval with respect to 0-5.54 m interval, these three contents of quartz, matrix and total grains remain relatively more stable and no sudden changes through the interval can be observed. That is because in this interval, the lithofacies are similar to each other. Quartz contents are relatively lower than those in previously discussed interval. When glauconite content is evaluated (Figure 36), it can be observed that glauconite is very scarce or even absent. However, at the top of the interval, glauconite increases suddenly and rapidly. This change is may be an indicator for a sequence boundary.

Between 11.82 and 17.64 m interval, when quartz-matrix-total grain contents (Figure 37) are evaluated, several statements can be interpreted: First, as similar to 0-5.54 m interval but different from the previous interval of 5.54-11.82, the variations through

these contents are high. Quartz content continues to decrease and reach up to a range of 0-20%. The strong relationship between the variations of quartz and total grain contents cannot be observed in this interval. The effect of quartz over total grain content ceases. In fact, the increase of rock fragment and feldspar content becomes more important to determine the total grain content. This is also suggested by the fact that the samples with inverse proportion between quartz and total grain content increases drastically. In other words, the fine grained facies are generally replaced by coarse grained facies. When glauconite content is evaluated (Figure 37), it can be stated that glauconite is absent through the studied interval except for the samples syh-52, syh-55, syh-57.

Between the interval of 17.64-23.33 m, when quartz, matrix and total grain contents (Figure 38), are evaluated, it can be stated that the direct proportional relationship between quartz and total grain content is observed. Quartz content starts to increase through the studied interval and its range is between 20 and 40%. This interval is also similar to the intervals 0-5.54 and 11.82-17.64 as there are relatively more vertical variations through the interval. Also, from the bottom of the interval to top of the interval, there is an increasing trend of quartz and total grain content. Another major difference in this interval is the abundance of glauconite content (Figure 39). At this interval, glauconite is very much higher relatively to the previous intervals of the studied sections (0-23.33 m). It is also highly variable within the interval. This is an indicator of fluctuations in sediment influx and energy level of the system.

Between 23.33-29.94 m interval, when quartz, matrix, and total grain contents are evaluated (Figure 40), it can be stated that the direct proportional relationship between quartz and total grain content still continues only with one exception at the sample syh-81. This difference is caused by the deposition of conglomerate. The variation for quartz and total grain contents is limited for the lower part of the studied interval. However, when the upper part of the interval is evaluated, also it can be observed that

these variations start to become more frequent and higher. When glauconite content of this interval (Figure 41) is studied, it can be concluded glauconite content in two different subinterval increases rapidly increase and forms two major peaks. These peaks are observed through the limestone facies as expected. However, glauconite is very low in marls.

Between 29.94-36.52 m interval of the studied section, when quartz, matrix and total grain contents are evaluated (Figure 42), it can be stated that the direct proportion between the quartz and total grain content still continues. Quartz content is relatively lower with respect to previous interval of 23.33-29.94 m. The whole interval seems to have more or less straight patterns for both quartz and total grain contents whereas there are slight local variations through this interval. When the glauconite contents of this interval is evaluated (Figure 43), it can be stated that glauconite content is relatively lower with respect to that of previous interval of 23.33-29.94 m, however, at this interval, sharp peaks of glauconite are replaced to the broaden peaks. That is because glauconite is observed more frequently at the samples of this interval with respect to previous interval.

Between 36.52-40.55 m interval of the studied section, when quartz, matrix and total grain contents are evaluated (Figure 44), following statements can be interpreted: The direct proportion between the quartz and total grain contents remains. However, quartz content is relatively low with respect to the previous interval. At the bottom of the interval, the quartz has a range of 20 to 30%, whereas it starts to fall up to the top of the interval and decreases to the levels with a range of 0 to 10%. This is a more or less linear decrease with slight variations. For the samples beginning from syh-112 to syh-117, the difference between quartz and total grain contents increases. This change is an indicator of the increase of other grains inside the sample. When the glauconite contents are evaluated (Figure 45), these statements can be interpreted: Glauconite levels are higher with respect to other intervals of the studied section. In fact, the

sample syh-117 has the highest peak for glauconite content. Glauconite is observed at more frequently through the samples collected from this interval, and they have sharp peaks. This interval can be determined to have relatively high variations of glauconite with respect to others with a range of 0-1.5%.
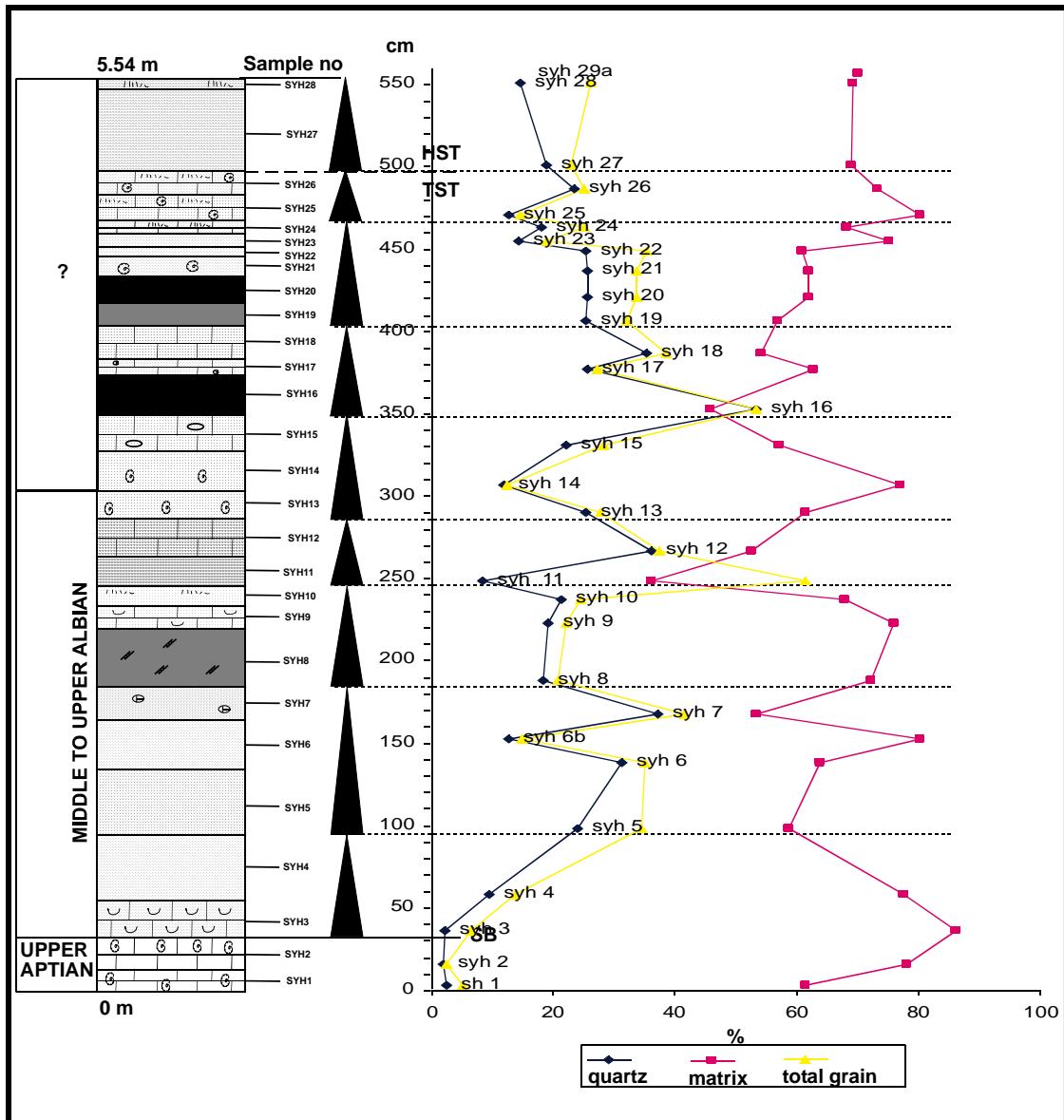
Figure 33: Quartz-Matrix-Total Grain Distribution Graphs (0-5.54 m)
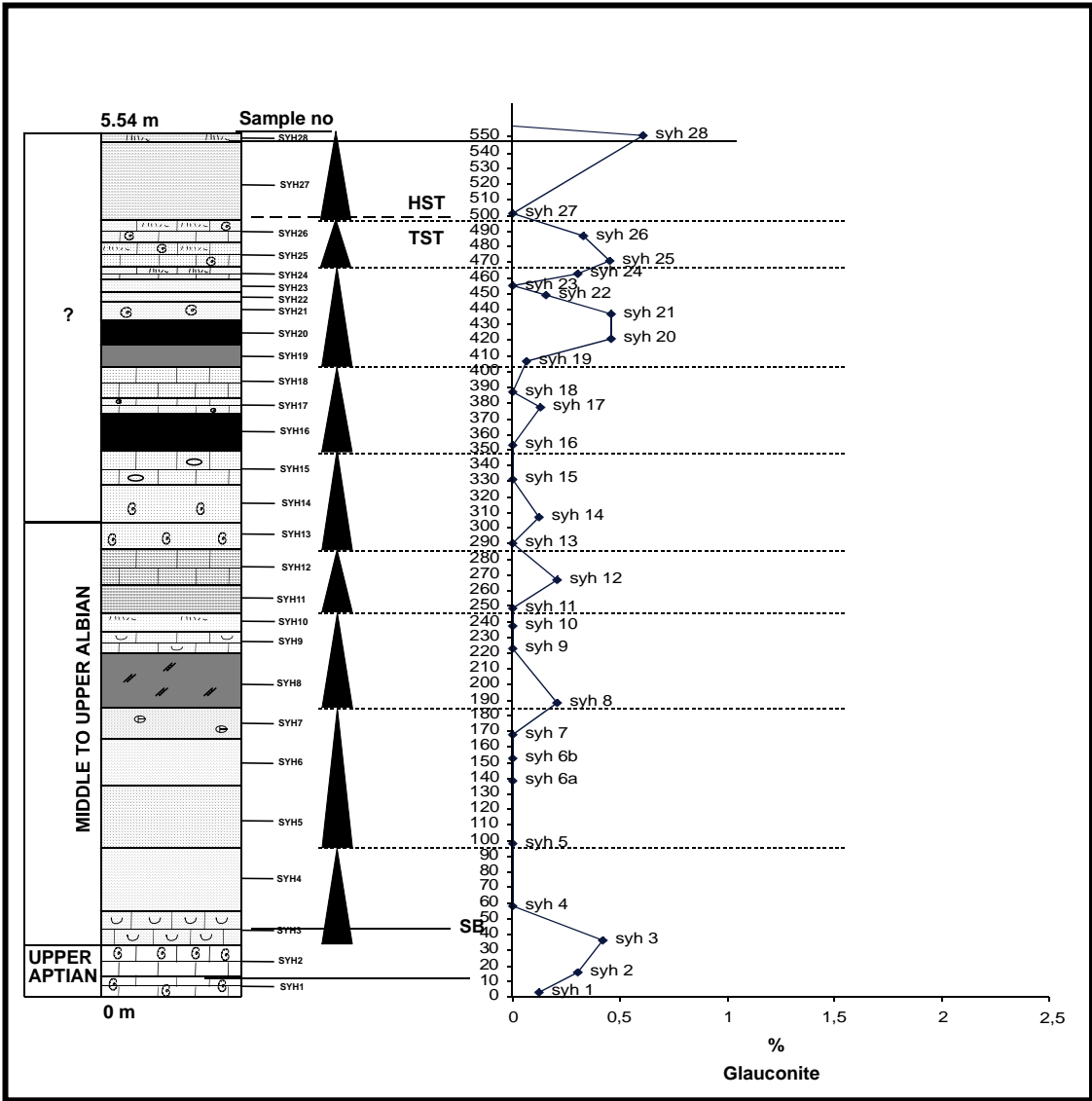
Figure 34: Glauconite Distribution Graphs (0-5.54 m)
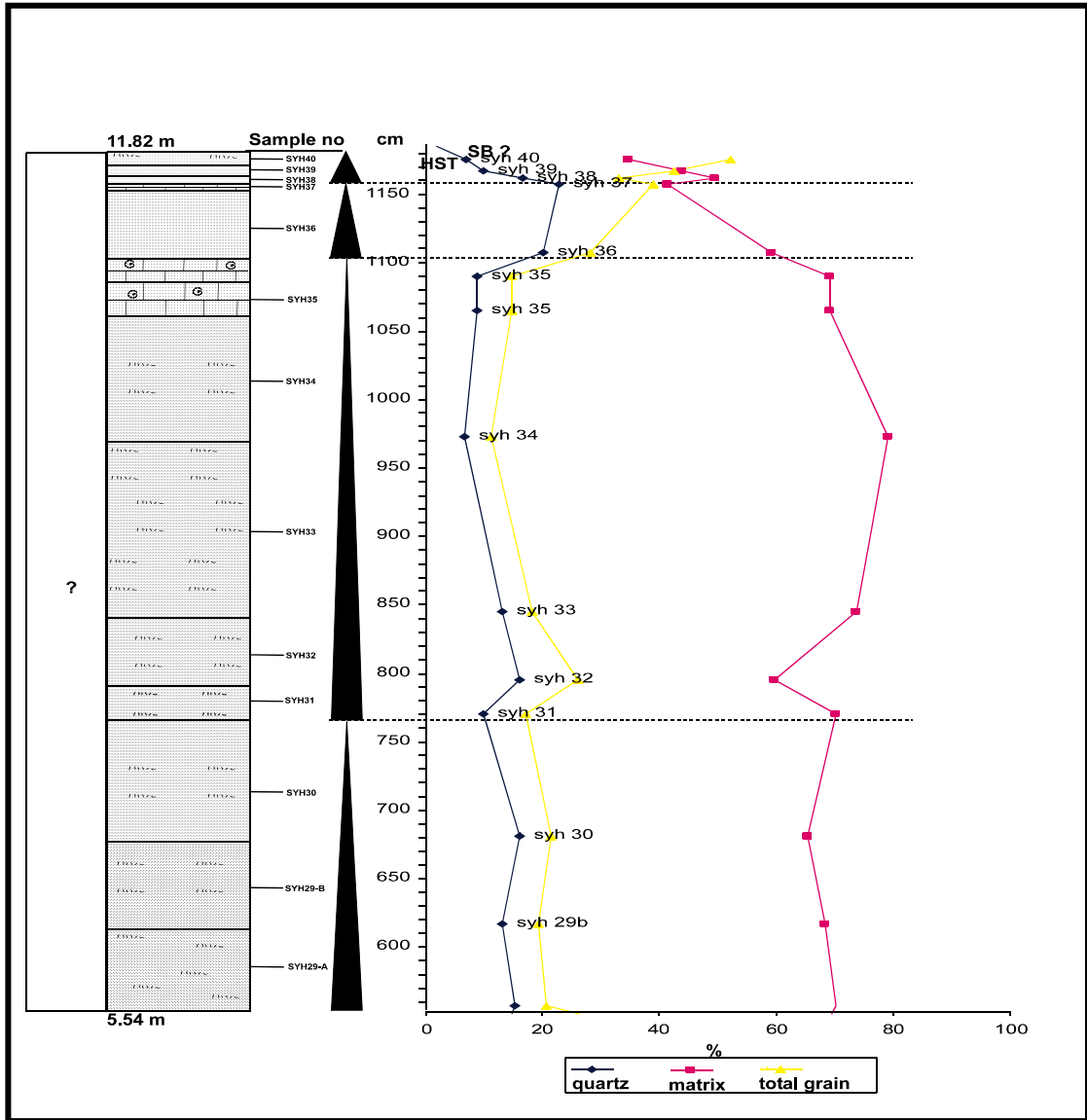
Figure 35: Quartz-Matrix-Total Grain Distribution Graphs (5.54-11.82 m)
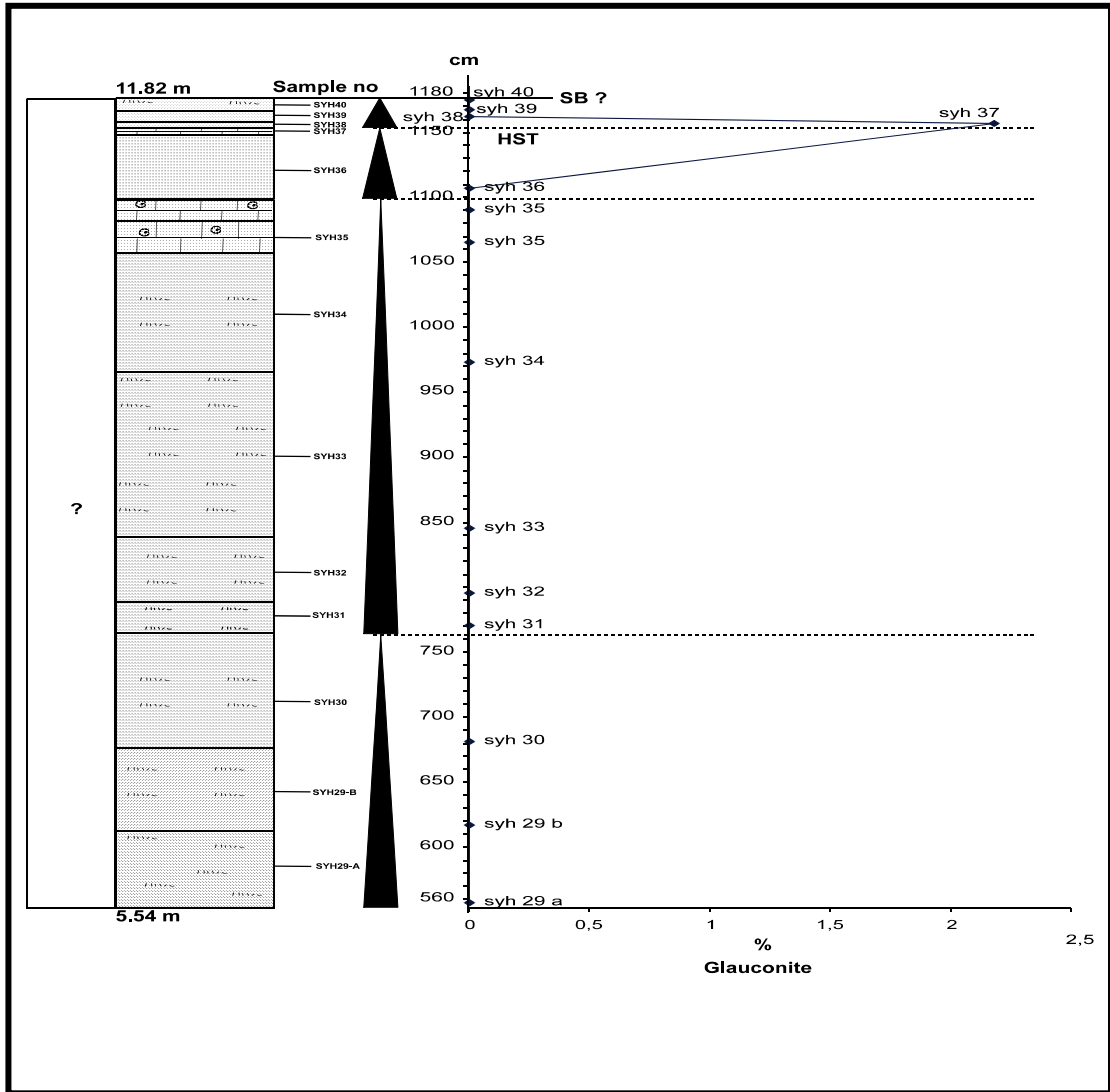
Figure 36: Glauconite Distribution Graphs (5.54-11.82 m)
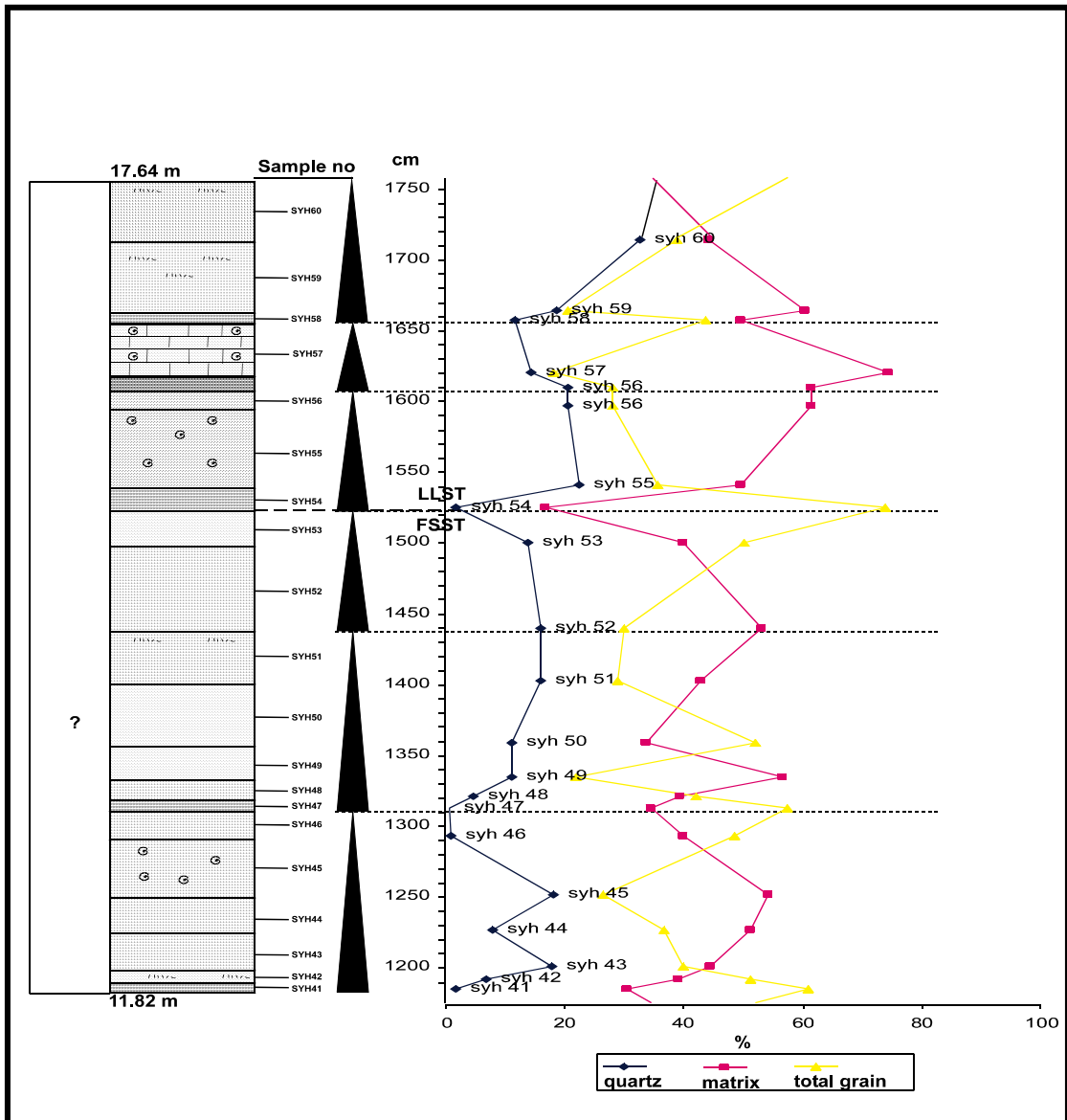
Figure 37: Quartz-Matrix-Total Grain Distribution Graphs (11.82-17.64 m)
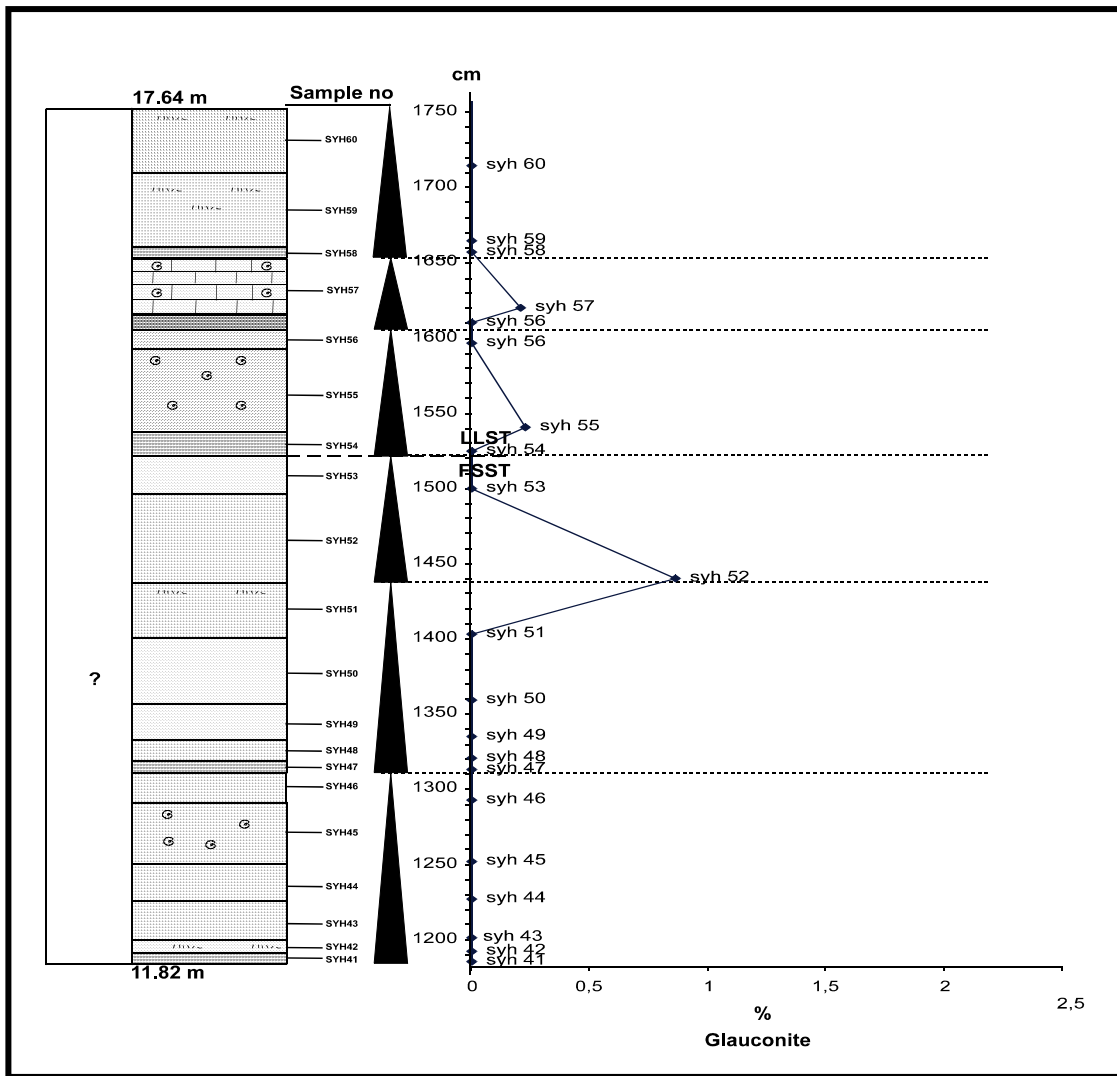
Figure 38: Glauconite Distribution Graphs (11.82-17.64 m)
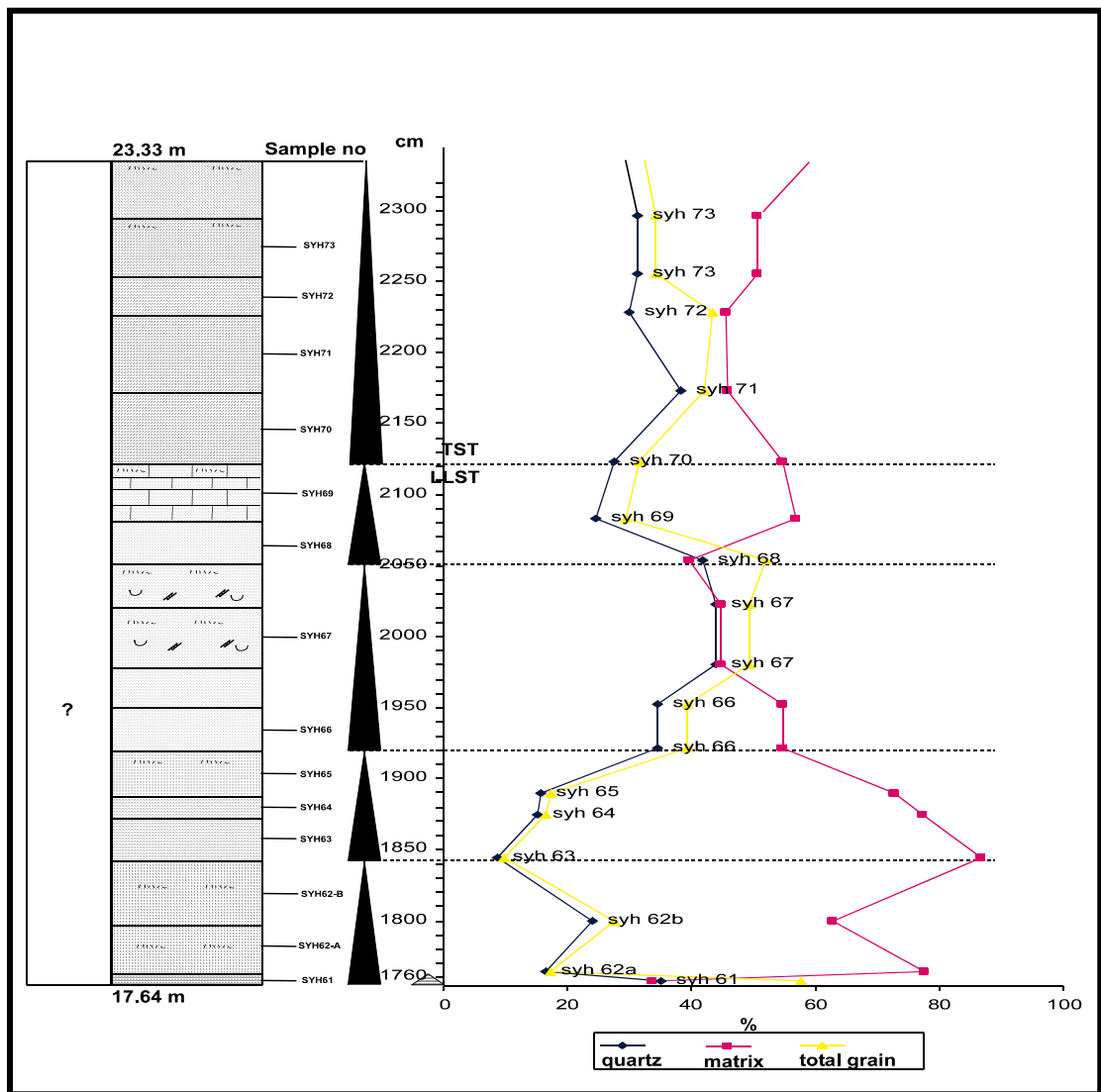
Figure 39: Quartz-Matrix-Total Grain Distribution Graphs (17.64-23.33 m)
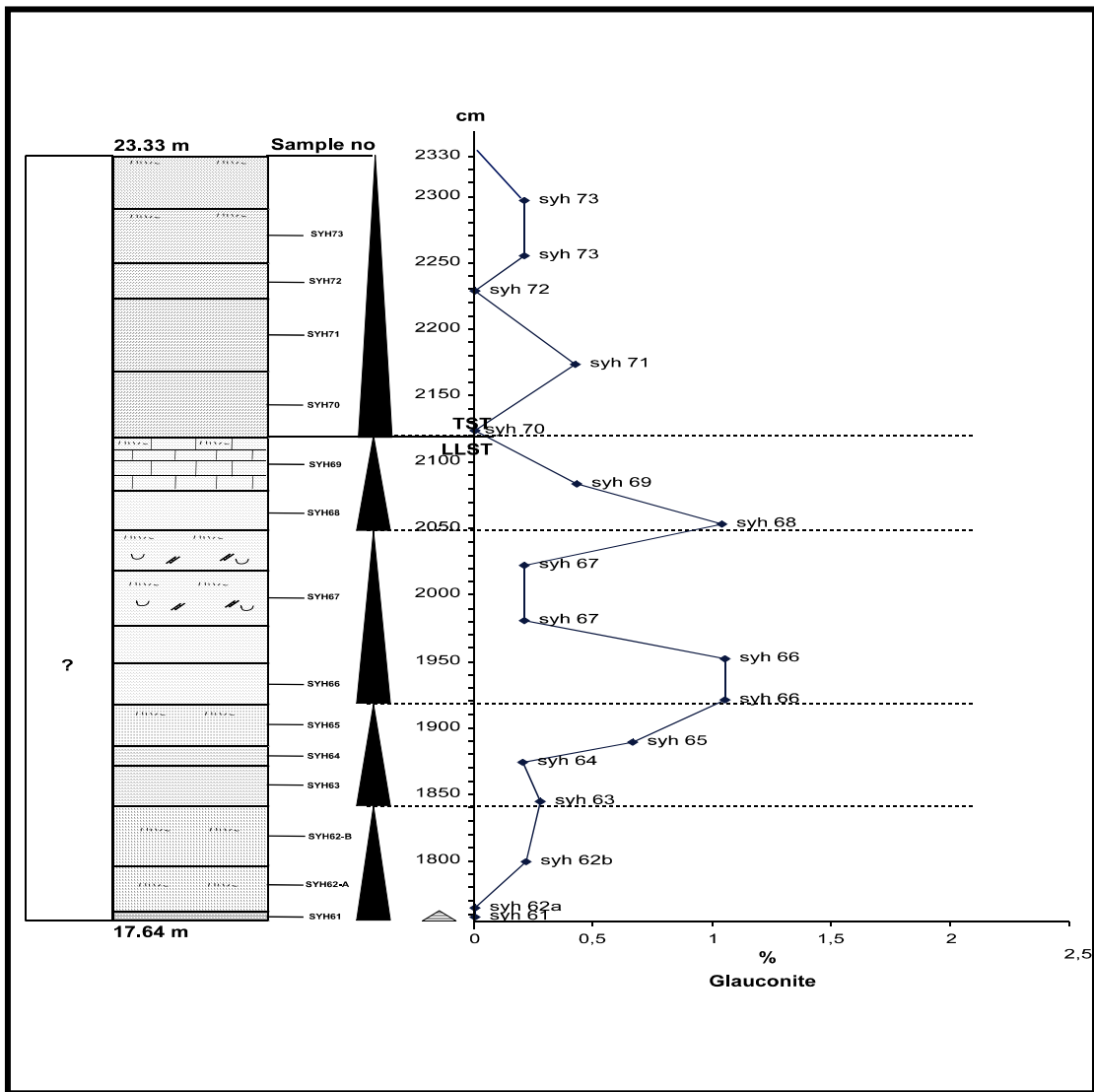
Figure 40: Glauconite Distribution Graphs (17.64-23.33 m)
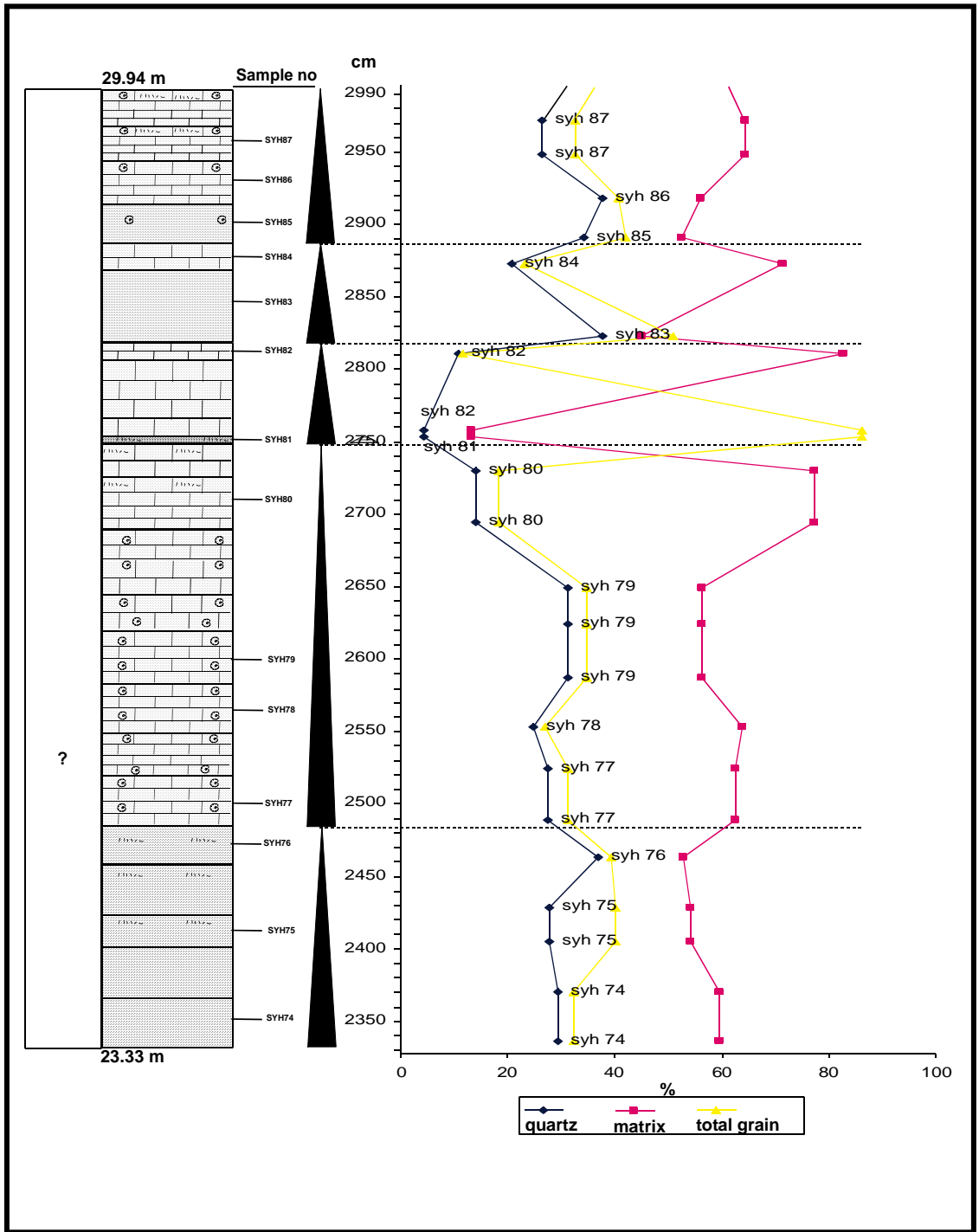
Figure 41: Quartz-Matrix-Total Grain Distribution Graphs (23.33-29.94 m)

69
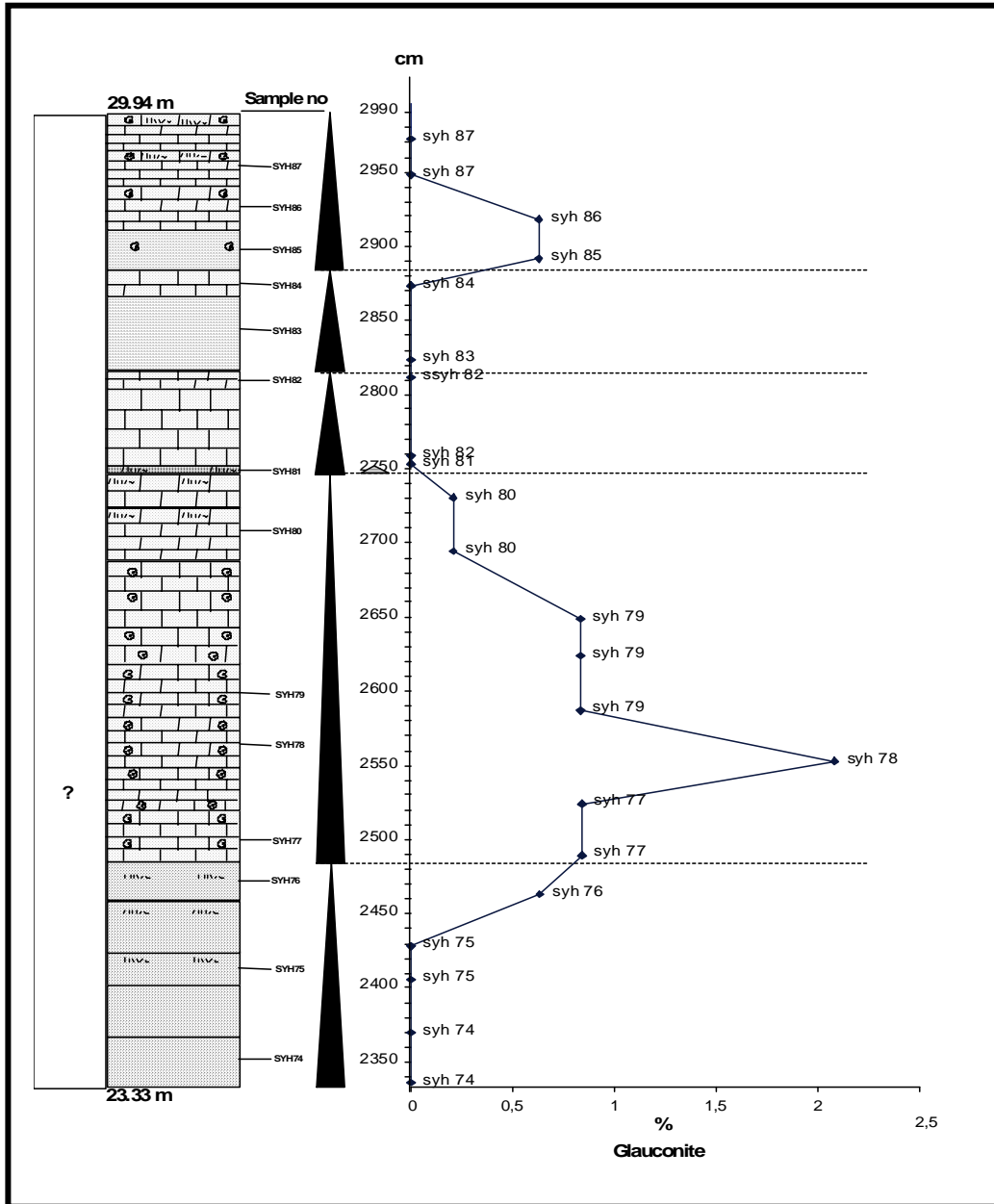
Figure 42: Glauconite Distribution Graphs (23.33-29.94 m)
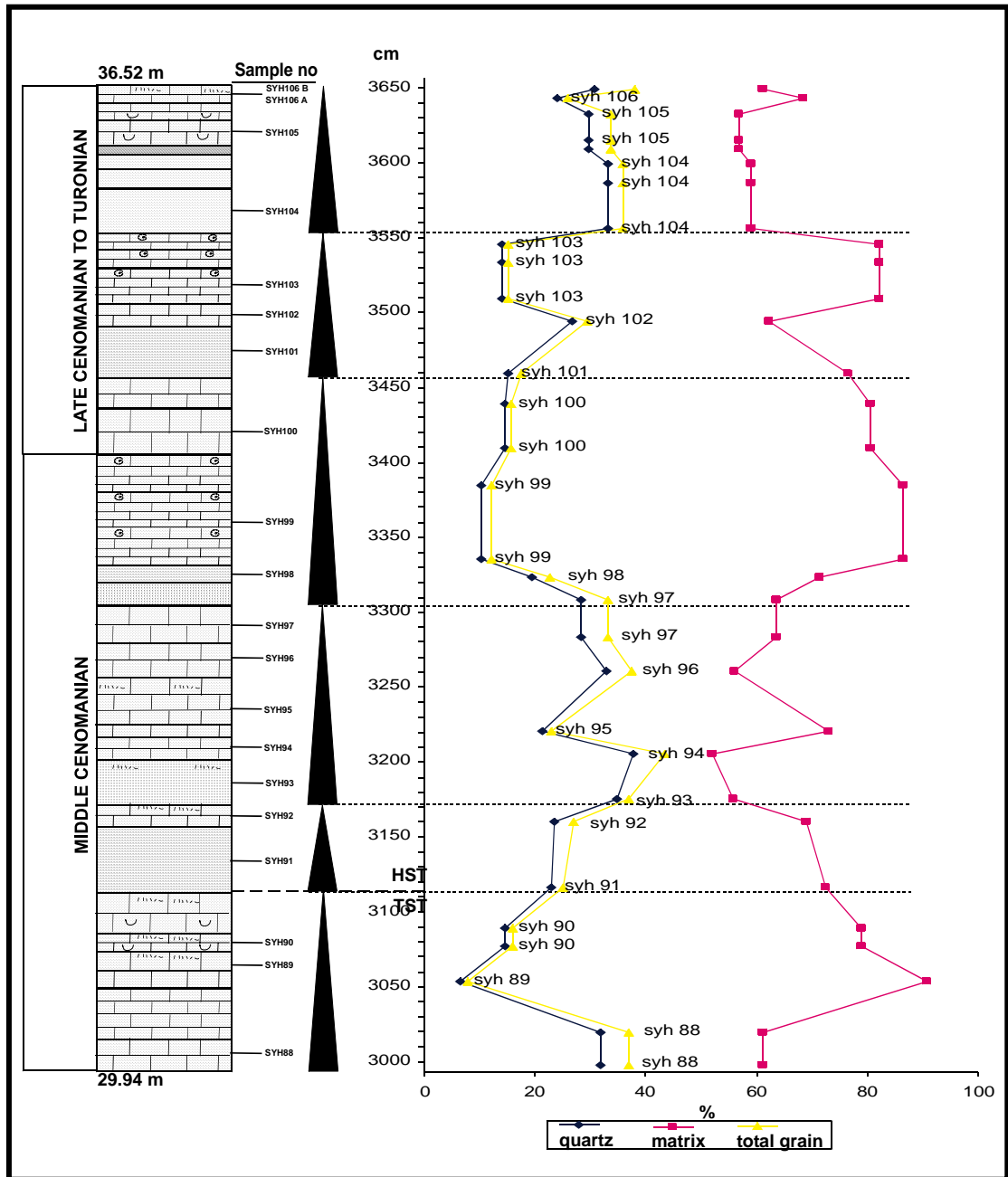
Figure 43: Quartz-Matrix-Total Grain Distribution Graphs (29.94-36.52 m)

71
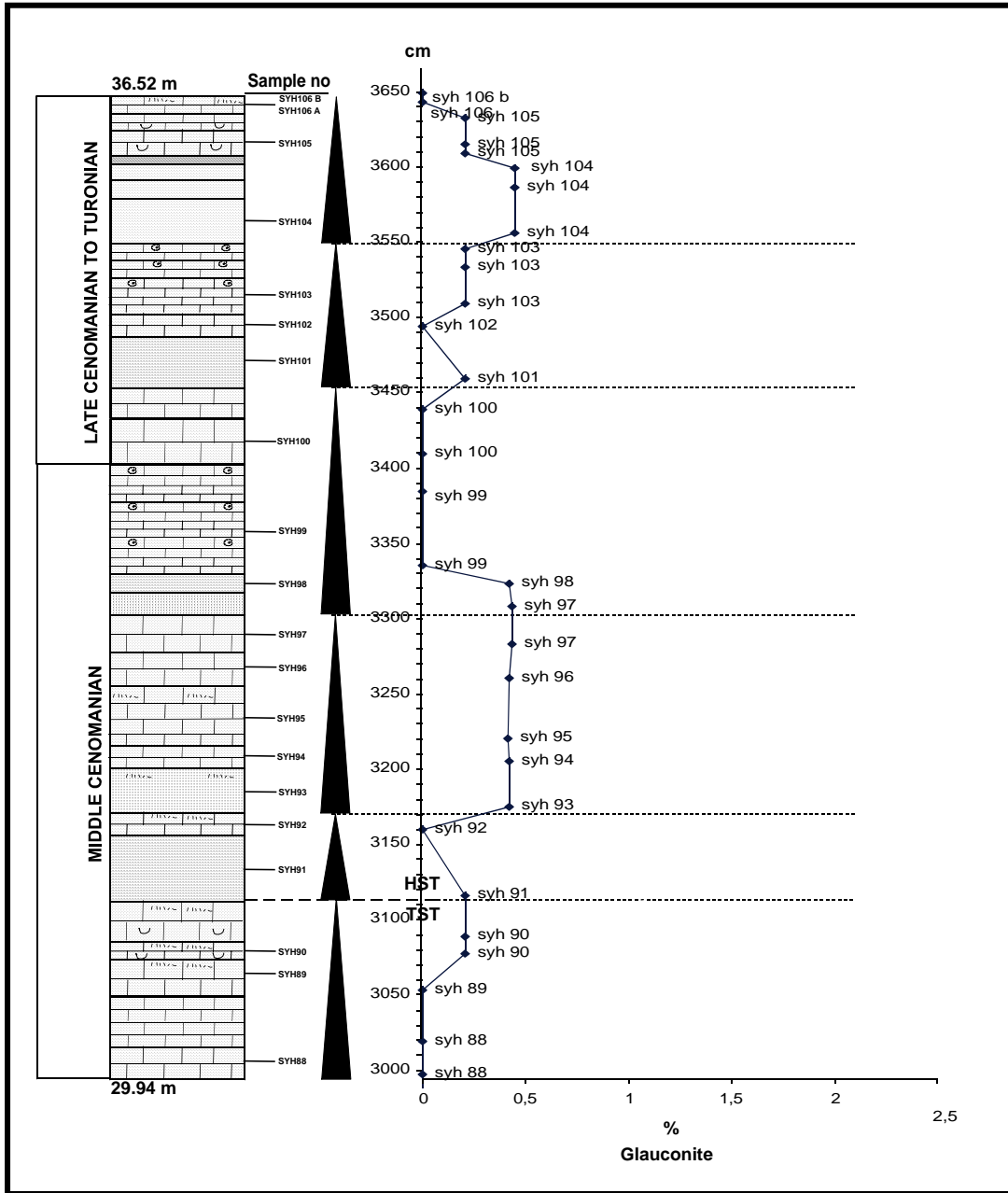
Figure 44: Glauconite Distribution Graphs (29.94-36.52 m)
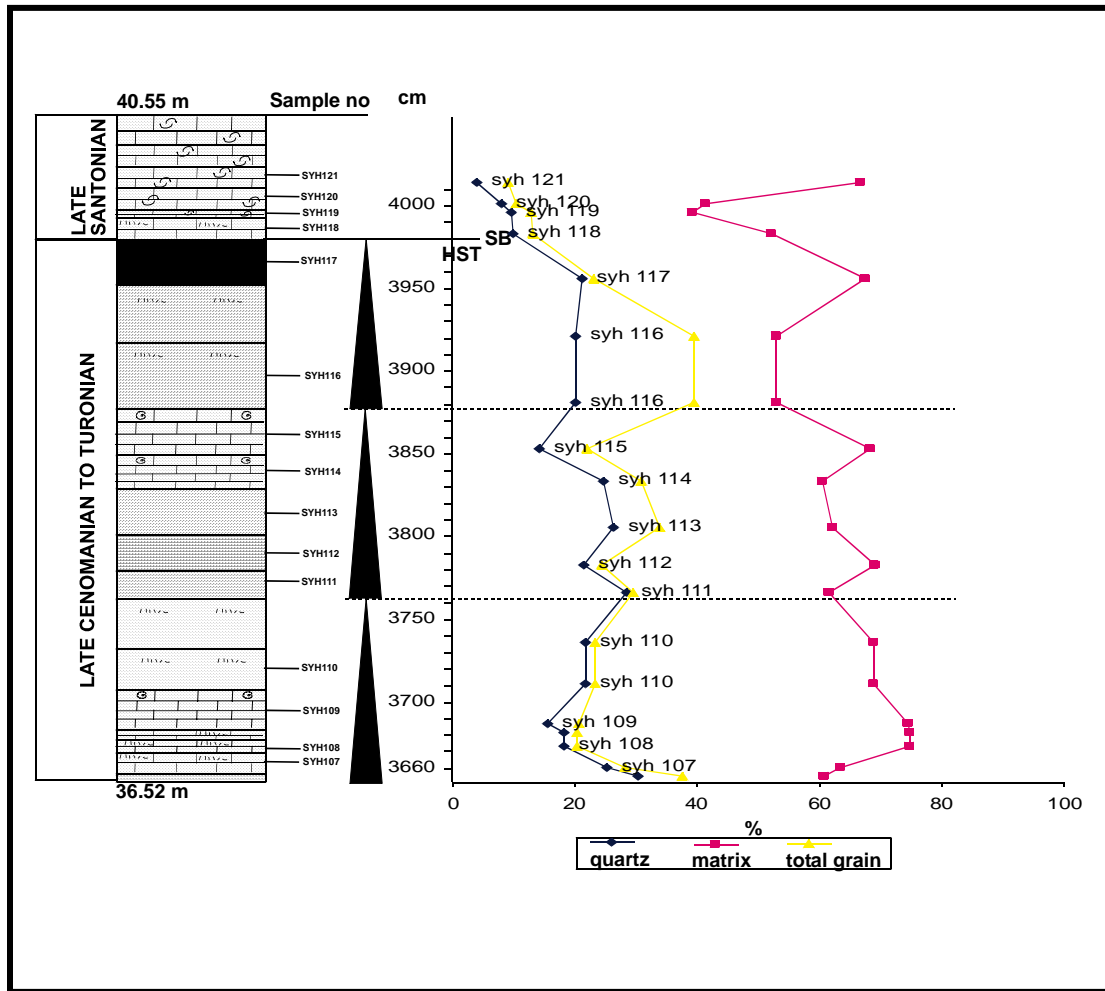
Figure 45:Quartz-Matrix-Total Grain Distribution Graphs (36.52-40.55 m)
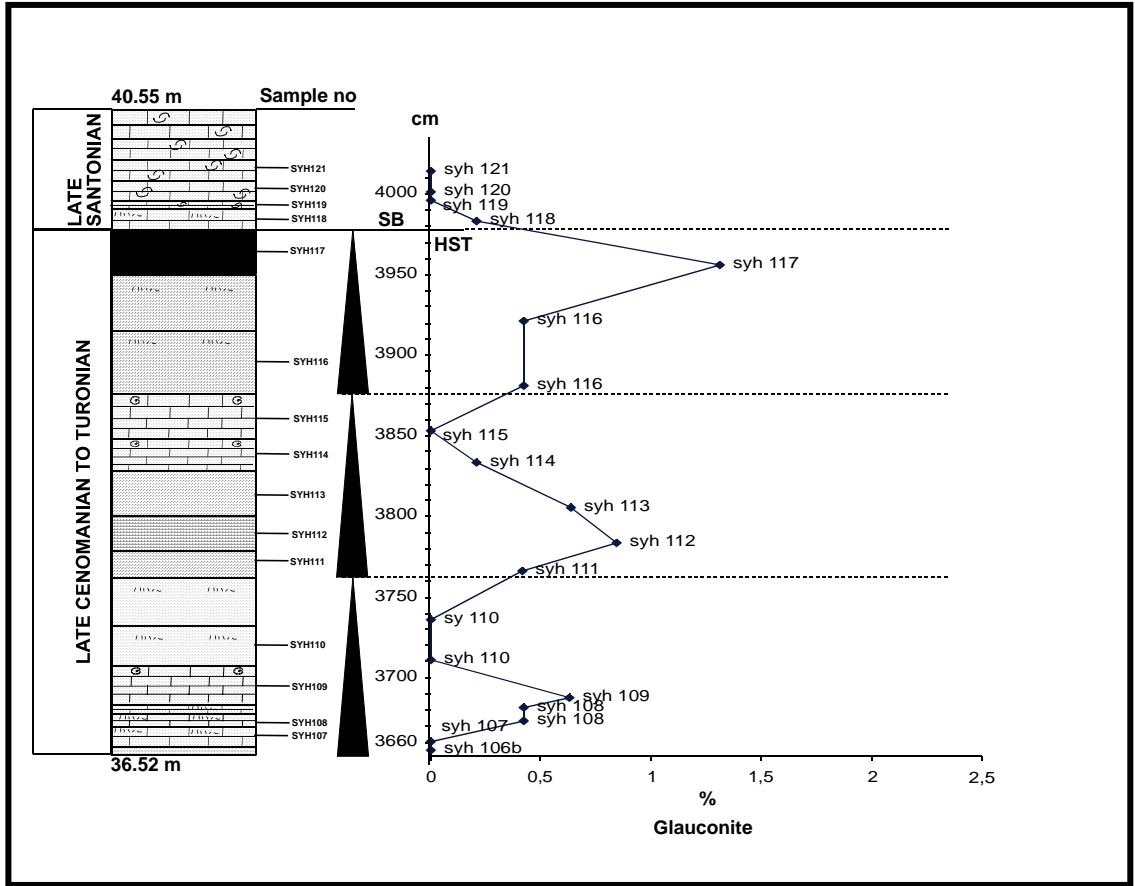
Figure 46: Glauconite Distribution Graphs (36.52-40.55 m)

CHAPTER 4

CYCLOSTRATIGRAPHY

The aim of cyclostratigraphy is to use cycles of any description for the construction and improvement of stratigraphic framework. Practically all cycles represent identifiable time periods, and are related to planetary movement (Schwarzacher, 1993). Cyclostratigraphy deals with mainly Milankovitch cycles.

Milankovitch theory states that climatic change is induced by variations in the orbital parameters of the Earth. These are the eccentricity, E, of the Earth's orbit around the sun, the deviation, tilt or obliquity, O, of the earth's axis of rotation from a vertical axis on the orbital plane, and the precession, P, expressing a certain relationship between obliquity and eccentricity. These parameters have the following periods: E between 100 ka and 400 ka, O 41 ka, P between 19-23 ka (Einsele, 2002). A sedimentary cycle is a group of different lithologies or textures which is repeated regularly in a sequence (Schwarzacher, 1993).

Determination of Milankovitch cycles for pelagic Üzümlü Formation has important consequences for understanding and evaluation of cycles observed through the formation. However, such determination for pelagic settings is also very difficult (Mayer and Appel, 1999).

As discussed in the preceding chapter, Üzümlü Formation consists of black shale-limestone alternations (redox cycles), and carbonaceous mudstone/marl-limestone

alternations which are disturbed by turbiditic currents. The identified cycles are interpreted as rhythmic cycles. Along the measured section four types of cycles are identified.

Cycle type A is characterized by the presence of the grey or black shales in the cycle (Figure 47). Sudden increase in accommodation space can create stagnant conditions hence the deposition of grey/black shales and/or limestones. Decrease in sea level yields to sandstone deposition and indicates shallowing upward trend. According to internal variations, within the cycle A, four subtypes are identified. A1 subtype starts with grey shales at the bottom and is followed by limestone facies and capped by sandstone facies at the top. A2 subtype starts with black shale beds and is capped by limestone facies. A3 subtype starts with grey shales at the bottom, black shales in the middle and limestone facies at the top. A4 subtype is composed of carbonaceous mudstone facies at the bottom and black shale facies at the top.

Cycle type B consists of carbonaceous facies with carbonate content relatively low at the bottom and relatively high at the top. Six subtypes are identified (Figure 47). When the carbonate source is distant, and sea level is high, carbonate input of the system is low. Henceforth, carbonaceous facies with low carbonate content are deposited at the bottom of the cycle. However, as the carbonate source gets closer and sea level falls as a result of a shallowing upward trend, then the carbonate input increases resulting the deposition of carbonaceous facies with high carbonate content at the top of the cycle. This can also be observed though the variations in the siliciclastic content. B1 subtype is composed of marls at the bottom and limestone facies at the top. B2 subtype starts with marl facies with relatively high siliciclastic input at the bottom and bioturbated marl facies with relatively low siliciclastic content at the top. B3 subtype starts with carbonaceous mudstone facies with relatively high siliciclastic content at the bottom and bioturbated mudstone facies with relatively low siliciclastic content at the top. B4 subtype is composed of limestone facies with relatively high siliciclastic content at the

bottom and bioturbated limestone facies with relatively low siliciclastic content at the top. B5 subtype is composed of carbonaceous mud facies at the bottom and marl facies at the top. B6 subtype contains marl facies at the bottom, limestone facies in the middle and sandstone facies at the top indicating a clear shallowing upward trend. Limestone-marl couplets are generated by (1) variations in carbonate production, (2) periodic carbonate dissolution and (3) periodic terrigeneous dissolution (Einsele, 2000). Between the middle Albian and early Cenomanian (?) the cycle generally composed of thick carbonaceous mudstones/marls and thinner limestones which indicates terrigeneous dilution. On the other hand between middle Cenomanian and late Santonian thick limestone beds indicate variations in carbonate production or dissolution.

Cycle type C is characterized by siliciclastic facies; hence, deposition took place in the relatively high energy conditions (Figure 47). The typical shallowing upward trend in these cycles can not be observed. In contrast, the cycle type indicates a deepening upward trend. This may be caused by the episodic (turbiditic) events. As a whole the cycle indicates low sea level conditions compared to other cycle types identified in the studied section. Two subtypes are identified. C1 subtype consists of conglomerate facies at the bottom and sandstone facies at the top. C2 subtype starts with sandstone facies at the bottom and bioturbated sandstone facies with relatively high siliciclastic material at the top.

Cycle type D is composed of siliciclastic facies at the bottom and carbonaceous facies at the top (Figure 47). At the bottom of these cycles, during the high sea level, deposition of siliciclastics took place due to high rate of sedimentation which is indicated by the lack of glauconites. When sea level falls, the unconsolidated and/or eroded carbonaceous material, already deposited in the shelf was reworked and/or transported to the top basin and formed the top of these cycles. Four subtypes are identified. D1 subtype is composed of sandstone facies at the bottom and limestone

77

facies at the top. D2 subtype starts with conglomerate facies at the bottom and capped by marl facies at the top. D3 subtype consists of conglomerate facies at the bottom and limestone facies at the top. D4 subtype is composed of siltstone facies at the bottom and limestone facies at the top.
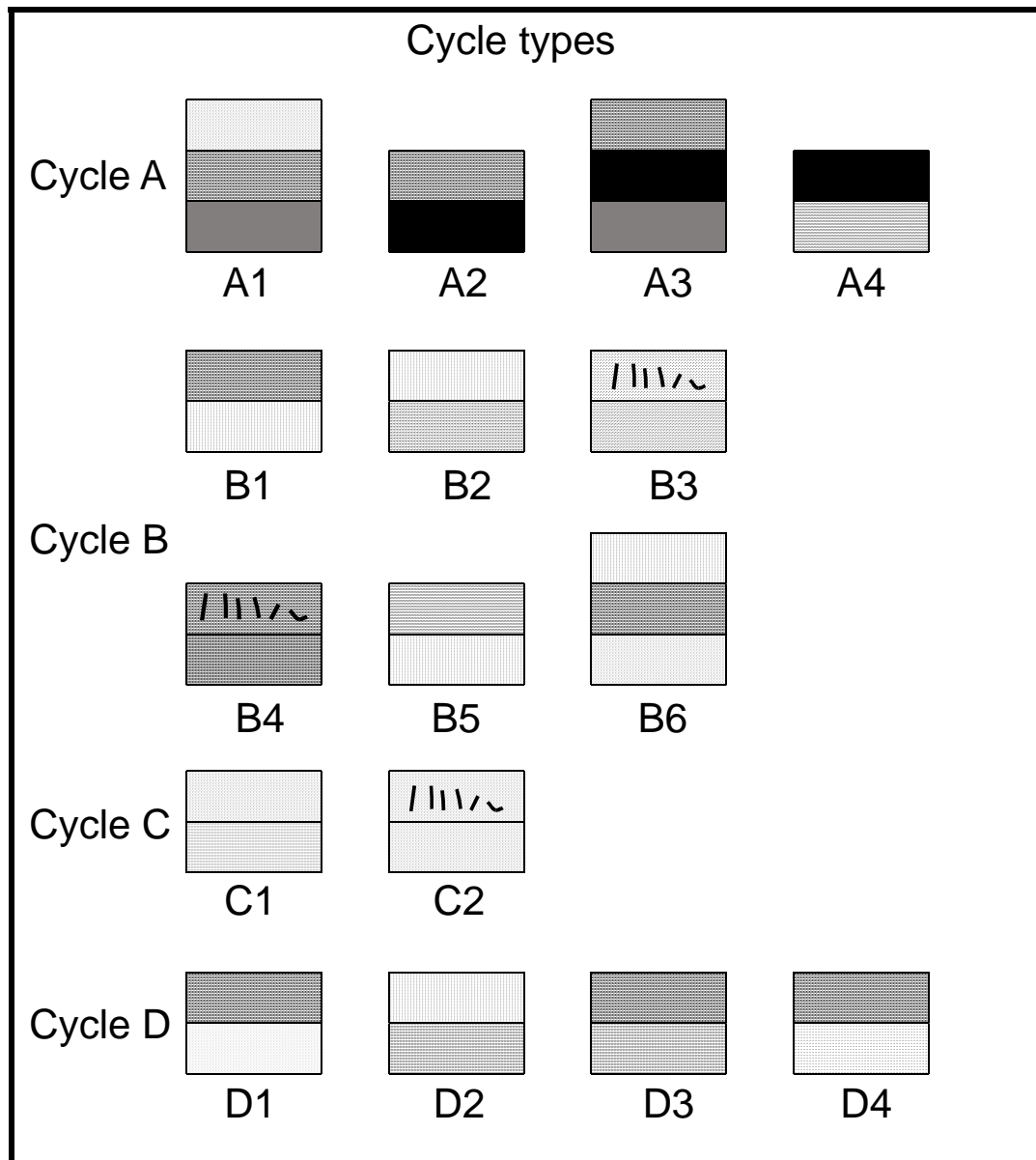
Figure 47: Identified cycle types in the studied section. See text for explanation.

It is very difficult to prove whether or not a given cyclic sequence is really caused by a mechanism with a constant time period. In general, the average cycle duration can only be determined by dating the beginning and end of a cyclic sequence (Einsele, 2000). 38 fifth order cycles are determined average time duration of each cycle is 0.4 Ma and this time range is in the eccentricity band of Milankovitch cycles.

The beginning of the Üzümlü Formation is middle-upper Albian, Aptian/Albian boundary 112 Ma, the middle Albian is represented by 105 Ma. Therefore, the beginning of the Üzümlü Formation is 105 Ma. The top of the Üzümlü Formation is Turonian and represented by 89 Ma. Therefore, time span for the cyclic Üzümlü Formation is (105-89=16) 16 Ma and the total number of cycles is 38 then the average cycle duration is (16/38=0.412 ~ 0.4) 0.4 Ma.

Cycles are determined by using lithofacies alternations. Quartz versus thickness, total terrigeneous material versus thickness and glauconite versus thickness graphs (Figures 33-46) have been drawn according to point-counting data (Appendix). These graphs are correlated with the cycles determined by lithofacies. This correlation shows that the graphs and cycle boundaries are well-matched. For that reason, small scale cycles determined by peak and trough points in the graphs. Decreasing terrigeneous percent is generally accompanied by the presence of glauconite; hence glauconite is interpreted as a primary mineral. As discussed in the forgoing chapter primary glauconite is an evidence of low terrigeneous influx. Low terrigeneous influx is occurred by virtue of two main reasons: Relative sea level rise or dry climate and low topography of the source rock. In both cases presence of primary glauconite related with climatic changes and in this study is accepted as indicative of cyclicity. Increasing terrigeneuos influx with the absence of glauconite may also indicate that during warmer climates more sediment is involved in the transportation by the running water (Einsele, 2000). The facies rich in siliciclastic content at the bottom of the cycles interpreted as the

transgressive part display enrichment in volcanic rock fragments, quartz and feldspar content. In contrast, the facies rich in carbonate at the top of the cycles interpreted as the regressive part display enrichment in matrix and decrease in terrigeneous grains.

Identified cycles are interpreted as 4th and 5th order cycles. Fourth order cycles are interpreted to represent eccentricity band of Milankovitch cyclicity. Fifth order cycles are rarely recorded in the studied section and interpreted to deposit by turbidity currents. These cycles are illustrated in figures 49, 50, 51, 52, 53, 54, 55 (from bottom to top respectively) and the symbols used in these figures are shown in figure 48.
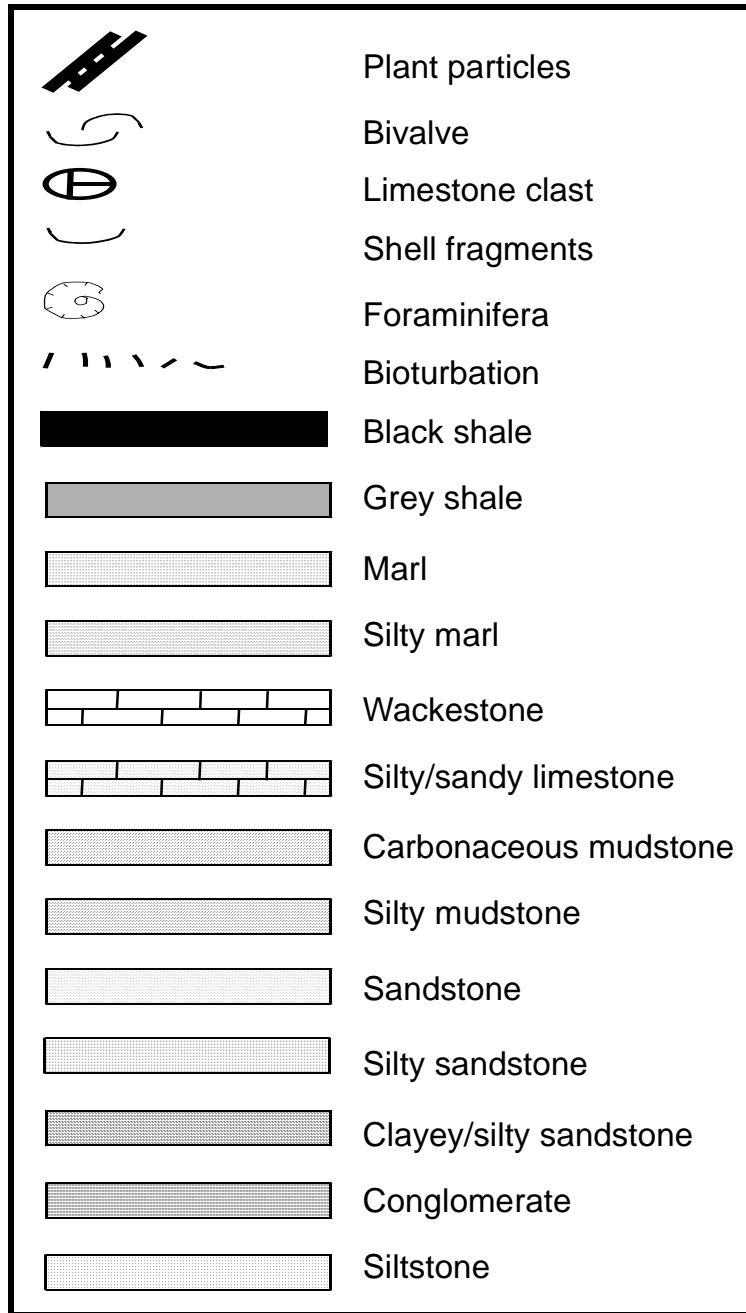
Figure 48: Symbols used in the stratigraphic sections.

- Plant particles
- Bivalve
- Limestone clast
- Shell fragments
- Foraminifera
- Bioturbation
- Black shale
- Grey shale
- Marl
- Silty marl
- Wackestone
- Silty/sandy limestone
- Carbonaceous mudstone
- Silty mudstone
- Sandstone
- Silty sandstone
- Clayey/silty sandstone
- Conglomerate
- Siltstone
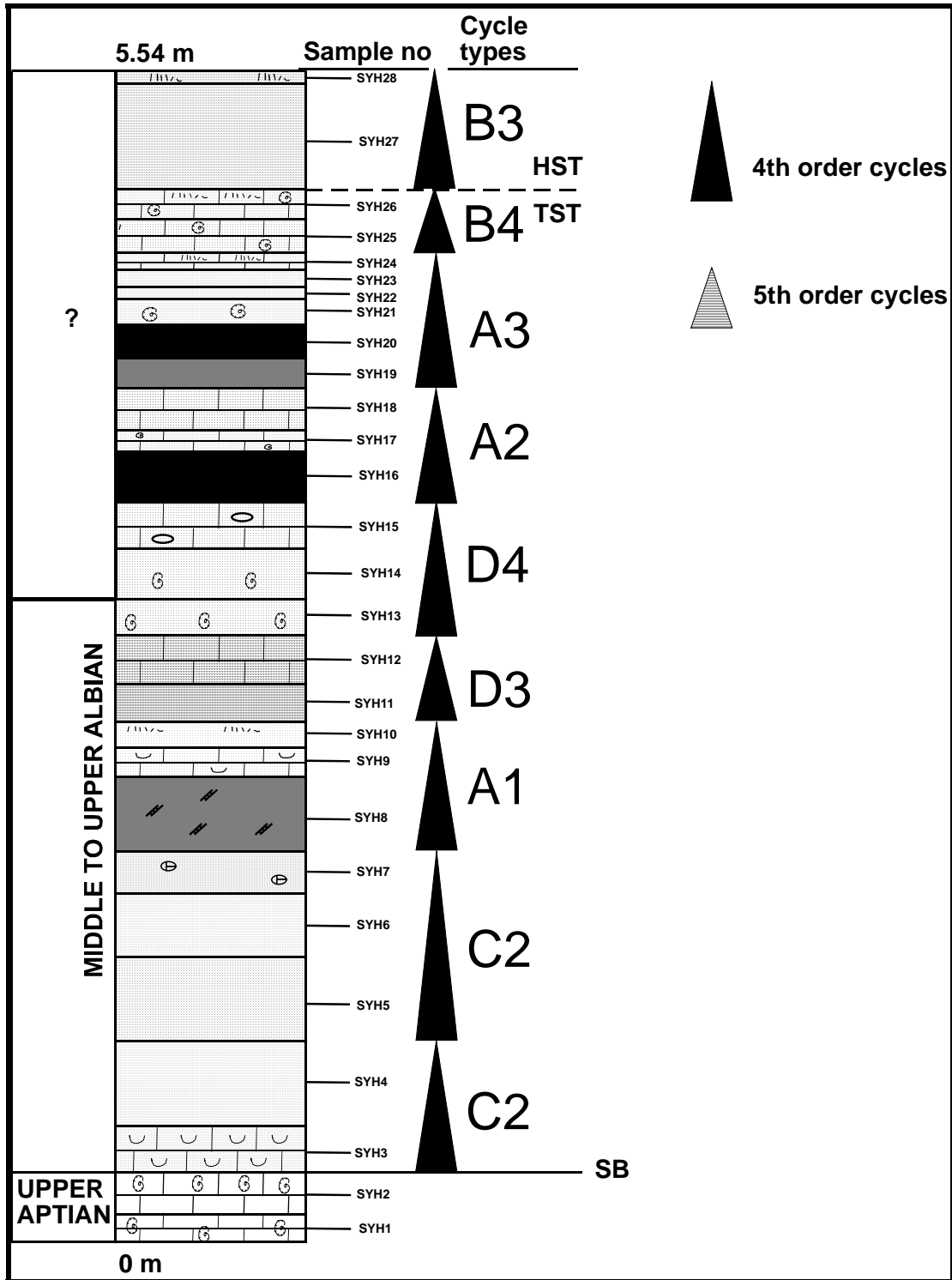
Figure 49: Stratigraphic section of measured succession (0-5.54 meters).
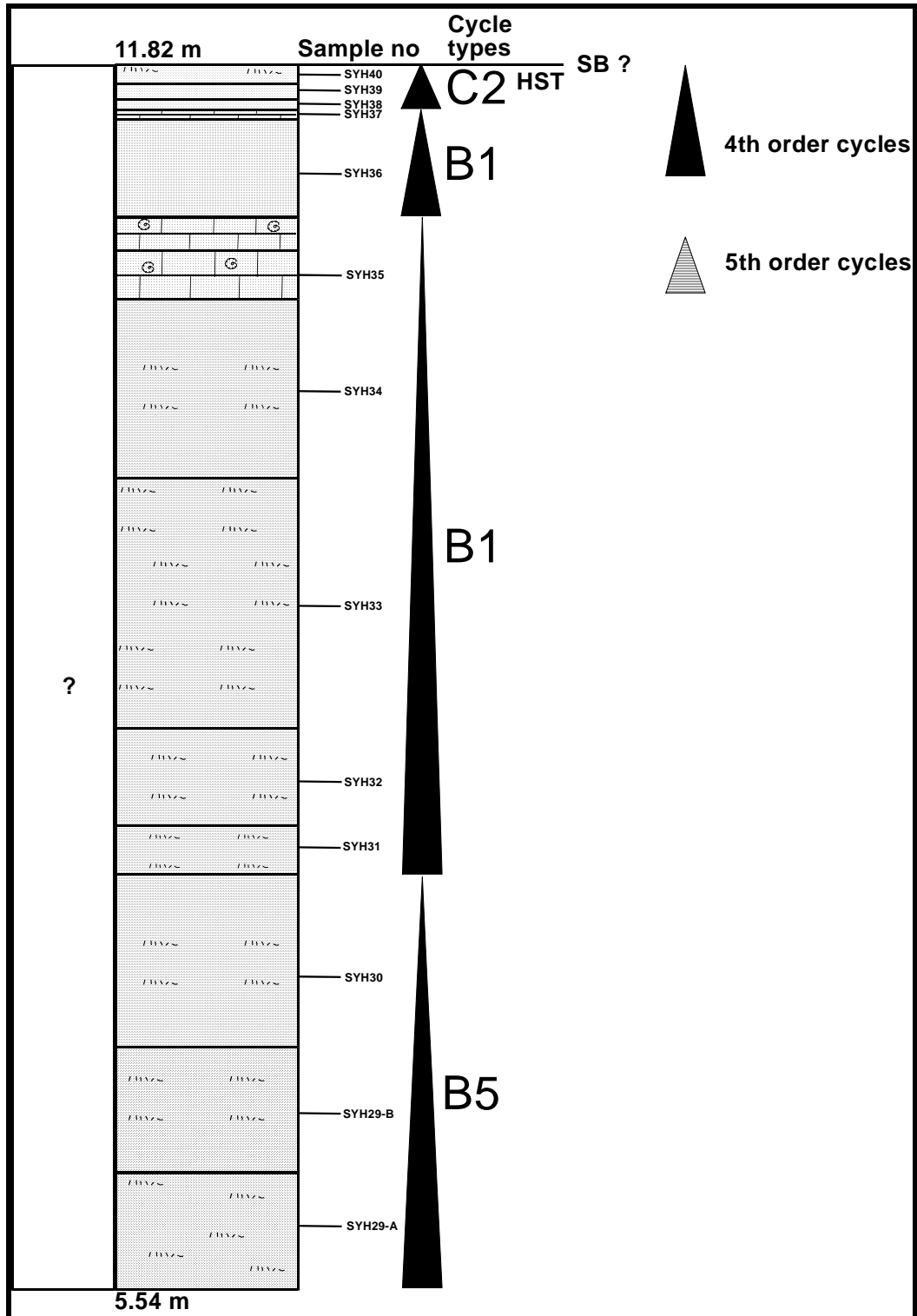
Figure 50: Stratigraphic section of measured succession (5.54-11.82 meters).
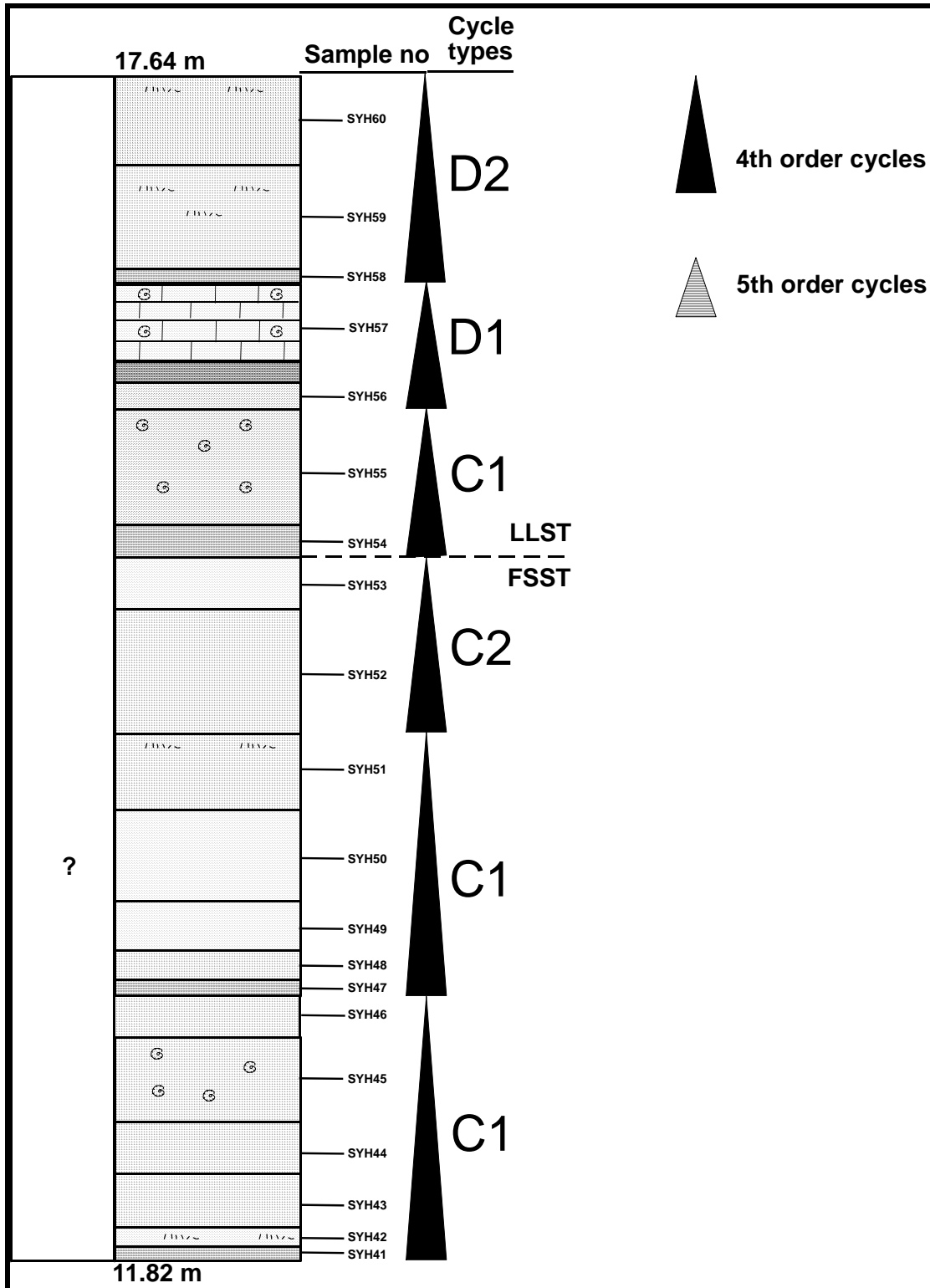
Figure 51: Stratigraphic section of measured succession (11.82-17.64 meters).

84
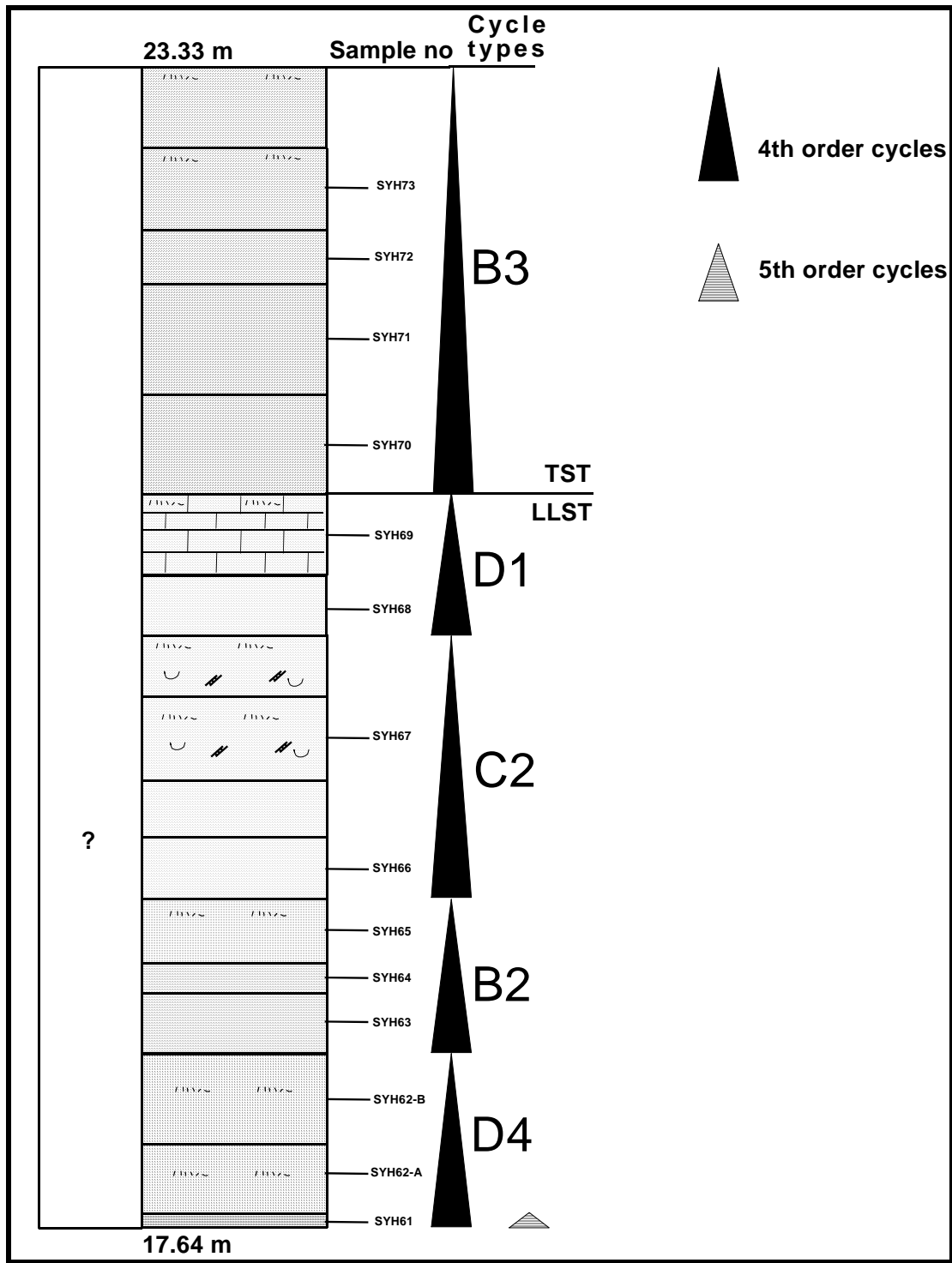
Figure 52: Stratigraphic section of measured succession (17.64-23.33 meters).
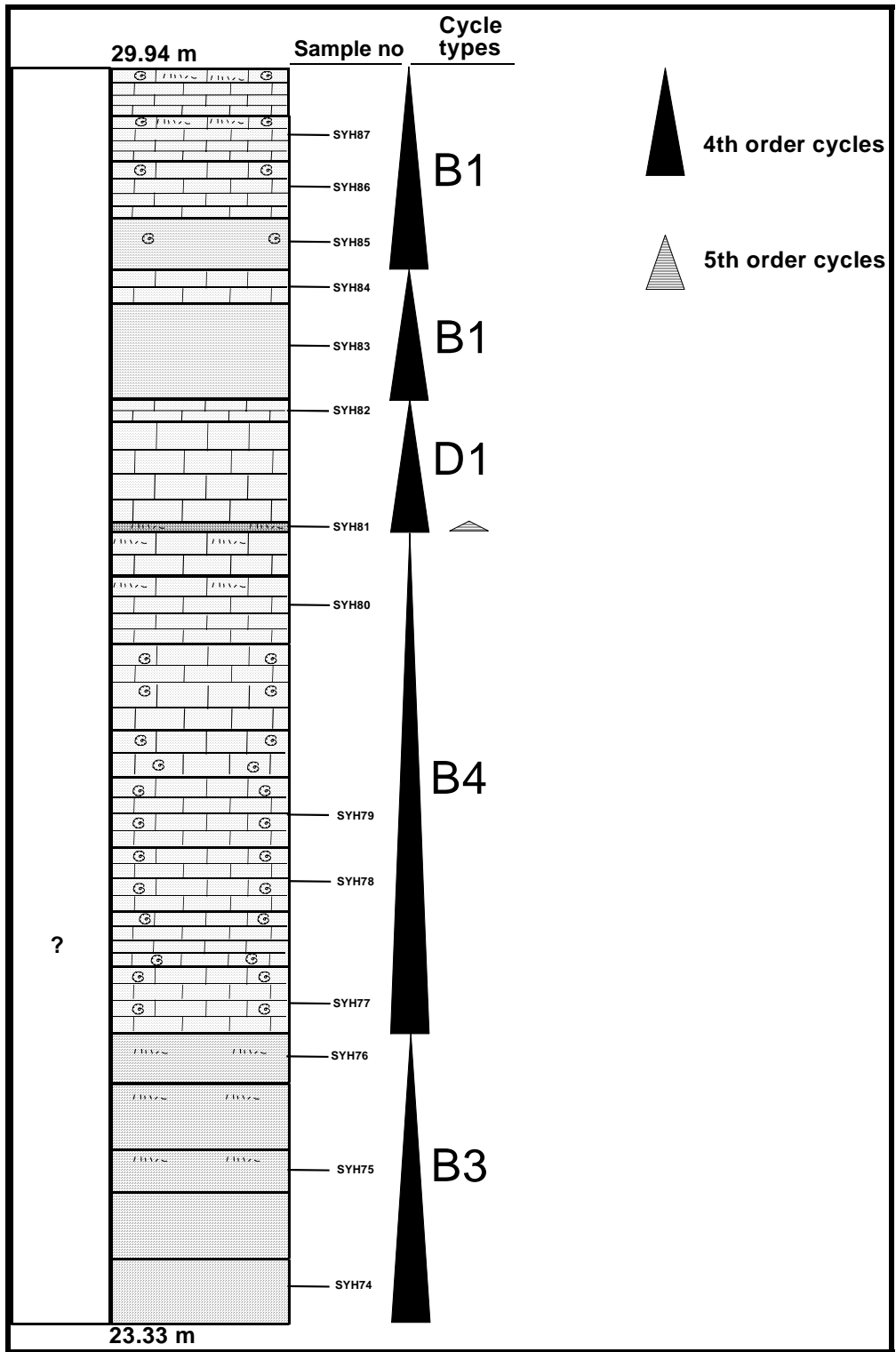
Figure 53: Stratigraphic section of measured succession (23.33-29.94meters).
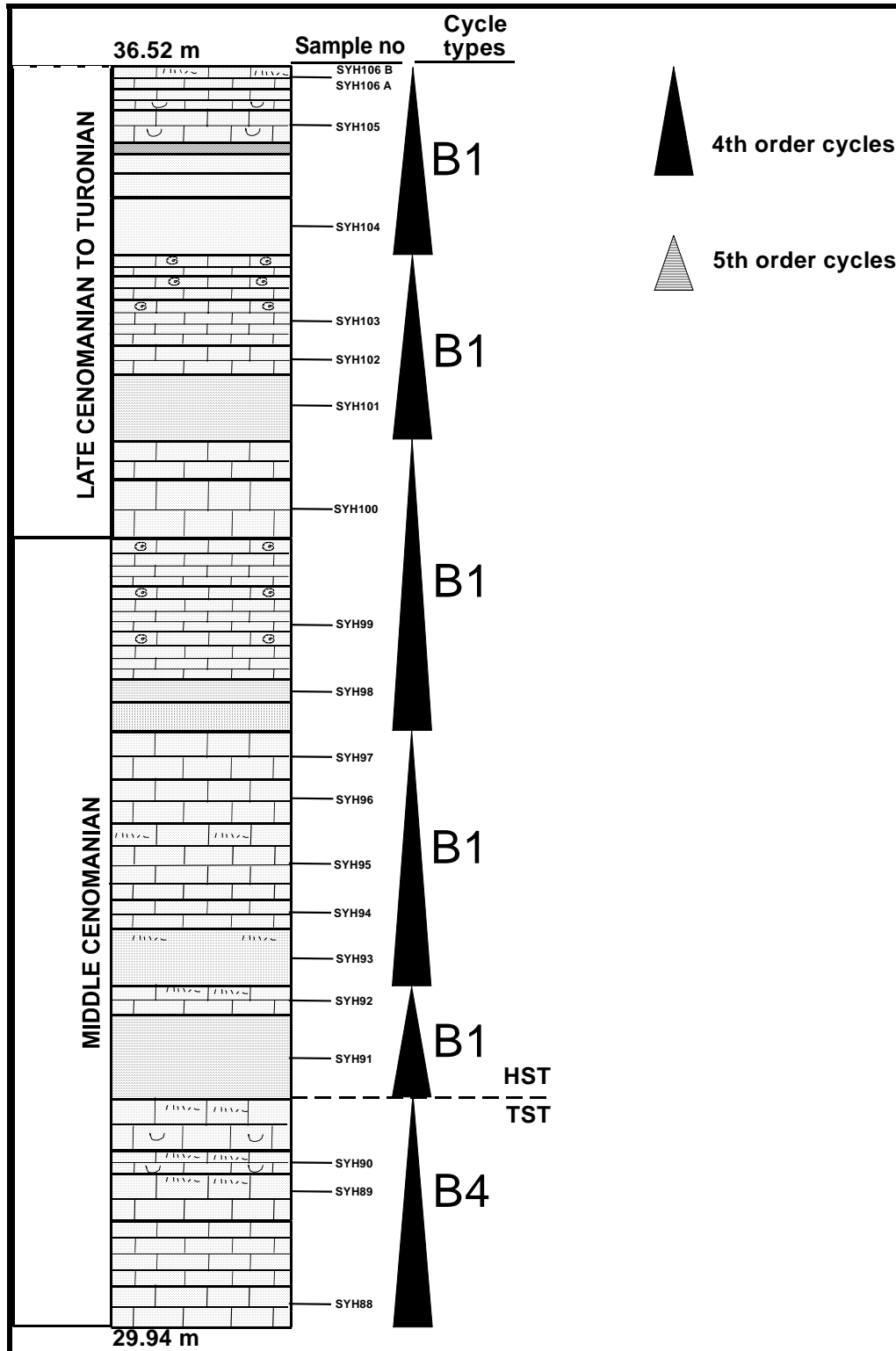
Figure 54: Stratigraphic section of measured succession (29.94-36.52 meters).
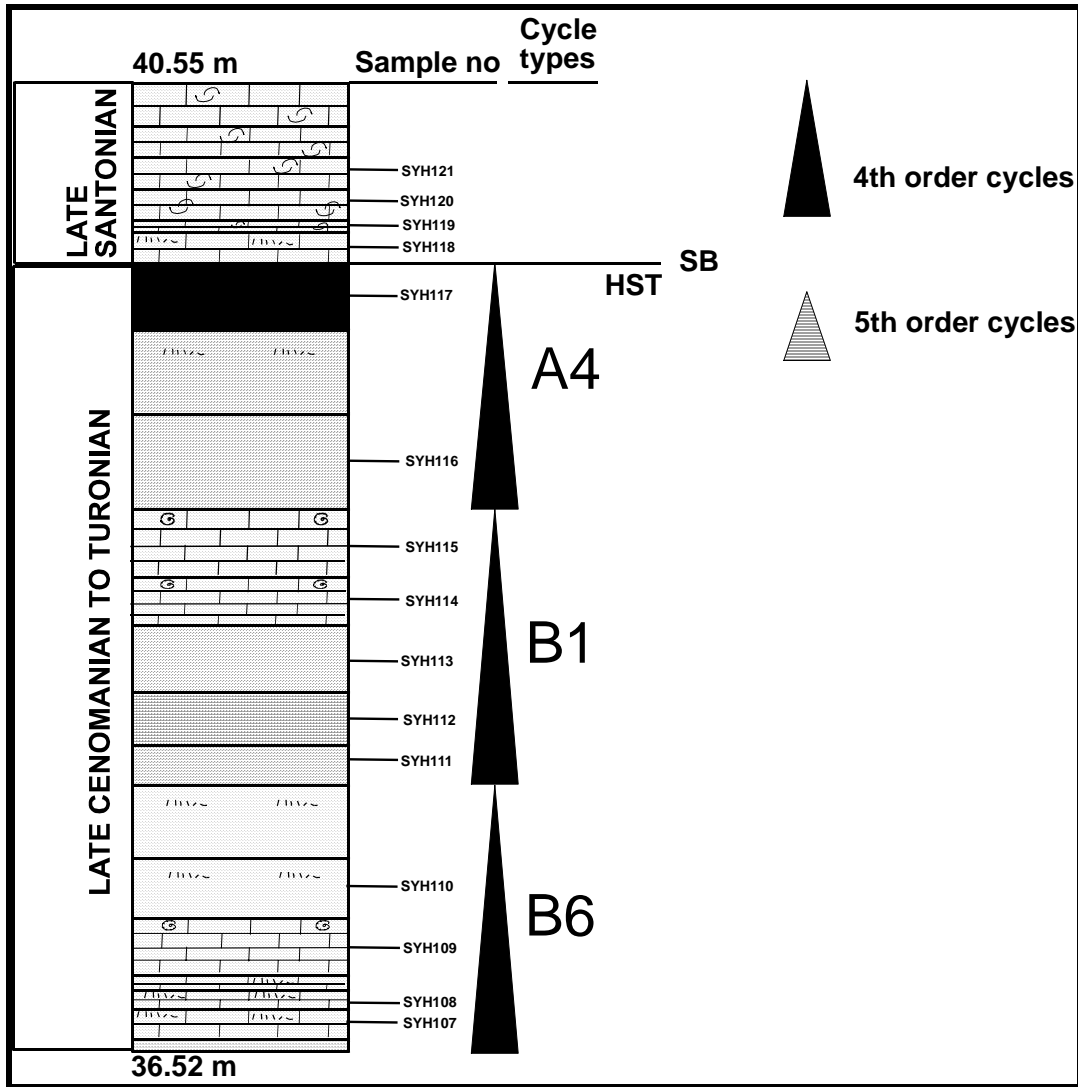
Figure 55: Stratigraphic section of measured succession (36.52-40.55 meters).

88

CHAPTER 5

SEQUENCE STRATIGRAPHY

Sequence stratigraphy arrived on the geologic "stage" in 1977 when Vail and his co-workers published on techniques they had developed at Esso Production Research to interpret seismic cross-sections. They assumed that continuous seismic reflectors on acoustic geophysical cross-sections are close matches to the chronostratigraphic surfaces, or time boundaries like bedding planes and unconformities. They had established that unconformities were clearly recognizable on marine seismic sections and assumed that like the unconformities of the Paleozoic identified by Wheeler (1958), Sloss (1963, 1972) and Sloss and Speed (1974) were the products of worldwide changes in sea level or eustasy. They noted that the unconformities enveloped packages of reflectors and called these seismic sequences. They remarked these with seismic reflectors onlapping and terminating either against the lower unconformity surface or against each other.

Using techniques developed by Schuchert (1916), Umbgrove (1939) and Wheeler (1958), they assumed that the position of onlapping seismic reflectors was controlled by the base level of the mean high water mark. Thus a sediment (or seismic) encroachment chart could be drawn that shows how far the sediment wedge of submarine, coastal and alluvial sediment (represented by the seismic) has onlapped a basin margin (Vail et al., 1977). A sediment (or seismic) aggradation chart was also constructed that shows the vertical component by which onlapped seismic reflectors had climbed or fallen (Vail et al., 1977). They then correlated the cycles of relative

89

changes of sea level at multiple locations and construct charts that incorporated the occurrence of global sediment (or seismic) onlap cycles. Using the aggradational measurements from the seismic, Vail et al, estimated the magnitude of relative sea-level excursions. However it was recognized the position of a eustatic event had on the continent is complicated by the local effects of tectonic subsidence. This may explain why sea-level curves for the Jurassic compiled by Hallam (1981) and Vail and Todd (1981) from different data sources record different positions for the same sea-level stands. Posamentier and Allen (1999) confirm this effect of local tectonism with a block diagram of a margin that has different tectonic signals along its length and consequently different relative sea level positions.

Following the Vail et al. (1977) publication, Jervey (1988) published an article that revolutionized the way we look at the relationship between tectonics, eustasy and sedimentation. He did this using a simple 2D sedimentary simulation. At the same time our understanding of system tracts expanded with the publications on these in Baum and Vail (1988), Donovan et al. (1988), and Loutit et al. (1988).

Measured section begins with wackestones of Soğukçam Limestone which are believed to deposited in pelagic setting (Yılmaz, 2002), unconformably overlain by pelagic packstones of Üzümlü formation. This unconformity is also represented as a time gap between late Aptian and middle Albian. The boundary between Soğukçam Limestone and Üzümlü Formation is interpreted as a type 3 (drowning unconformity) sequence boundary. Type 3 sequence boundary is defined by Schlager (1999) as the flooding surface between a highstand system tract and transgressive system tract where rate of subsidence exceeds the rapid fall of sea-level.

Type 3 boundary is overlain by limestone - black shale alternations which are interrupted by turbidity currents. Limestone - black shale interval is interpreted as transgressive deposits and so a Transgressive Systems Tract. This system tract is

composed of C type cycles at the bottom, A and D type cycles in middle and a B type cycle at the top (Figure 49). As discussed in the preceding chapter, C type cycles indicate low sea level conditions, A type cycles, also indicated by the presence of black shale levels, are transgressive. B type cycles at the top indicate deposition in a deeper environment. As indicated by the organization of the cycle types, the system tract shows a clear evidence for landward propagation of the sea towards the land. Hence, the system tract is interpreted as Transgressive System Tract.

The limestone-black shale alternation followed by carbonaceous mudstone/marl – limestone alternation which is interpreted as Highstand Systems Tract. The Highstand System Tract of type 3 boundary is characterized by the dominancy of B type cycles (Figure 50, 51). C2 cycle is observed at the top of the system tract. This organization indicates a high stand regressive phase. The regressive deposits that form when sediment accumulation rates exceed the rate of relative sea-level rise and increase in accommodation constitute the upper systems tract in either a type 1 or type 2 sequence.

Carbonaceous mudstone/marl-limestone sequence is capped by conglomerate-sandstone cycles. The abrupt change of coarse grained deposits on top of fine grained Highstand Systems Tract deposits may indicate a correlative conformity of a sequence boundary and beginning of Falling Stage System Tract (FSST) or Early Lowstand Systems Tract (ELST). FSST of this sequence is composed of C type cycles (Figure 51). In general, active supply of coarse-grained terrigeneous sediments to a deep-water environment commences in response to relative sea-level fall (Mutti, 1985; Posamentier et al., 1988). The correlative conformity of this sequence boundary is thought to be represented by one of the conglomerate levels which constitute the bottom of the C1 type cycles in the middle of the succession. The considerable thickness of these cycles is interpreted as deposited as a result of sudden fall of sea level. Sudden fall of the sea level results in sub aerial exposure of shallow marine sediments and coarse grained sediments are by-passed to the deep sea.

Posamentier and Allen (1999) divided a Lowstand Systems Tract into Early and Late Phases. They indicated that during early lowstand, relative sea level is falling, forced regression takes place, and an unconformity forms a sequence boundary on the exposed surface landward of the shoreline, representing a surface of sedimentary bypass. Incised valleys may form in the interfluve lows. Vail et al 1977, like many other referenced authors, also equate this Systems Tract to the accumulation of sediments as basin floor fans. However, Posamentier and Allen (1999) suggest that care should be taken with this interpretation since the formation of these fans may often be independent of a relative fall in sea level and are instead tied to higher rates of sedimentation and the character of the up dip slope since this Systems Tract is equated with the relative fall in sea level. In the studied section, presence of glauconite minerals in the C type cycles indicates that these cycles are deposited with low sediment influx. Therefore, it can be stated that these cycles are deposited during the relative fall of sea level.

Falling Stage Systems Tract deposits are followed by Late Lowstand Systems Tract (LLST) deposits. LLST is represented by B, C and D type cycles (Figure 51, 52). In the studied section this systems tract sediments are characterized by the dominancy of D type cycles. B and C type cycles are observed at the bottom and the top of the LLST. During the LLST the rate of relative sea level fall decreases and accommodation space is greater then the FSST. Therefore, deposition of pelagic sediments commences while the siliciclastics are still continues to deposit. As a result, B, C and D cycles were formed.

Overlying thick carbonaceous mudstone and limestone cycle is interpreted as Transgressive System Tracts of type 1 sequence which is represented by B and D types of cycles (Figure 52, 53, 54). D type cycles are the dominant cycle type in the TST. Only one occurrence of D1 type cycle observed. When the relative sea level begins to raise the pelagic sedimentation rate increases and B type cycles were deposited.

However, siliclastic influx to the system was continuing due to turbidity currents and D type cycles were deposited.

Carbonaceous mudstone and limestone cycle is capped by marl-limestone alternation. Glauconite content of this alternation show low sediment influx. This alternation is interpreted as HST and composed of B and A types of cycles (Figure 54, 55) B type cycles dominate this system tract. A type cycle is observed at the top of the HST. Limestone-marl successions and black shale - limestone alternations occurring in the deep sea, preferentially form during the transition from transgressive to highstand deposits (Einsele et al., 1991). In this study limestone-marl/carbonaceous mudstone alternations are interpreted as Transgressive Systems Tract and Highstand Systems Tract deposits.

The upper-most sequence boundary (type 3) (Figure 55) is indicated as time gap between Turonian and Late Santonian. This sequence boundary is overlain by red colored sandy silty limestones of Yenipazar Formation.

Sequence boundary types determined and defined in the studied section can also be correlated with global examples (De Graciansky et al., 1998) Type 3 boundary separating Üzümlü Formation from Soğukçam Limestone may be correlated with Ap6 level of De Graciansky et al. (1998). However, as the area is tectonically affected, there is more time gap. The bottom part of Üzümlü Formation belonging to middle to upper Albian is represented by the fossil species of *T. roberti* represented in the biozone of *B. breggiensis*. Type 1 sequence boundary in the middle part of the section can be correlated with Al7-11 of De Graciansky et al. (1998). The second type 3 boundary at the top part of the section is separating Üzümlü Formation from Yenipazar formations and may be correlated with Ce3 of De Graciansky et al. (1998).

CHAPTER 6

DISCUSSION AND CONCLUSION

Sedimentological analysis of Üzümlü Formation is based on point-counting of collected samples, thin section investigations and interpretation of vertical facies association. Investigation of vertical facies associations revealed that the Üzümlü Formation is deposited at the toe of continental slope. The overall carbonate rich characteristics of lithofacies indicate that deposition took place well above the carbonate compensation depth and just above the lysocline. The presence of siltstones, sandstones and conglomerates between the fine grained carbonaceous rocks with conformable boundaries indicate that these coarse grained rocks are deposited by turbidity currents. In addition, dominance of dark colored beds show that the depositional environment suffered from the oxygen deficiency especially during the middle to late? Albian. Occurrence of black shale levels in the latest Albian (?) and late Cenomanian to Turonian is correlative to the oceanic anoxic events in the mid-Cretaceous equivalents (OAE1d and OAE2) in different parts of the world.

Modal analysis of sandstone facies show that the tectonic setting of the region was considerably changed in the late Cenomanian. Sandstone provenance analysis indicates that between the middle Albian to middle Cenomanian the basin is dominated by the terrigeneous material derived from magmatic arc and recycled orogen. During the late Cenomanian, tectonic setting changed from magmatic arc to basement uplift and transitional continental settings which are tectonically consolidated regions of amalgamated ancient orogenic belts.

High-resolution cyclostratigraphical studies based on the cm-m scaled cyclic occurrences of lithofacies and vertical variations of rock forming minerals along the measured section. Üzümlü Formation is characterized by redox (black shale-limestone) cycles at the bottom, conglomerate – sandstone cycles in the middle and carbonaceous mudstone/marl-limestone cycles at the top. The determination of exact shallowing-upward Milankovitch cycles is rather difficult in pelagic settings. However, in black/grey shale-limestone cycles, plant particles within the black/grey shales are derived from the flooded vegetated lands during relatively high sea levels. The average cycle duration of 0.4 Ma is determined.

The direct evidence of sequence boundaries with subaerial exposure and erosion could not be recorded in pelagic successions. However, the sudden and prolonged sediment influx which results in deposition of thicker sandstones and conglomerates in the continental slope or basins may be indicative of correlative conformities of sequence boundaries in the pelagic settings. Three sequence boundaries are identified along the measured section. Two type 3 sequence boundaries; one of them is separating the pelagic carbonates of Soğukçam Limestone and pelagic deposits of Üzümlü Formation and the other one is at the top of the section. One type 1 sequence boundary found in the middle of the succession. Within the cycle types determined, cycle types dominated with black-grey shales – limestones are associated with the Transgressive Systems Tracts. Carbonaceous mudstone/marl-limestone cycles with low terrigeneous content and relatively high terrigeneous content are interpreted as Highstand Systems Tracts and Transgressive Systems Tracts respectively. Cycles composed of thick sandstone beds and thin conglomerate beds are interpreted as deposited during Falling Stage System Tracts including the type 1 sequence boundary. Conglomerate/sandstone-marl cycles are recorded in the Falling Stage Systems Tracts.

As a conclusion, Üzümlü Formation shows the records of high frequency and low frequency sea level fluctuations, mid-Cretaceous oceanic events related with the anoxia and black shale formation and tectonic setting of the region.

REFERENCES

Abdüsselamoğlu, S., 1959. Almacıkdağı ile Mudurnu ve Göynük civarının jeolojisi, İstanbul Üniversitesi, Fen Fakültesi Monografileri, 14.

Altıner D., 1991. Microfossil biostratigraphy (mainly foraminifers) of the Jurassic-Cretaceous carbonate successions in northwestern Anatolia (Turkey). Geologica Romana, 27, 1, 167-213.

Altiner D. and Özkan S., 1991. Calpionellid zonation in North-Western Anatolia (Turkey) and calibration of the stratigraphyc ranger of some benthic Foraminifera at the Jurassic - Cretaceous boundary. Geologica Romana, 27, 1, 215-236

Altiner D., Koçyigit A., Farinacci A., Nicosia U. and Conti M.A., 1991. Jurassic-Lower Cretaceous stratigraphy and paleogeographic evolution of the southern part of North-Western Anatolia (Turkey). Geologica Romana, 27, 1, 13-80

Altınlı, İ. E., 1975. Orta Sakarya'nın jeolojisi : Cumhuriyetin 50, yılı Yerbilimleri Kongresi, Maden Tetkik Arama Enst. yayınları, 11-25.

Altınlı, İ. E., 1976. Geology of the northern portion of the middle Sakarya river: I.Ü. Fen Fak. Mecmuası, S.B. 41, 15-56, İstanbul.

Altınlı, İ. E., 1978. Geology of the eastern territiory of Nallıhan: I.Ü. Fen Fak. Mecmuası, S.B. 41, 29-44, İstanbul.

Arthur, M. A. 1979. North Atlantic Cretaceous black shales: the record at Site 398 and a brief comparison with other occurrences. In: Ryan, W. B. F. and Sibuet, I. C. et al. Initial Reports Deep Sea Drilling Project, 47/2**.** U.S. Government Printing Office, Washington D.C. 719-38.

Arthur, M.A., Brumsack, H.-J., Jenkyns, H.C., Schlanger, S.O., 1990. Stratigraphy, geochemistry, and paleoceanography of organic carbon-rich Cretaceous sequence. In: Ginsburg, R.N., Beaudoin, B. (Eds.), Cretaceous Resources, Events and Rhythms. Kluwer Academic, 75-119.

Arthur, M. A. and Natland, J. H. 1979. Carbonaceous sediments in the North and South Atlantic: the role of salinity in stable stratification of Early Cretaceous basins. In: Talwani, M., Hay, W. and Ryan, W. B. F. (eds.). Deep Drilling Results in the Atlantic Ocean: continental margins and paleoenvironment. Maurice Ewing Ser. 3, Am. Geophys. union, 375-401

Arthur and Schlanger, S. O. 1979. Cretaceous 'oceanic anoxic events' as causal factors in development of reef-reservoired giant oil fields. Bull. Am. Ass. Petrol. Geol. 63, 870-85.

Aydın, M., Serdar, H.S., Şahintürk, Ö., Yazman, M., Çokuğraş, R., Demir, O. ve Özçelik, Y., 1987. Çamdağ (Sakarya) - Sünnicedağ (Bolu) yöresinin jeolojisi. Türkiye Jeol. Kur. Bült., 30, 1-14.

Bak K., 2005. Sedimentological, geochemical and microfaunal responses to environmental changes around the Cenomanian–Turonian boundary in the

Outer Carpathian Basin; a record from the Subsilesian Nappe, Poland. Palaeogeography, Palaeoclimatology, Palaeoecology.

Baum, G.R., and P.R. Vail, 1988. Sequence Stratigraphic concepts applied to Paleogene outcrops, Gulf and Atlantic basins: in C. K. Wilgus, B. K. Hastings, H. Posamentier, J. Van Wagoner, C. A. Ross, and C. G. St. C. Kendall, (eds.), Sea-Level changes: an integrated approach, Soc. Econ. Paleon. and Min. Special Publication No. 42, 309-327.

Berry, W. B. N. and Wilde, P. 1978. Progressive ventilation of the oceans—an explanation for the distribution of the Lower Paleozoic black shales. Am. J. Sci. 278, 257-75.

Boggs S. JR., 1995. Principles of sedimentology and stratigraphy second edition. Prentice Hall Inc. 160-161

Cobianchi, M., Luciani, V., Bosellini, A., 1997. Early Cretaceous nannofossils and planktonic foraminifera from northern Gargano (Apulia, southern Italy). Cretaceous Research 18, 249–293.

Coccioni, R., De Poli, A., Erba, E., Lottaroli, F., Premoli Silva, I., 1990. Lithostratigraphy and biostratigraphy of the ptian-Albian Scisti a Fucoidi Formation (central Italy): evidence for hiatuses and their paleotectonic and paleoenviromental implications. 3rd Convegno Internazionale 'Fossili, Evoluzione, Ambiente', Pergola, 21October 1990, 41 (abstract).

Coccioni, R., Galeotti, S., 1993. Orbitally induced cycles in benthonic foraminiferal morphogroups and trophic structure distribution patterns from the Late Albian "Amadeus segment" (Central Italy). Micropalaeontology 12, 227–239.

Collinson J.D., Thompson D.B., 1989. Sedimentary structures. Second edition. Chapman and Hall, London., 207.

Dickinson, W.R., 1985. Interpreting provenance relations from detrital modes of sandstones. In: Provenance of Arenites (ed. By G.G Zulfa), 333-361

Donovan, A.D., G.R. Baum, G.L. Blechschmidt, T.S. Loutit, C.E. Pflum, and P.R. Vail, 1988. Sequence stratigraphic setting of the Cretaceous-Tertiary Boundary in Central Alabama: in C. K. Wilgus, B. K. Hastings, H. Posamentier, J. Van Wagoner, C. A. Ross, and C. G. St. C. Kendall, (eds.), Sea-Level changes: an integrated approach, SEPM Special Publication No. 42, 299-307.

Dott RH Jr, 1998. An episodic view of shallow marine clastic sedimentation. Reidel, Dordrecht, 3-12

Dunham, R.J., 1962. Classification of carbonate rocks according to depositional texture. In: Classification of Carbonate Rocks (Ed. by W.E. Ham), 108-121 Mem. Am. Ass. Petrol. Geol., 1.

Einsele G., 2000. Sedimentary Basins. Evolution, Facies, and Sediment Budget. Springer-Verlag Berlin Heidelberg. 291-381

Einsele G and Ricken W ,1991. Limestone-marl alternations – an overview. In: Einsele G, Ricken W, Seilacher Cycles and Events in strattigraphy. Springer, Berlin Heidelberg New York., 1-19

Embry. A.F. and Klovan, J.E. ,1971. A late Devonian reef tract on northeastern Banks Island, Northwest Territories. Bull. Can. Petrol. Geol. 19. 730-781

99

Erbacher, J., Thurow, J., Little, R., 1996. Evolution patterns of radiolaria and organic matter variation: A new approach to identify sea-level changes in mid-Cretaceous pelagic environments. Geology, 24, 499-502.

Erbacher, J., Thurow, J., 1997. Influence of anoxic events on the evolution of mid-Cretaceous radiolaria in the North Atlantic and western Tethys. Marine Micropalaeontology 30, 139–158.

Fenner, J., 2001. Middle and Late Albian geography, and climate and the setting of the Kirckrode I and II berehole sites. Palaeogeography, Palaeoclimatology, Palaeoecology 174, 5–32.

Fisher J. K., Price G. D., Hart M. B., Leng M. J., 2005. Stable isotope analysis of the CenomanianeTuronian (Late Cretaceous) oceanic anoxic event in the Crimea. Cretaceous Research 26, 853-863.

Fourquin, CI., 1975. L'Anatolie du Nord-Ouest, marge meridionale du continent curcpeen. Bull. Soc. Giol. France, (7), XVII, 1058-1069.

Galeotti S., Sprovieri M., Coccioni R., Bellanca A, Neri R., 2003. Orbitally modulated black shale deposition in the upper Albian Amadeus Segment (central Italy): a multi- proxy reconstruction. Palaeogeography, Palaeoclimatology, Palaeoecology 190, 441- 58

Görür N., Şengör A.M.C., Akkök R., Yılmaz Y., 1983. Pontidler'de Neo-Tetisin kuzey kolunun açılmasına ilişkin sedimentolojik veriler. Türkiye Jeoloji Kurumu Bülteni, s.26, 11-20

Hernandez-Romano U., Aguilera-Franco N., Martinez-Medrano M., and Barcelo-Duarte J., 1997. Guerrero-Morelos Platform drowning at the Cenomanian – Turonian boundary, Huitziltepec area, Guerrero State, southern Mexico. Cretaceous Research 18, 661 – 686.

Jenkyns H. C., 1980. Cretaceous anoxic events: from continents to oceans. Journal of the Geological Society, London 137, 171-188.

Kellera G., Bernerb Z., Adattec T., Stueben D., 2004. Cenomanian–Turonian and d13C, and d18O, sea level and salinity variations at Pueblo, Colorado. Palaeogeography, Palaeoclimatology, Palaeoecology 211, 19– 43.

Koçyigit A., Altiner D., Farinacci A., Nicosia U., and Conti M.A., 1991. Late Triassic-Aptian evolution of the Sakarya divergen margin: implications for the opening history of the Northern neo-Tethys, in North-Western Anatolia, Turkey. Geologica Romana, 27, 1, 81-100.

Kuypers M. M. M., Lourens L. J., Rijpstra W.I. C., Pancost R. D., Nijenhuis I.A., Damste J. S. S., 2004. Orbital forcing of organic carbon burial in the proto-North Atlantic during oceanic anoxic event 2. Earth and Planetary Science Letters 228, 465–482.

Larson, R.L., 1991. Latest pulse of the earth: Evidence for a mid-Cretaceous superplume. Geology, 19: 547-550. Larson, R.L., 1991b. Geological consequences of superplumes. Geology, 19, 963-966.

Loutit, T.S., J. Hardenbol, P.R. Vail, and G.R. Baum, 1988. Condensed Sections: The key to age dating and correlation of continental margin sequences: in Wilgus, et al, (eds.), Sea-Level in C. K. Wilgus, B. K. Hastings, H. Posamentier, J. Van

Wagoner, C. A. Ross, and C. G. St. C. Kendall, (eds.), Sea-Level changes: an integrated approach, SEPM Special Publication No. 42, 183-213.

Lowe. D.R., 1982. Sediment Gravity Flows: II. Depositional models with special reference to the deposits of high density turbidity currents. J. Sedim Petrol. 52, 279-297.

Mayer H. and Appel E., 1999. Milankovitch cyclicity and rock-magnetic signatures of paleoclimatic change in the Early Cretaceous Biancone Formation of the Southern Alps, Italy. Cretaceous Research, 20, 2, 189-214

Morris SA, Kenyon NH, Limonov AF, Alexander J, 1998. Downstream changes of large-scale bedforms in turbidites around the Valencia cannel mouth, north-west Mediterranean: implications for paleflow reconstruction. Sedimentology 45: 365-377.

Nederbragt A. J., and Fiorentino A., 1999. Stratigraphy and palaeoceanography of the Cenomanian-Turonian Boundary Event in Oued Mellegue, north-western Tunisia. Cretaceous Research 20, 47–62.

Nzoussi-Mbassania P., Khamlib N., Disnara J.R., Laggoun-Defargea F., Boussafir T. M., 2005. Cenomanian–Turonian organic sedimentation in North-West Africa: A comparison between the Tarfaya (Morocco) and Senegal Basins. Sedimentary Geology 177, 271–295

Önal, M., Helvacı, C, İnci, U., Yağmurlu, F., Meriç, E. Ve Tansel, 1., 1988. Çayırhan, kuzeybatı Ankara kuzeyindeki Soğukçam Kireçtaşı, Nardin Formasyonu ve Kızılçay Grubunun stratigrafisi, yaşı, fasiyes ve depolama ortamları: TPJD Bülteni, C-l/2, 153-163.

Özkan-Altıner, S., 1999. Rock-forming Nannofossils in Uppermost Jurassic-Lower Cretaceous Rock Units of Northwest Anatolia: Nannoconus and Its Revised Taxonomy. Turkish Journal of Earth Sciences, 8, 19-43.

Pettijohn, F.J.: Sedimentary Rocks. New York: Harper and Brothers 1949.

Pettijohn, F. J. (Francis John), 1972. Sand and Sandstone. Berlin, New York, Springer-Verlag, 67-113

Posamentier, H.W., Allen, G.P., 1999. Siliciclastic sequence stratigraphy: concepts and applications. SEPM Concepts in Sedimentology and Paleontology no. 7, 210pp

Saner, S., 1980a. Batı Ponditler'in komᵒu havzaların oluşumlarının levha tektoniği kuramıyla açıklaması, KB Türkiye: MTA Dergi., 93/94, 1-20.

Saner, S., 1980b. Mudurnu-Göynük havzasının Jura ve sonrası çökelim nitelikleriyle paleocoğrafya yorumlaması: Türkiye Jeol. Kur. Bült. 23, 39-52.

Schlanger, S. O. and Jenkyns, H. C. 1976. Cretaceous oceanic anoxic events: causes and consequences. Geol. Mijnbouw. 55, 179-84.

Schalager, W., 1999. Type-3 sequence boundaries. In: Harris, P.M., saller, A. H., and Simo, J. A. T. (eds). Advaces in carbonate sequence stratigraphy: application to resevoirs, outcrops and models. S. E. P. M. Special Publication No:63, 35-45.

Schuchert, C., 1916. Correlation and chronology in geology in the basis of paleogeography. Bull. Geol. Soc. Am., 27, 491-514.

Schurrenberger, D., Russell, J. and Kerry Kelts. 2003. Classification of lacustrine sediments based on sedimentary components. Journal of Paleolimnology 29, 141-154

Schwarzacher W., 1993. Cyclostratigraphy and the milankovitch theory. Elseveier Amsterdam, London, New York, Tokyo. 1-10

Scopellitia G., Bellancaa A., Coccionib R., Lucianic V., Neria R., Baudind F., Chiarie M., Marcucci M., 2004. High-resolution geochemical and biotic records of the Tethyan 'Bonarelli Level' (OAE2, latest Cenomanian) from the Calabianca–Guidaloca composite section, north-western Sicily, Italy. Palaeogeography, Palaeoclimatology, Palaeoecology 208, 293–317.

Sloss, L.L., 1963. Sequences in the cratonic interior of North America. Geol. Soc. Am. Bull., 74, 93-113.

Sloss, L.L., 1972. Synchrony of Phanerozoic sedimentary-tectonic events of the North American craton and the Russian Platform. 24th Int. Geol. Congr. Sect. 6, 24-32

Sloss, L.L. and Speed, R.C., 1974. Relationships of cratonic and continental margin tectonics episodes. In: W.R. Dickinson (Editor), Tectonics and Sedimentation. Soc. Econ. Paleontol. Miner. Spec. Publ., 22, 98-119.

Strasser A., Caron M., and Gjermeni M., 2001. The Aptian, Albian and Cenomanian of Roter Sattel, Romandes Prealps, Switzerland: a high-resolution record of oceanographic changes. Cretaceous Research 22, 173–199.

Şengör, A. M. C. ve Yılmaz, Y., 1981. Tethyan evolution of Turkey: a plate tectonic approach. Tectonophysics, 75, 181-241.

Takashima R., Kawabe F., Nishi H., Moriya K., Wani R., Ando H., 2004. Geology and stratigraphy of forearc basin sediments in Hokkaido, Japan: Cretaceous environmental events on the north-west Pacific margin. Cretaceous Research 25, 365-390.

Toker. V.. 1976. Stratigraphical Studies of the area located between Nallıhan and Bozkaya villages along the Sorgun river Communications de la Faculte des Science de I'Univ d'Ankara, seri C. 19. 1-63, 1-5.

Tucker M. E., 1991. Sedimentary Petrology An Introduction to the origin of sedimentary Rocks, Blackwell Scientific Publications. 53-54

Vail, P. R. , R. G. Todd,and J. B. Sangree, 1977. Seismic Stratigraphy and Global Changes of Sea Level: Part 5. Chronostratigraphic Significance of Seismic Reflections: Section 2. Application of Seismic Reflection Configuration to Stratigraphic Interpretation Memoir 26, 99 – 116.

Vail, P.R., Mitchum, R.M., Jr., Todd, R.G., Widmier, J.M., Thompson, S., III., Sangree, J.B., Bubb, J.N. and Hatleilid, W.G., 1977. Seismic stratigraphy and global changes of sea level. In: C.E. Payton (Editor), Seismic Stratigraphy-Applications to Hydrocarbon Exploration. Am. Assoc. Pet. Geol. Mem., 26, 49-212.

Vail, P.R. and Todd, R.G., 1981. Northern North Sea Jurassic unconformities, chronostratigraphy and sea level changes from seismic stratigraphy. In: L.V. Illing and G.D. Hobson (Editors), Proceeding of the Petroleum Geology of the

Continental Shelf of NW Europe Conf., March 4-6, 1980. London. Heydon and Son Ltd., London, pp. 216-235.

Valeria Luciani, Miriam Cobianchi, Stefano Fabbri, 2006, The regional record of Albian oceanic anoxic events at the Apulian Platform Margin (Gargano Promontory, southern Italy), Revue de micropaleontology

Varol, B. and Kazancı, N., 1981. Litho- and biofacies characteristics of upper Jurassic-lower Cretaceous carbonate sequence in the Nallıhan- Seben (Bolu) region. Geol.Soc. Bull.Turkey, 24, 111-118. (in Turkish).

Wheeler, H.E., 1958. Time stratigraphy. Am. Assoc. Pet. Geol. Bull., 42: 1047-1063.

Yağmurlu, F., Helvacı, C, İnci, U. and Önal, M., 1988. Tectonic characteristics and structural evolution of the Beypazarı and Nallıhan Neogene basin, central Anatolia: Metu Journal of Pure and Applied sciences, 21, 1-3, 127-143.

Yılmaz İ.Ö., 2002. Applications of cyclostratigraphy and sequence stratigraphy in determination of the hierarchy in peritidal and pelagic successions (NW, SW and WNW of Turkey) by using sedimentology and sedimentary geochemistry (Stable isotopes) METU, 248 pp.

Yılmaz, İ. Ö., and Altıner, D. 2005a. Records of Early Cretaceous (Aptian-Albian) and Late Cretaceous (Santonian-Campanian) Red Beds and possible Oceanic Anoxic Events: their meaning in Sequence Stratigraphic framework (NW Turkey). International Geosciences Programme Project (IGCP) 463 and 494, Workshop on Cretaceous Oceanic Red Beds, CORB, September 1-2, 2005, Neuchâtel, Switzerland. Abstract Book, 240-241.

Yılmaz, İ. Ö., and Altıner, D. 2005b. Cyclostratigraphic, sequence stratigraphic and sedimentological approaches in platform to platform and platform to basin correlations (Tauride and Pontide platforms and Mudurnu-Nallihan basins 20-(Barremian-Aptian), SW, NW and NW Turkey). 7th International Symposium on Cretaceous, 5-7 September 2005,Neuchâtel, Switzerland. Abstract Book, 239-240.

Yılmaz, İ. Ö., and Altıner, D. 2006. Fischer plot analysis, sedimentology and cyclostratigraphy of the turbidite succession above a drowning unconformity recorded in a pelagic sequence (Aptian-Cenomanian, NW Turkey). SEDIMENT2006, the 4th annual conference of SEPM (Society for Sedimentary Geology). June, 6-11, 2006 in Göttingen, Germany, Abstract Book, p., 187.

Yılmaz, Y. Tüysüz, O., Gözübol, A.M. ve Yiğitbaş, E., 1980. Abant (Bolu)-Dokurcun (Sakarya) arasında Kuzey Anadolu Fay zonunun kuzey ve güneyinde kalan tektonik birliklerin jeolojik evrimi : istanbul Yerbilimleri, *2,* 239=261.

Yılmaz, Y., 1981. Sakarya kıtasının güney kenarının tektonik evrimi : istanbul Yerbilimleri, 1, 33-52.

APPENDIX

Results of Point Counting from Samples (units in %)

The thin section of samples were prepared and analyzed on the basis of their major mineral constituents and the frequency of mineral constituents has been counted by point-counting method under the microscope. Identified minerals are quartz, orthoclase, MRF, VRF, SRF, matrix, calcite, skeletal grains, pyroxene, opaque, plagioclase, amphibole, glauconite, biotite, muscovite.

Sample No	Quartz	Orthoclase	MRF	VRF	SRF	Matrix	Calcite	Skeletal grains	Pyroxene	Opaque	Plagioclase	Amphibole	Glauconite	Biotite	Muscovite
syh.1	2,31	0,36	0,00	0,00	2,06	55,10	6,55	32,77	0,00	0,00	0,73	0,00	0,12	0,00	0,00
syh.2	1,82	0,30	0,00	0,61	0,00	59,57	18,84	17,37	0,00	1,22	0,00	0,00	0,30	0,00	0,00
syh.3	1,67	0,84	0,00	4,18	0,00	41,21	45,40	6,07	0,00	0,00	0,00	0,21	0,42	0,00	0,00
syh.4	2,62	7,06	0,00	4,44	0,00	0,00	78,02	0,20	0,00	7,66	0,00	0,00	0,00	0,00	0,00
syh.5	20,81	3,43	0,00	10,51	0,00	57,98	1,01	0,20	0,00	3,03	0,00	3,03	0,00	0,00	0,00
syh.6A	9,51	22,06	0,00	3,64	0,00	64,17	0,00	0,00	0,00	0,61	0,00	0,00	0,00	0,00	0,00
syh.6B	8,73	4,22	0,00	2,26	0,00	51,96	28,61	1,36	0,00	2,86	0,00	0,00	0,00	0,00	0,00
syh.7	24,02	13,35	0,00	4,31	0,00	45,79	7,80	1,23	0,00	3,49	0,00	0,00	0,00	0,00	0,00
syh.8	14,58	4,11	0,00	2,26	0,00	68,17	4,31	0,00	0,00	5,54	0,00	0,82	0,21	0,00	0,00
syh.9	15,38	4,05	0,00	3,04	0,00	68,62	7,69	0,00	0,00	0,81	0,00	0,40	0,00	0,00	0,00
syh.10	16,77	4,85	0,00	3,23	0,00	52,93	15,15	2,22	0,00	3,03	0,00	1,82	0,00	0,00	0,00
syh.11	6,20	2,40	0,00	53,20	0,00	27,40	9,00	0,00	0,00	1,40	0,00	0,00	0,00	0,40	0,00
syh.12	28,10	8,26	0,00	1,45	0,00	49,38	3,51	0,41	0,00	7,23	0,00	1,45	0,21	0,00	0,00
syh.13	21,15	4,52	0,00	2,46	0,00	59,34	2,46	0,00	0,00	8,42	0,00	1,64	0,00	0,00	0,00
syh.14	9,19	3,00	0,00	0,37	0,00	72,06	5,27	3,07	0,00	6,31	0,00	0,61	0,12	0,00	0,00
syh.15	12,81	9,48	0,00	6,28	0,00	52,96	4,56	2,95	0,00	10,84	0,00	0,12	0,00	0,00	0,00
syh.16	50,40	3,33	0,00	0,00	0,00	45,96	0,16	0,00	0,00	0,00	0,00	0,16	0,00	0,00	0,00
syh.17	21,00	4,87	0,00	1,66	0,00	58,64	4,35	6,27	0,00	2,43	0,00	0,64	0,13	0,00	0,00
syh.18	29,29	6,37	0,00	3,19	0,00	48,25	6,22	0,00	0,00	6,53	0,00	0,15	0,00	0,00	0,00
syh.19	8,00	17,69	0,00	6,65	0,00	55,32	1,85	0,00	0,00	10,32	0,00	0,10	0,07	0,00	0,00
syh.20	0,00	0,00	0,00	0,00	0,00	0,00	0,00	0,00	0,00	0,00	0,00	0,15	0,46	0,00	0,00
syh.21	13,72	12,20	0,00	8,08	0,00	57,01	5,34	0,30	0,00	2,74	0,00	0,15	0,46	0,00	0,00
syh.22	1,84	23,81	0,00	9,98	0,00	52,53	8,60	0,00	0,00	2,30	0,00	0,77	0,15	0,00	0,00
syh.23	0,77	13,87	0,00	4,47	0,00	67,03	8,47	1,54	0,00	3,39	0,00	0,46	0,00	0,00	0,00
syh.24	1,52	16,77	0,00	7,01	0,00	39,94	28,51	2,90	0,00	2,90	0,00	0,15	0,30	0,00	0,00
syh.25	3,93	9,06	0,00	1,81	0,00	47,73	32,93	0,15	0,00	3,93	0,00	0,00	0,45	0,00	0,00

Sample No	Quartz	Orthoclase	MRF	VRF	SRF	Matrix	Calcite	Skeletal grains	Pyroxene	Opaque	Plagioclase	Amphibole	Glauconite	Biotite	Muscovite
syh.26	2,64	21,09	0,00	1,48	0,00	64,91	8,73	0,16	0,00	0,33	0,00	0,33	0,33	0,00	0,00
syh.27	2,27	16,99	0,00	4,05	0,00	66,83	2,43	0,49	0,00	4,05	0,00	2,91	0,00	0,00	0,00
syh.28	1,21	13,62	0,00	11,65	0,00	31,47	37,97	0,00	0,00	3,33	0,00	0,15	0,61	0,00	0,00
syh.29A	3,30	11,95	0,05	0,65	2,74	50,23	20,14	2,00	0,00	6,56	2,09	0,28	0,00	0,00	0,00
syh.29B	3,73	9,44	0,10	0,35	2,73	54,77	13,57	1,29	0,00	10,69	3,13	0,15	0,00	0,00	0,00
syh.30	6,13	10,13	0,00	1,15	1,04	56,81	8,70	0,66	0,00	12,21	3,07	0,11	0,00	0,00	0,00
syh.31	3,67	6,26	0,00	0,57	2,79	45,44	25,01	3,63	0,00	8,55	4,07	0,00	0,00	0,00	0,00
syh.32	6,61	9,60	0,00	0,65	5,40	32,98	26,77	1,13	0,00	12,82	3,95	0,08	0,00	0,00	0,00
syh.33	5,79	7,40	0,00	0,32	0,96	61,09	12,86	0,32	0,00	7,40	3,86	0,00	0,00	0,00	0,00
syh.34	2,07	4,77	0,00	0,00	2,49	69,50	9,75	1,25	0,00	8,30	1,87	0,00	0,00	0,00	0,00
syh.35	1,62	7,27	0,00	0,00	2,42	41,01	28,28	3,64	0,00	12,12	3,64	0,00	0,00	0,00	0,00
syh.36	2,61	17,67	0,00	0,80	4,62	22,89	36,35	0,40	0,00	10,24	2,61	1,81	0,00	0,00	0,00
syh.37	2,87	20,11	0,00	10,54	0,96	27,59	13,98	0,19	3,64	10,73	4,60	2,68	2,11	0,00	0,00
syh.38	4,69	12,04	0,61	10,61	1,63	37,55	12,04	0,61	4,29	8,16	3,67	4,08	0,00	0,00	0,00
syh.39	3,22	6,84	0,20	25,15	1,01	40,44	3,62	0,20	5,23	4,63	6,04	3,42	0,00	0,00	0,00
syh.40	0,40	6,67	0,00	37,37	1,62	6,26	28,48	0,00	5,86	0,20	6,26	6,87	0,00	0,00	0,00
syh.41	0,00	1,86	0,00	58,39	0,00	0,62	30,23	0,83	4,55	2,07	0,83	0,62	0,00	0,00	0,00
syh.42	0,44	6,67	0,00	36,22	1,78	24,67	14,67	0,00	4,22	2,89	6,44	2,00	0,00	0,00	0,00
syh.43	5,03	13,00	0,00	14,47	1,05	31,03	13,84	0,21	5,87	6,92	6,50	2,10	0,00	0,00	0,00
syh.44	2,12	5,93	0,00	25,21	1,06	29,03	22,46	0,00	2,97	3,18	2,54	5,51	0,00	0,00	0,00
syh.45	5,23	13,18	0,00	3,86	0,00	37,50	17,05	8,86	0,00	5,68	4,55	4,09	0,00	0,00	0,00
syh.46	1,21	0,00	0,00	41,85	4,43	16,70	23,54	0,00	9,05	0,00	1,41	1,81	0,00	0,00	0,00
syh.47	0,80	0,00	0,00	49,50	4,41	1,60	33,27	0,00	4,01	0,00	3,01	3,41	0,00	0,00	0,00
syh.48	4,03	0,81	0,00	20,36	9,27	8,47	31,25	0,40	6,05	7,66	7,86	3,83	0,00	0,00	0,00
syh.49	5,60	5,60	0,00	3,20	0,80	31,40	25,60	6,60	6,60	4,00	7,00	3,60	0,00	0,00	0,00
syh.50	6,80	4,60	0,60	30,60	1,00	26,40	7,60	0,00	5,80	3,20	8,60	3,80	0,00	0,00	0,00

Sample No	Quartz	Orthoclase	MRF	VRF	SRF	Matrix	Calcite	Skeletal grains	Pyroxene	Opaque	Plagioclase	Amphibole	Glauconite	Biotite	Muscovite
syh.51	6.64	9.46	0.00	4.83	1.01	37.63	5.43	1.21	14.69	3.42	7.24	8.45	0.00	0.00	0.00
syh.52	11.90	4.38	0.00	6.26	3.76	43.63	9.60	0.00	4.59	4.38	3.76	6.89	0.84	0.00	0.00
syh.53	6.41	7.62	0.00	22.65	6.61	27.45	12.63	0.00	1.40	1.80	7.21	6.21	0.00	0.00	0.00
syh.54	1.41	0.60	0.00	61.97	8.45	0.60	16.30	0.00	4.23	2.21	1.81	2.41	0.00	0.00	0.00
syh.55	13.91	8.83	0.00	5.96	0.22	40.18	9.71	0.00	4.19	6.40	6.84	3.53	0.22	0.00	0.00
syh.56	12.27	8.45	0.00	3.02	0.20	51.51	10.26	0.00	0.00	10.06	4.23	0.00	0.00	0.00	0.00
syh.57	6.41	8.22	0.00	0.20	2.00	54.71	19.84	0.00	0.00	6.41	1.40	0.60	0.20	0.00	0.00
syh.58	4.95	6.80	0.00	25.77	2.27	42.06	7.84	0.00	0.82	1.44	4.12	3.92	0.00	0.00	0.00
syh.59	11.18	7.66	0.00	0.62	0.21	42.65	18.01	0.00	0.21	18.22	1.04	0.21	0.00	0.00	0.00
syh.60	19.80	13.06	0.00	1.02	0.20	36.53	7.96	0.00	0.82	13.88	5.10	1.63	0.00	0.00	0.00
syh.61	9.30	26.05	0.00	10.47	0.00	4.65	29.30	0.00	2.79	3.72	12.09	1.63	0.00	0.00	0.00
syh.62A	9.15	7.63	0.00	0.00	0.00	54.47	23.31	0.00	0.00	4.79	0.65	0.00	0.00	0.00	0.00
syh.62B	12.47	11.85	0.00	0.42	0.00	43.24	19.75	0.00	0.00	6.65	3.12	2.29	0.21	0.00	0.00
syh.63	3.44	5.56	0.00	0.00	0.00	76.72	10.32	0.00	0.00	2.65	1.06	0.00	0.26	0.00	0.00
syh.64	8.06	7.27	0.00	0.00	0.00	73.28	4.32	0.00	0.00	5.50	1.38	0.00	0.20	0.00	0.00
syh.65	6.58	9.34	0.00	0.00	0.00	70.28	2.76	0.00	0.85	7.86	1.70	0.00	0.64	0.00	0.00
syh.66	11.97	22.72	0.00	0.20	0.20	47.46	7.51	0.00	0.00	4.46	4.46	0.00	1.01	0.00	0.00
syh.67	13.36	30.77	0.00	0.61	0.00	24.49	20.45	0.00	0.20	5.06	4.86	0.00	0.20	0.00	0.00
syh.68	15.86	26.31	0.00	2.81	0.00	23.90	16.06	0.00	0.00	6.83	7.23	0.00	1.00	0.00	0.00
syh.69	11.52	13.37	0.00	0.21	0.21	22.22	34.98	0.00	0.00	12.76	4.32	0.00	0.41	0.00	0.00
syh.70	11.92	15.96	0.00	0.00	0.00	47.88	7.07	0.00	0.00	13.33	3.84	0.00	0.00	0.00	0.00
syh.71	15.27	23.22	0.00	0.61	0.00	39.51	6.52	0.00	0.00	11.20	3.26	0.00	0.41	0.00	0.00
syh.72	12.30	17.94	0.00	6.25	0.00	36.09	9.68	0.00	0.81	9.48	7.06	0.40	0.00	0.00	0.20
syh.73	10.51	21.01	0.00	1.01	0.00	41.82	9.09	0.00	0.00	14.34	2.02	0.00	0.20	0.00	0.00
syh.74	8.83	20.74	0.00	0.41	0.21	44.56	15.40	0.00	0.00	7.39	2.46	0.00	0.00	0.00	0.00
syh.75	12.78	15.21	0.00	8.92	0.20	44.62	9.94	0.00	0.61	4.46	3.25	0.00	0.00	0.00	0.00

Sample No	Quartz	Orthoclase	MRF	VRF	SRF	Matrix	Calcite	Skeletal grains	Pyroxene	Opaque	Plagioclase	Amphibole	Glauconite	Biotite	Muscovite
syh.76	17,42	19,67	0,00	0,00	0,00	34,22	18,85	0,00	0,00	6,56	2,66	0,00	0,61	0,00	0,00
syh.77	11,16	16,63	0,00	0,61	0,20	51,93	10,75	0,00	0,00	5,07	2,84	0,00	0,81	0,00	0,00
syh.78	15,70	9,42	0,00	0,00	0,00	47,09	17,04	0,00	0,67	5,83	2,24	0,00	2,02	0,00	0,00
syh.79	15,52	16,13	0,00	0,40	0,00	34,48	22,18	0,00	0,00	7,46	3,02	0,00	0,81	0,00	0,00
syh.80	4,77	9,54	0,00	0,40	1,59	29,42	48,11	0,20	0,00	3,58	2,19	0,00	0,20	0,00	0,00
syh.81	1,23	3,28	0,00	77,66	1,23	13,52	0,00	0,00	0,00	0,00	3,07	0,00	0,00	0,00	0,00
syh.82	5,43	5,63	0,00	0,40	0,00	48,49	34,61	0,00	0,00	5,03	0,40	0,00	0,00	0,00	0,00
syh.83	17,42	20,59	0,00	3,39	0,45	37,10	8,14	0,00	0,00	3,62	9,28	0,00	0,00	0,00	0,00
syh.84	12,68	8,45	0,00	0,00	0,00	33,20	38,63	0,00	0,00	4,83	2,21	0,00	0,00	0,00	0,00
syh.85	18,50	16,06	0,00	1,63	0,81	41,67	11,18	0,00	0,41	3,86	5,28	0,00	0,61	0,00	0,00
syh.86	13,91	24,19	0,00	0,20	0,81	32,26	24,19	0,00	0,20	1,81	1,81	0,00	0,60	0,00	0,00
syh.87	9,31	17,41	0,00	0,20	2,02	35,22	29,55	0,00	0,20	2,02	4,05	0,00	0,00	0,00	0,00
syh.88	13,47	18,32	0,00	0,63	0,42	31,79	29,26	0,00	0,00	2,11	4,00	0,00	0,00	0,00	0,00
syh.89	3,44	3,04	0,00	0,00	0,40	51,82	39,07	0,00	0,00	1,21	1,01	0,00	0,00	0,00	0,00
syh.90	5,28	9,35	0,00	0,00	0,20	37,60	41,26	0,00	0,00	5,08	1,02	0,00	0,20	0,00	0,00
syh.91	11,45	11,45	0,00	0,00	0,20	37,55	34,94	0,00	0,00	2,21	2,01	0,00	0,20	0,00	0,00
syh.92	9,71	13,84	0,00	0,62	0,62	40,29	28,72	0,00	2,69	1,45	2,07	0,00	0,00	0,00	0,00
syh.93	16,23	18,46	0,00	0,20	0,00	34,28	21,50	1,01	0,00	5,68	2,03	0,00	0,41	0,20	0,00
syh.94	18,62	19,23	0,00	0,00	0,00	33,81	18,22	0,20	0,00	3,85	5,47	0,00	0,40	0,20	0,00
syh.95	9,48	11,69	0,00	0,00	0,20	42,74	30,24	0,60	0,00	2,82	1,41	0,00	0,40	0,40	0,00
syh.96	15,37	17,42	0,00	0,20	0,82	47,75	8,20	0,00	0,00	6,15	3,69	0,00	0,41	0,00	0,00
syh.97	12,94	15,45	0,00	0,84	0,84	58,46	5,22	0,00	0,00	2,30	3,13	0,42	0,42	0,00	0,00
syh.98	11,11	8,28	0,00	0,40	2,02	54,14	17,17	0,00	0,00	5,66	0,81	0,00	0,40	0,00	0,00
syh.99	6,29	4,06	0,00	0,00	1,01	58,22	28,19	0,00	0,00	1,42	0,81	0,00	0,00	0,00	0,00
syh.100	6,73	7,76	0,00	0,00	0,61	52,65	27,96	0,00	0,00	3,88	0,41	0,00	0,00	0,00	0,00
syh.101	10,10	5,05	0,00	0,00	1,82	52,12	24,44	0,00	0,00	5,66	0,61	0,00	0,20	0,00	0,00

112

Sample No	Quartz	Orthoclase	MRF	VRF	SRF	Matrix	Calcite	Skeletal grains	Pyroxene	Opaque	Plagioclase	Amphibole	Glauconite	Biotite	Muscovite
syh.102	19,67	6,90	0,00	0,84	0,21	36,82	25,52	0,00	0,00	8,37	1,67	0,00	0,00	0,00	0,00
syh.103	8,52	5,48	0,00	0,00	0,41	51,12	31,03	0,00	0,00	2,64	0,61	0,00	0,20	0,00	0,00
syh.104	11,18	21,94	0,00	0,00	0,00	39,78	19,14	0,00	0,00	4,73	2,80	0,00	0,43	0,00	0,00
syh.105	18,29	11,38	0,00	0,00	0,00	33,94	22,97	0,00	0,00	8,94	4,07	0,20	0,20	0,00	0,00
syh.106A	7,88	16,16	0,00	0,20	0,00	31,92	36,57	0,00	0,00	5,66	1,62	0,00	0,00	0,00	0,00
syh.106B	13,42	17,19	0,00	1,26	0,00	54,93	6,29	0,00	0,00	0,84	6,08	0,00	0,00	0,00	2,10
syh.107	11,47	14,08	0,00	0,20	0,20	39,44	24,55	0,00	0,00	7,24	2,62	0,20	0,00	0,00	0,00
syh.108	9,18	9,39	0,00	0,20	0,20	38,16	37,14	0,00	0,41	3,06	1,84	0,00	0,41	0,00	0,00
syh.109	6,69	9,33	0,00	3,65	0,00	49,29	25,76	0,00	0,00	3,25	1,42	0,00	0,61	0,00	0,00
syh.110	10,48	11,69	0,00	1,01	0,00	35,08	34,27	0,00	0,00	6,85	0,60	0,00	0,00	0,00	0,00
syh.111	13,10	15,73	0,00	0,00	0,00	42,34	19,76	0,00	0,00	7,66	1,01	0,00	0,40	0,00	0,00
syh.112	6,71	15,04	0,00	0,00	1,02	35,57	33,94	3,46	0,00	1,42	2,03	0,00	0,81	0,00	0,00
syh.113	8,83	17,86	0,00	0,62	1,44	37,58	25,05	0,00	0,00	2,46	5,54	0,00	0,62	0,00	0,00
syh.114	10,48	14,52	0,00	2,42	0,20	40,93	19,96	0,00	3,63	3,63	3,63	0,40	0,20	0,00	0,00
syh.115	5,61	8,82	0,00	2,40	3,41	46,09	22,65	6,41	0,00	2,40	2,20	0,00	0,00	0,00	0,00
syh.116	9,09	11,52	0,00	0,20	11,31	35,76	17,58	0,00	0,20	2,42	7,68	3,84	0,40	0,00	0,00
syh.117	11,37	10,11	0,00	0,00	0,00	68,00	0,00	0,00	0,00	7,16	2,11	0,00	1,26	0,00	0,00
syh.118	5,68	4,67	0,00	0,00	2,23	38,54	14,00	30,63	0,00	3,04	1,01	0,00	0,20	0,00	0,00
syh.119	4,81	5,23	0,00	0,42	1,67	31,38	8,16	46,03	0,00	1,26	1,05	0,00	0,00	0,00	0,00
syh.120	4,43	3,82	0,00	0,20	2,21	26,16	15,69	46,28	0,00	1,21	0,00	0,00	0,00	0,00	0,00
syh.121	2,41	2,01	0,00	0,00	4,83	38,43	28,57	20,52	0,00	3,02	0,20	0,00	0,00	0,00	0,00